

Supporting Information

Redox Property of Enamines

Yao Li,^{†,§} Dehong Wang,^{‡,§} Long Zhang,^{†,‡} and Sanzhong Luo^{*,†,‡}

[†] *Center of Basic Molecular Science (CBMS), Department of Chemistry, Tsinghua University, Beijing 100084, China*

[‡] *Key Laboratory of Molecular Recognition and Function, Institute of Chemistry, Chinese Academy of Sciences, Beijing 100190, China*

E-mail: luosz@tsinghua.edu.cn

Content

1. Cyclic Voltammograms of enamines	S2
2. NMR spectra of enamines	S30
3. Calculation details and additional data	S100
4. Reference.....	S104

1. Cyclic Voltammograms of enamines

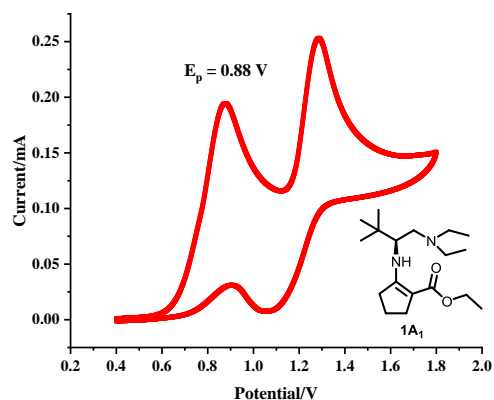


Figure S1. Cyclic voltammogram of $1A_1$.

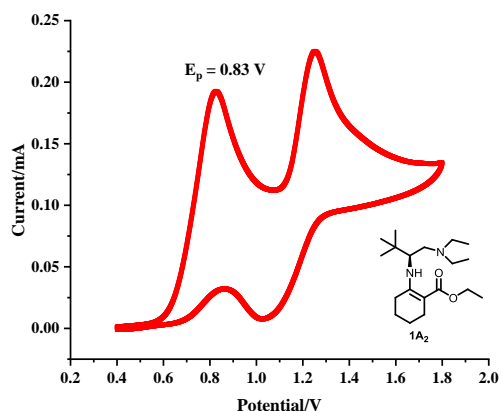


Figure S2. Cyclic voltammogram of $1A_2$.

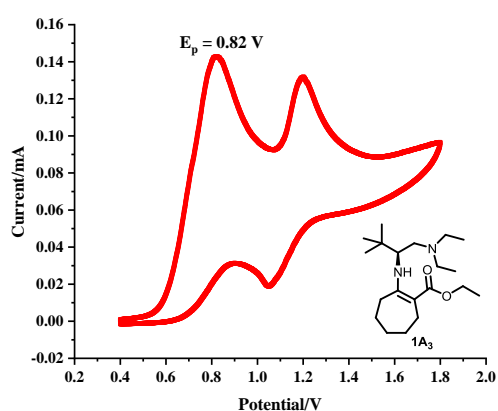


Figure S3. Cyclic voltammogram of $1A_3$.

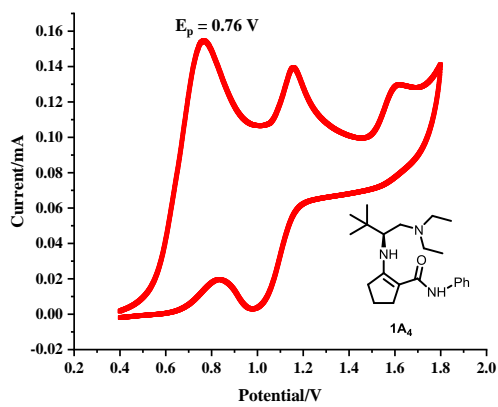


Figure S4. Cyclic voltammogram of $\mathbf{1A_4}$.

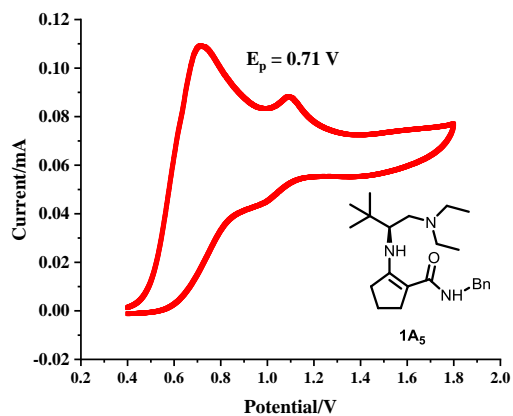


Figure S5. Cyclic voltammogram of $\mathbf{1A_5}$.

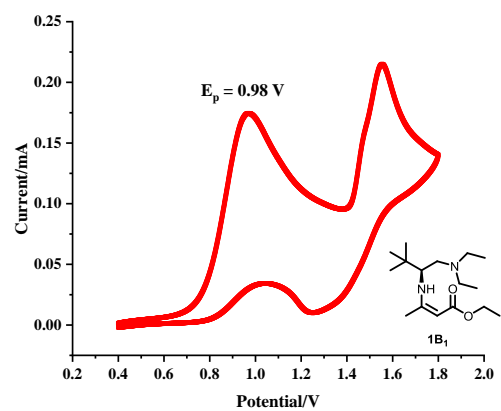


Figure S6. Cyclic voltammogram of $\mathbf{1B_1}$.

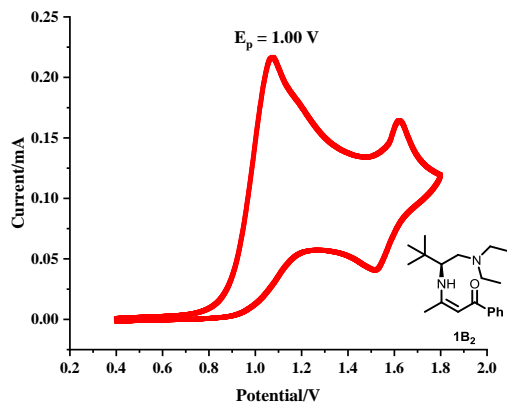


Figure S7. Cyclic voltammogram of 1B_2 .

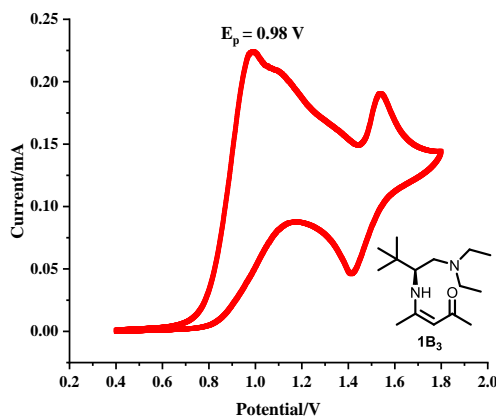


Figure S8. Cyclic voltammogram of 1B_3 .

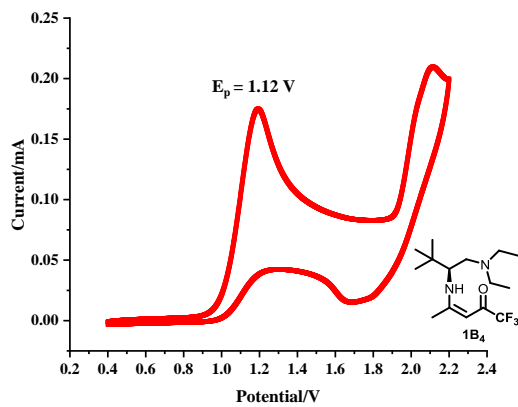


Figure S9. Cyclic voltammogram of 1B_4 .

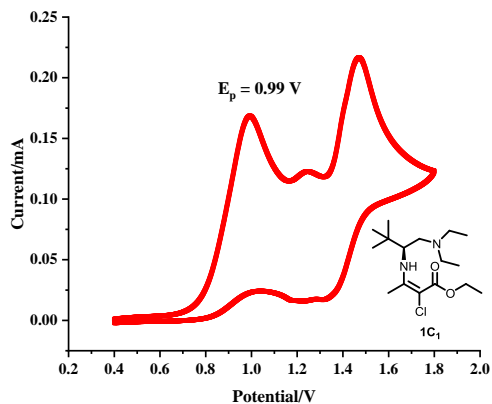


Figure S10. Cyclic voltammogram of $\mathbf{1C_1}$.

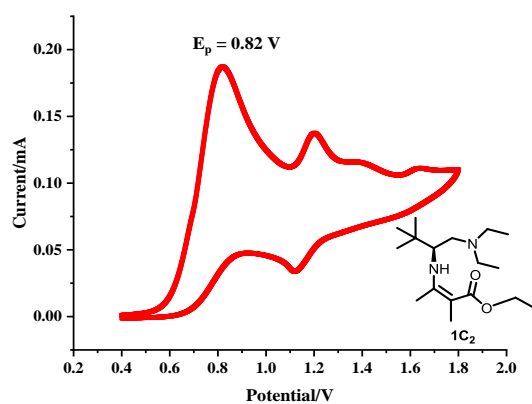


Figure S11. Cyclic voltammogram of $\mathbf{1C_2}$.

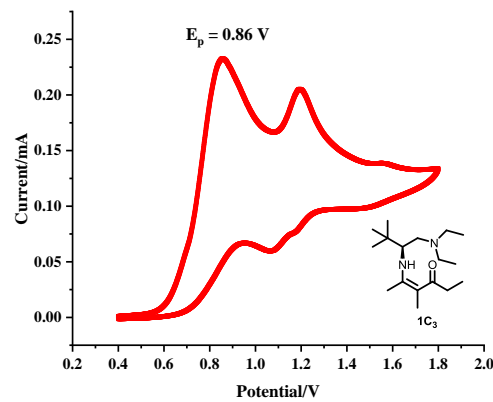


Figure S12. Cyclic voltammogram of $\mathbf{1C_3}$.

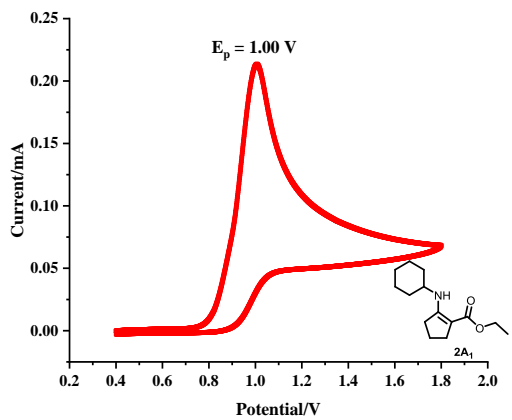


Figure S13. Cyclic voltammogram of 2A_1 .

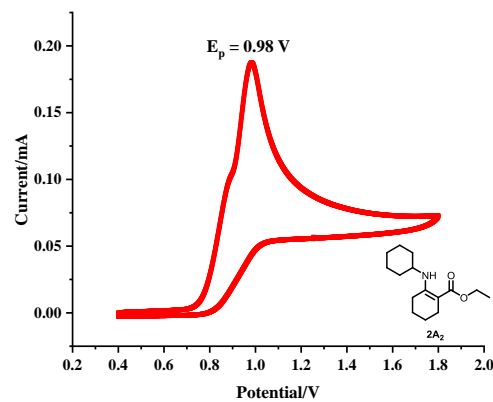


Figure S14. Cyclic voltammogram of 2A_2 .

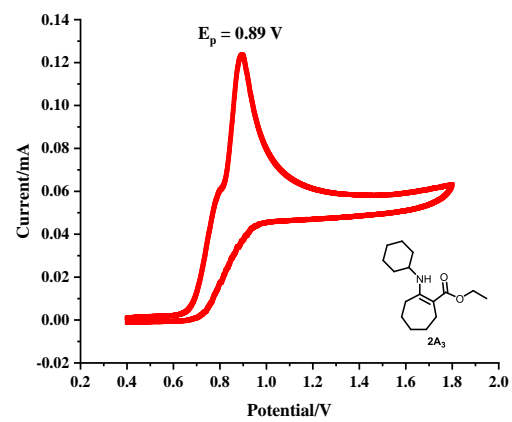


Figure S15. Cyclic voltammogram of 2A_3 .

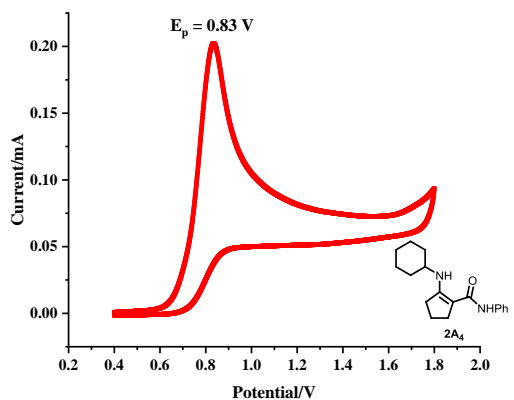


Figure S16. Cyclic voltammogram of 2A_4 .

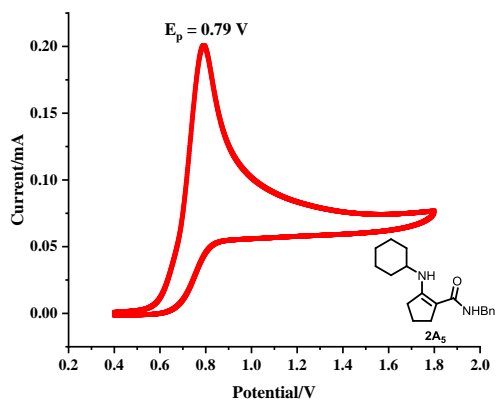


Figure S17. Cyclic voltammogram of 2A_5 .

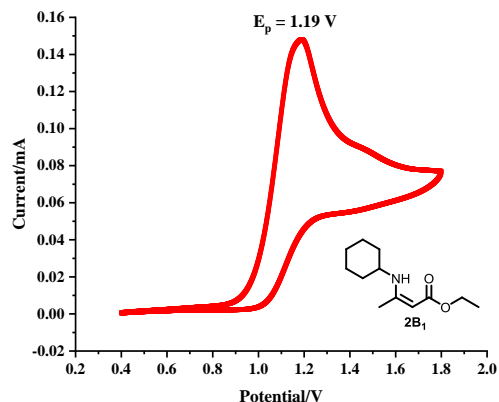


Figure S18. Cyclic voltammogram of 2B_1 .

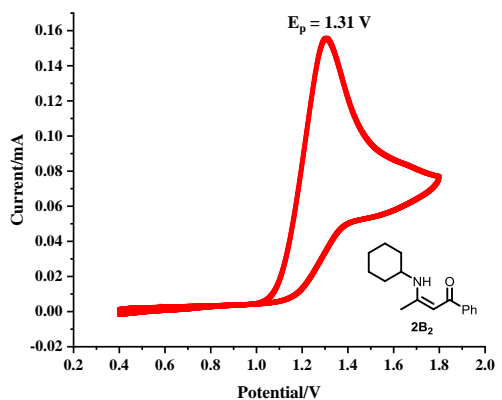


Figure S19. Cyclic voltammogram of $2B_2$.

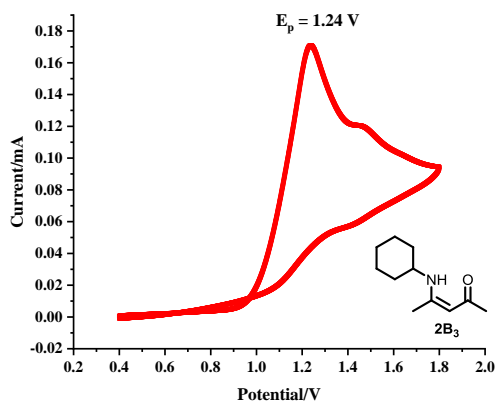


Figure S20. Cyclic voltammogram of $2B_3$.

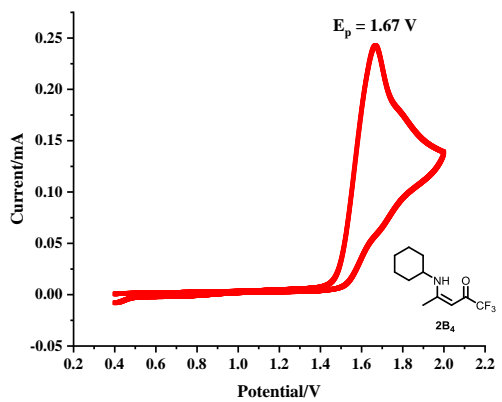


Figure S21. Cyclic voltammogram of $2B_4$.

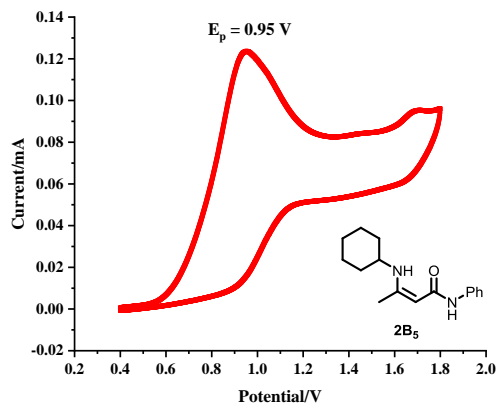


Figure S22. Cyclic voltammogram of 2B_5 .

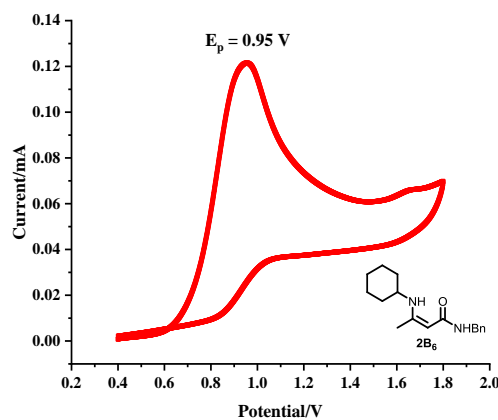


Figure S23. Cyclic voltammogram of 2B_6 .

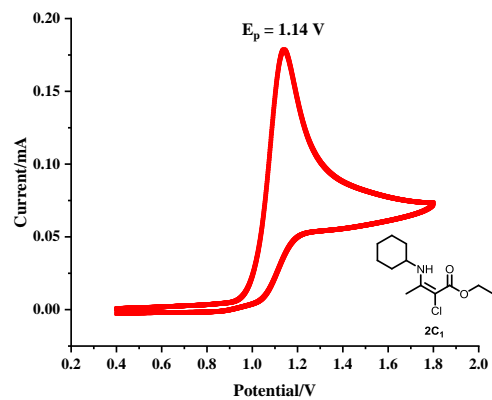


Figure S24. Cyclic voltammogram of 2C_1 .

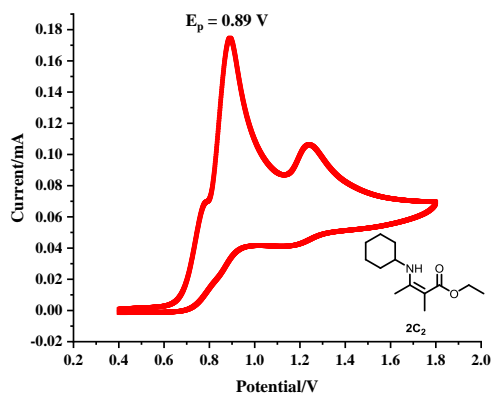


Figure S25. Cyclic voltammogram of 2C_2 .

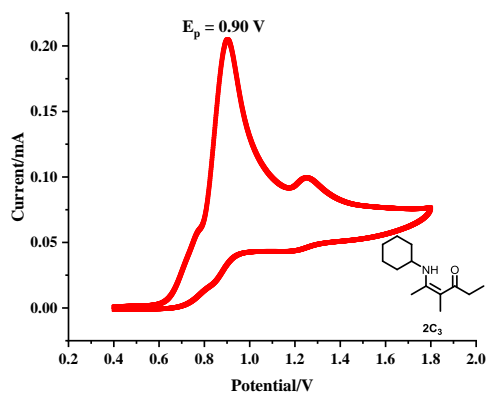


Figure S26. Cyclic voltammogram of 2C_3 .

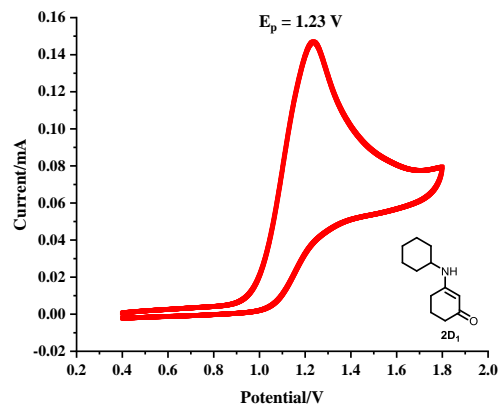


Figure S27. Cyclic voltammogram of 2D_1 .

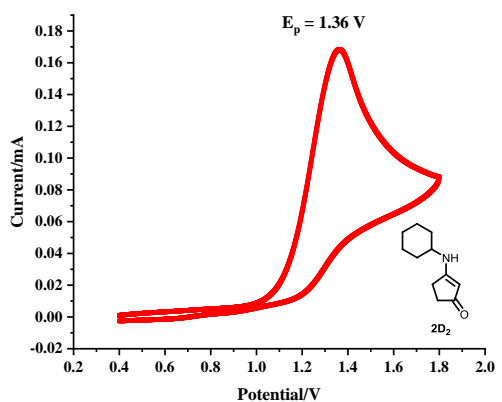


Figure S28. Cyclic voltammogram of $2D_2$.

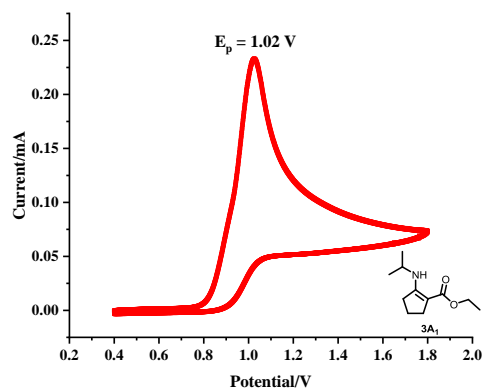


Figure S29. Cyclic voltammogram of $3A_1$.

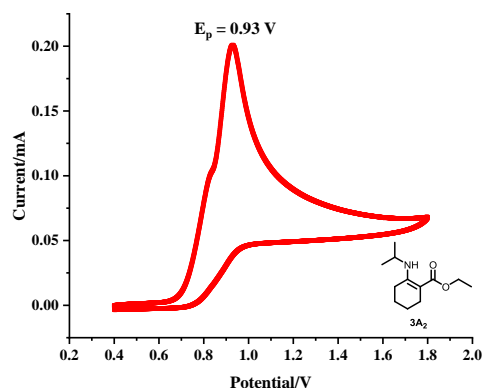


Figure S30. Cyclic voltammogram of $3A_2$.

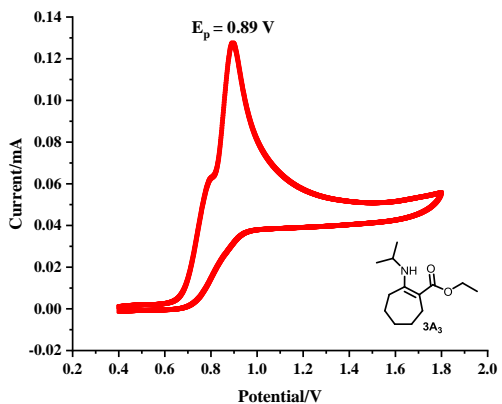


Figure S31. Cyclic voltammogram of 3A_3 .

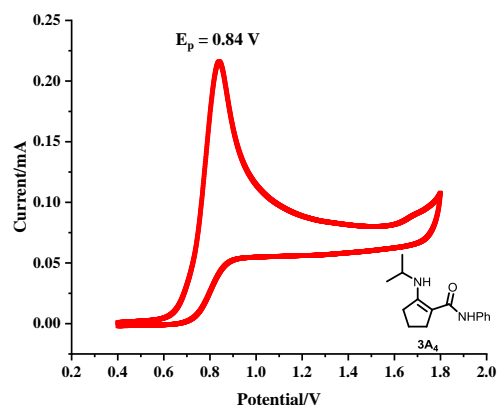


Figure S32. Cyclic voltammogram of 3A_4 .

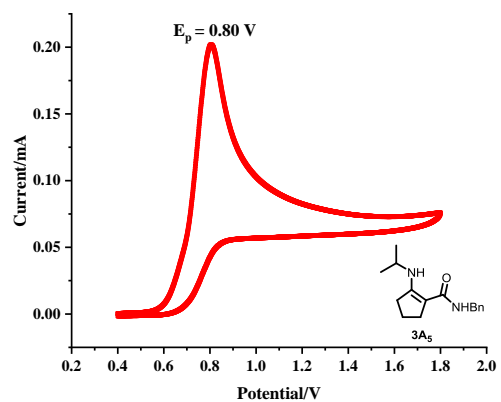


Figure S33. Cyclic voltammogram of 3A_5 .

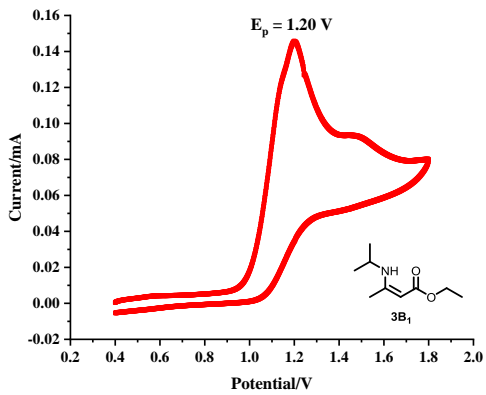


Figure S34. Cyclic voltammogram of $3B_1$.

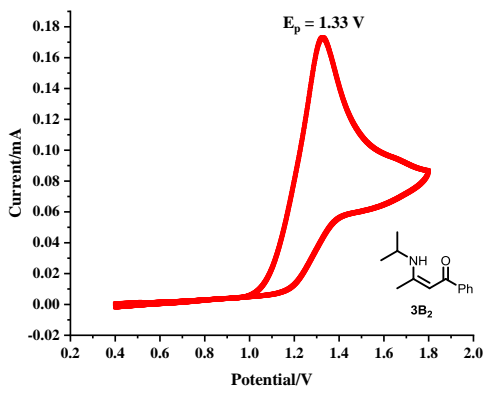


Figure S35. Cyclic voltammogram of $3B_2$.

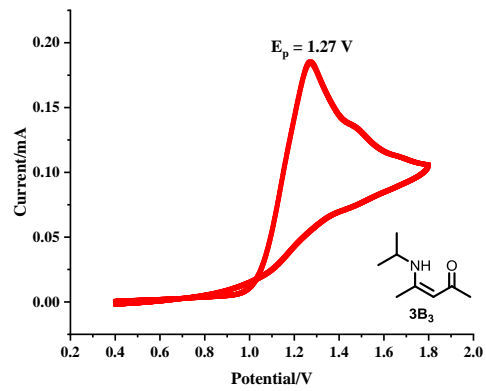


Figure S36. Cyclic voltammogram of $3B_3$.

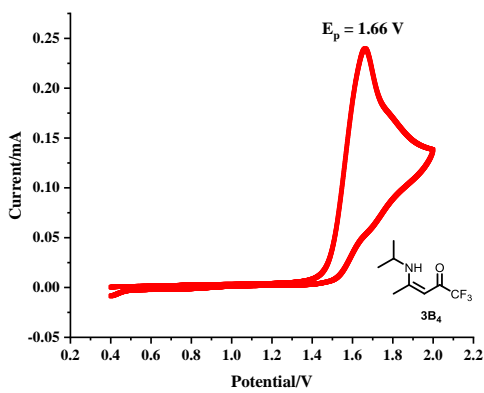


Figure S37. Cyclic voltammogram of $3\mathbf{B}_4$.

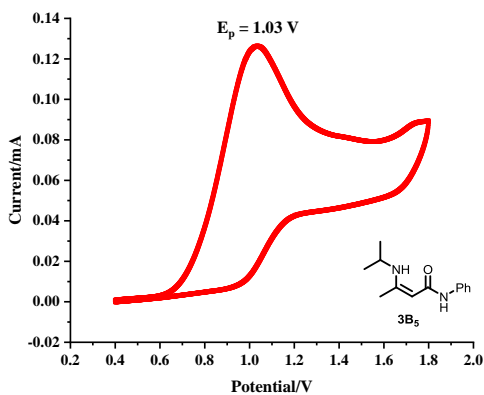


Figure S38. Cyclic voltammogram of $3\mathbf{B}_5$.

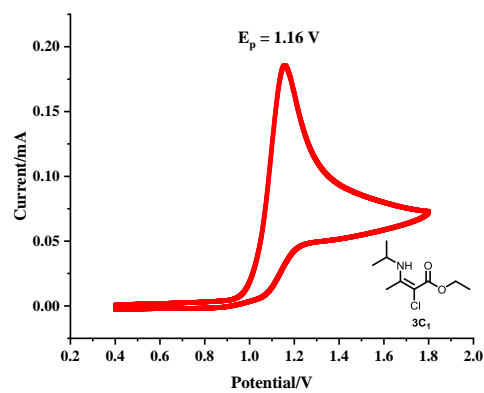


Figure S39. Cyclic voltammogram of $3\mathbf{C}_1$.

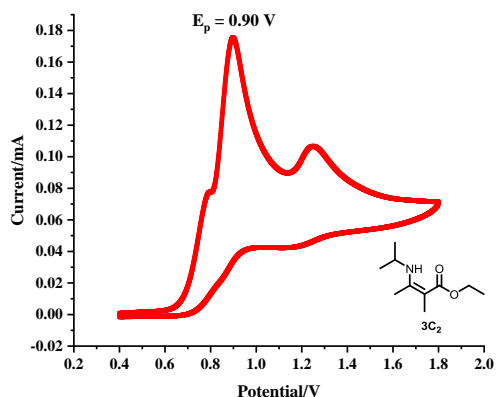


Figure S40. Cyclic voltammogram of 3C_2 .

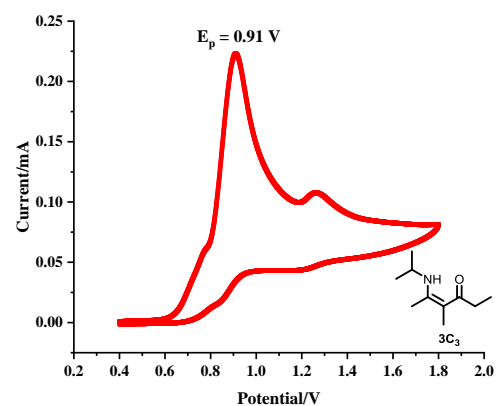


Figure S41. Cyclic voltammogram of 3C_3 .

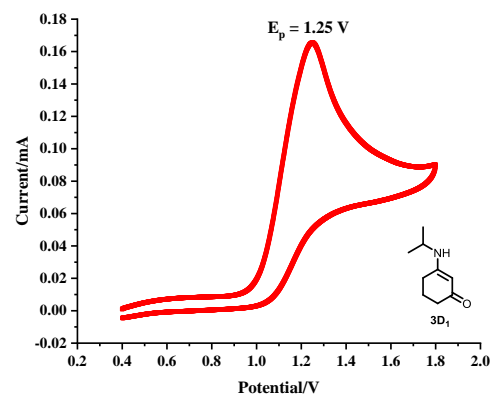


Figure S42. Cyclic voltammogram of 3D_1 .

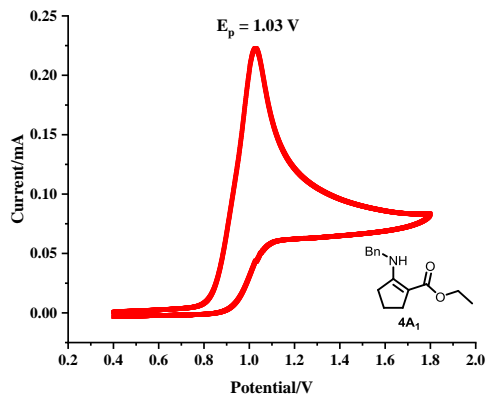


Figure S43. Cyclic voltammogram of **4A₁**.

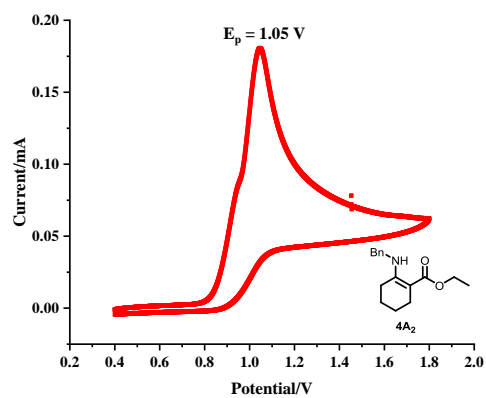


Figure S44. Cyclic voltammogram of **4A₂**.

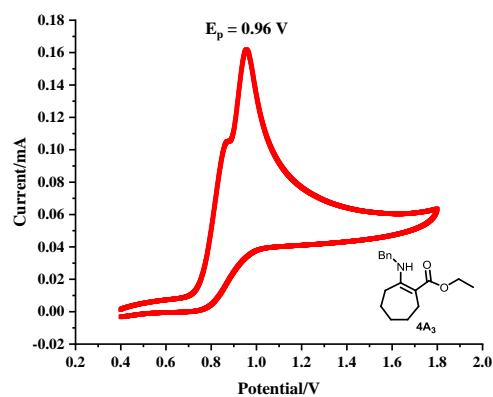


Figure S45. Cyclic voltammogram of **4A₃**.

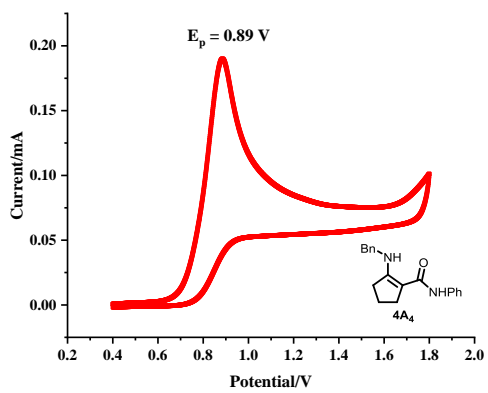


Figure S46. Cyclic voltammogram of 4A_4 .

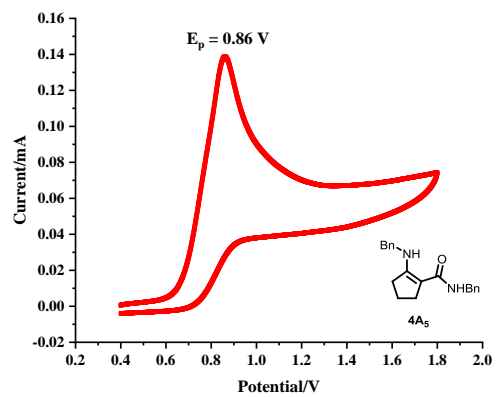


Figure S47. Cyclic voltammogram of 4A_5 .

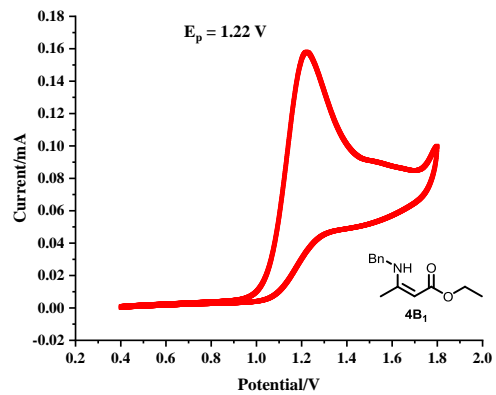


Figure S48. Cyclic voltammogram of 4B_1 .

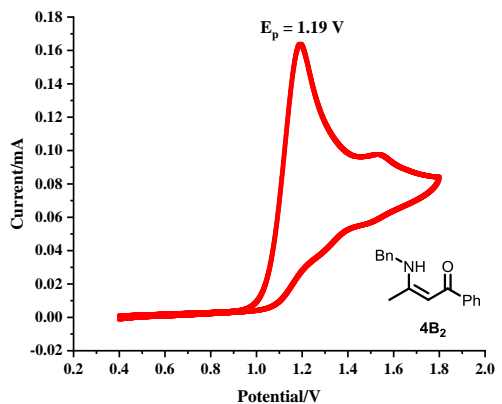


Figure S49. Cyclic voltammogram of $4B_2$.

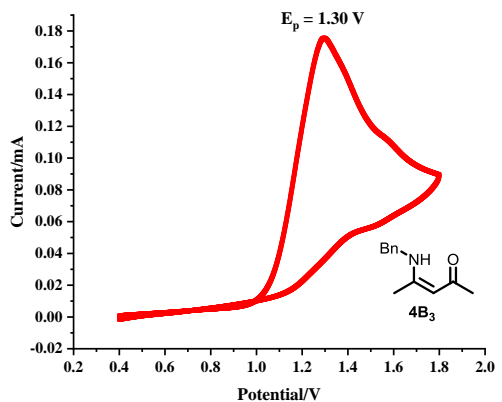


Figure S50. Cyclic voltammogram of $4B_3$.

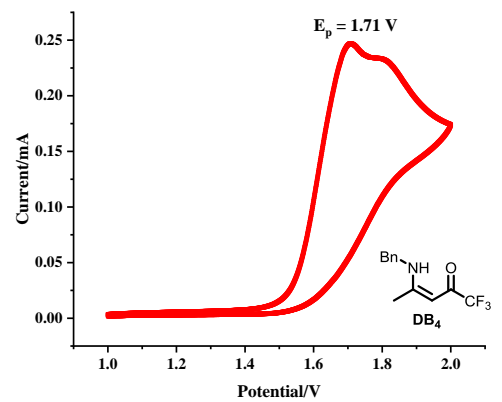


Figure S51. Cyclic voltammogram of $4B_4$.

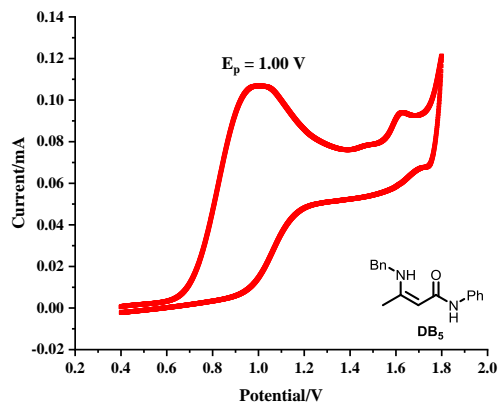


Figure S52. Cyclic voltammogram of **4B₅**.

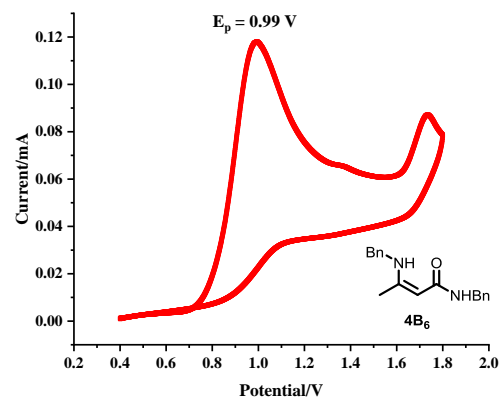


Figure S53. Cyclic voltammogram of **4B₆**.

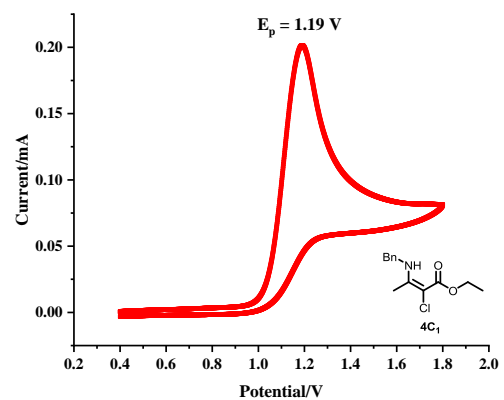


Figure S54. Cyclic voltammogram of **4C₁**.

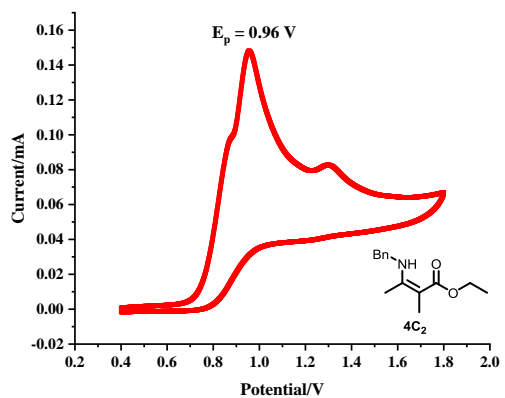


Figure S55. Cyclic voltammogram of 4C_2 .

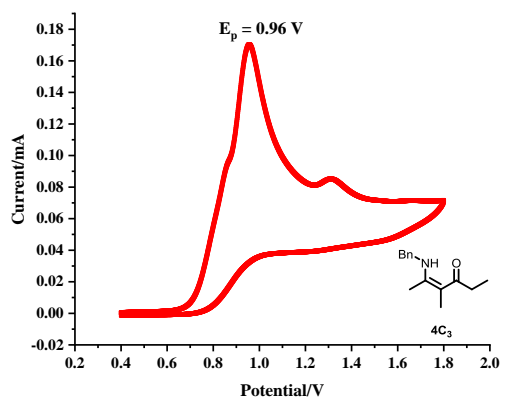


Figure S56. Cyclic voltammogram of 4C_3 .

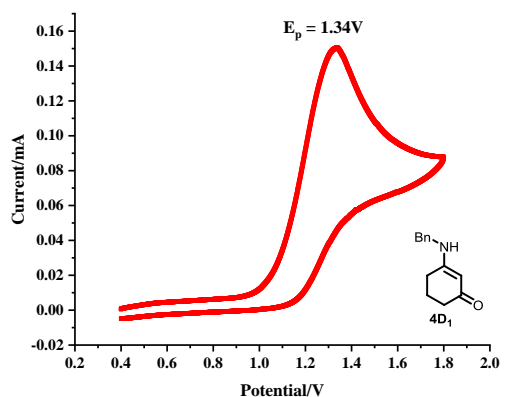


Figure S57. Cyclic voltammogram of 4D_1 .

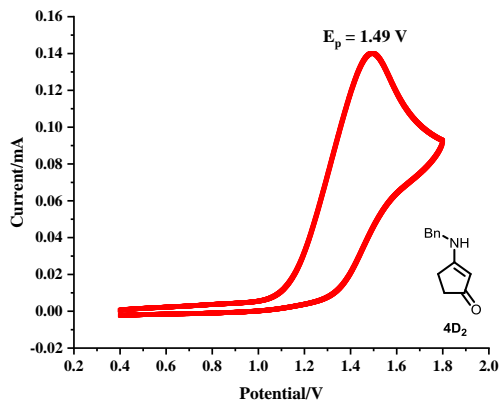


Figure S58. Cyclic voltammogram of $4D_2$.

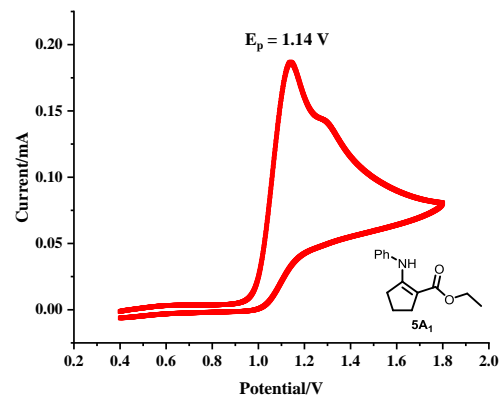


Figure S59. Cyclic voltammogram of $5A_1$.

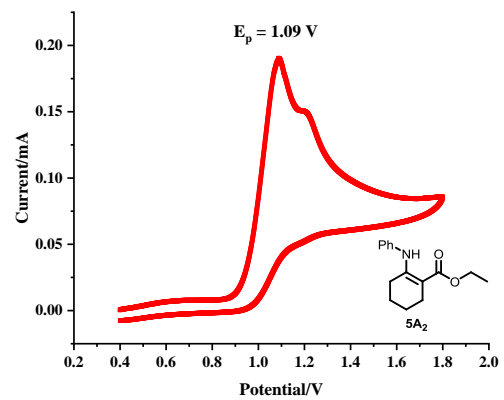


Figure S60. Cyclic voltammogram of $5A_2$.

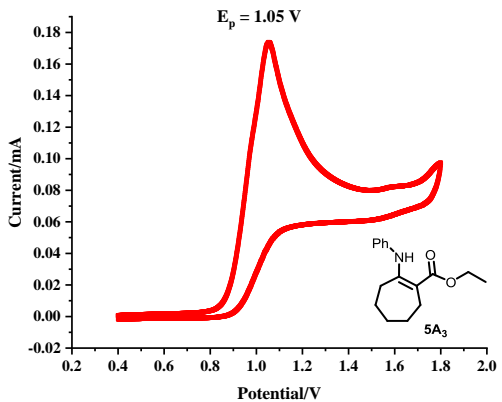


Figure S61. Cyclic voltammogram of 5A_3 .

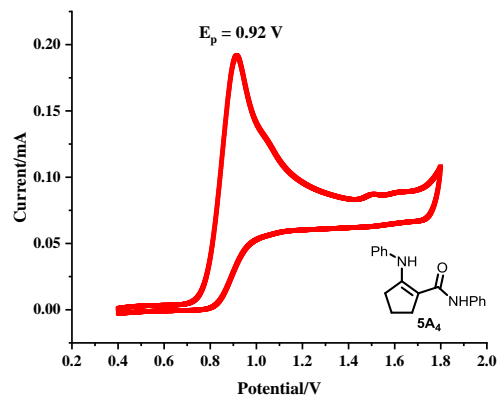


Figure S62. Cyclic voltammogram of 5A_4 .

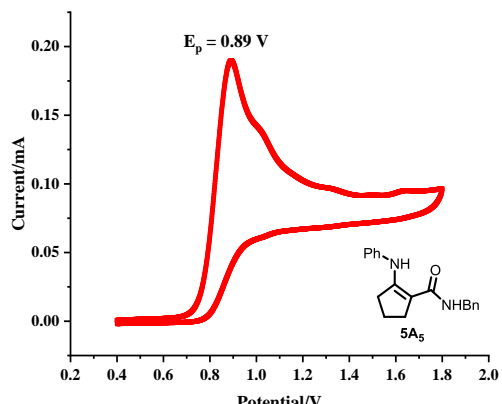


Figure S63. Cyclic voltammogram of 5A_5 .

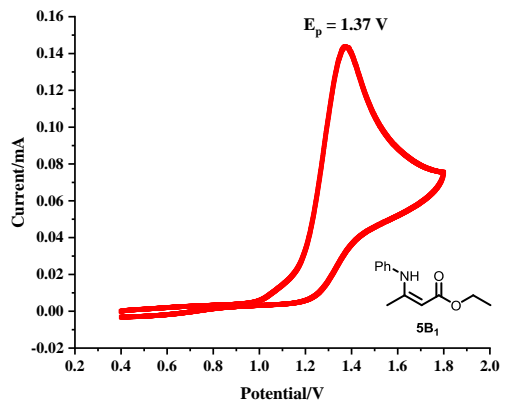


Figure S64. Cyclic voltammogram of $5B_1$.

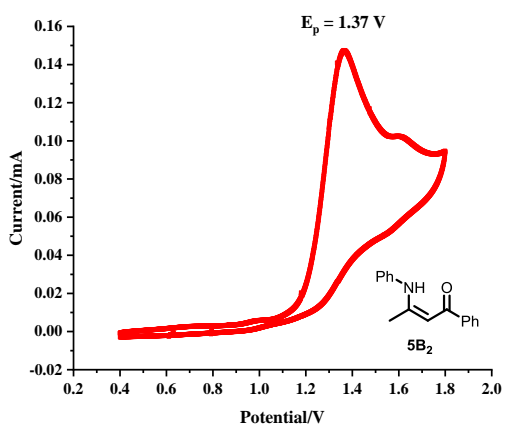


Figure S65. Cyclic voltammogram of $5B_2$.

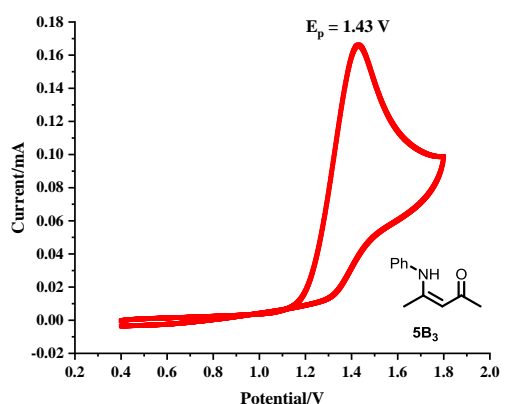


Figure S66. Cyclic voltammogram of $5B_3$.

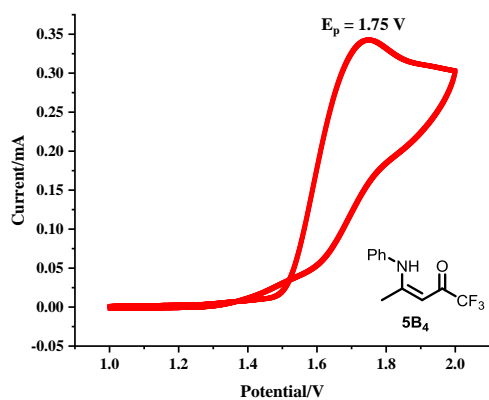


Figure S67. Cyclic voltammogram of $5\mathbf{B}_4$.

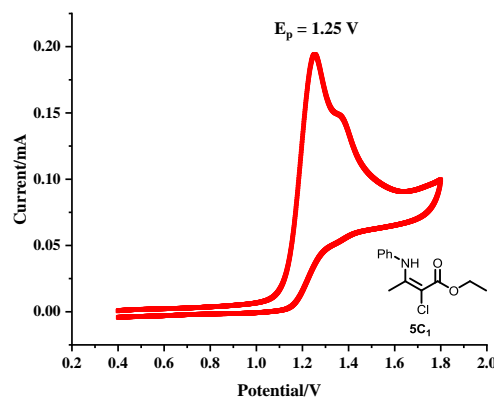


Figure S68. Cyclic voltammogram of $5\mathbf{C}_1$.

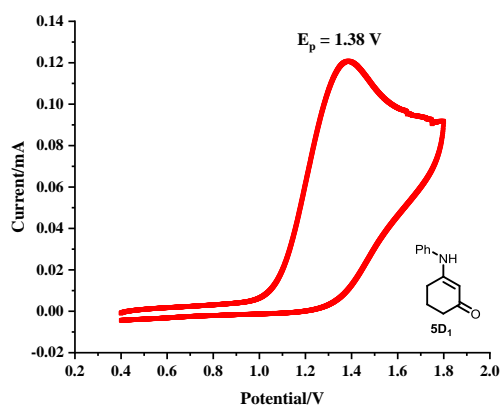


Figure S69. Cyclic voltammogram of $5\mathbf{D}_1$.

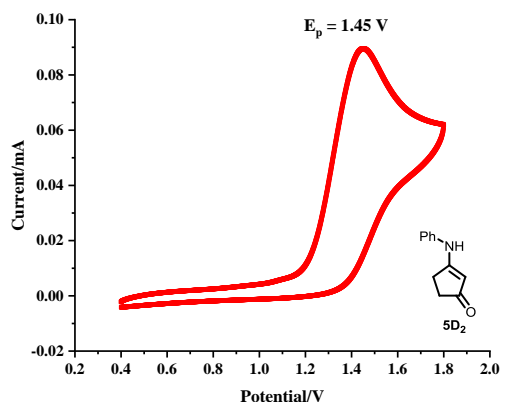


Figure S70. Cyclic voltammogram of $5D_2$.

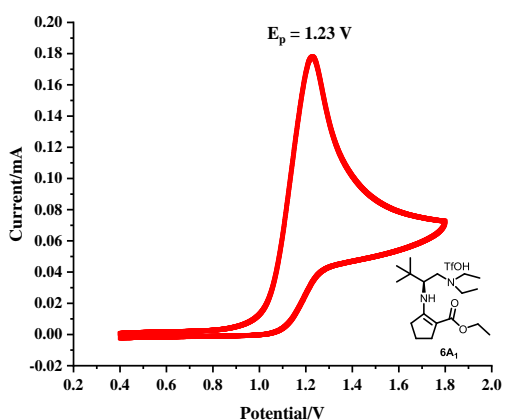


Figure S71. Cyclic voltammogram of $6A_1$.

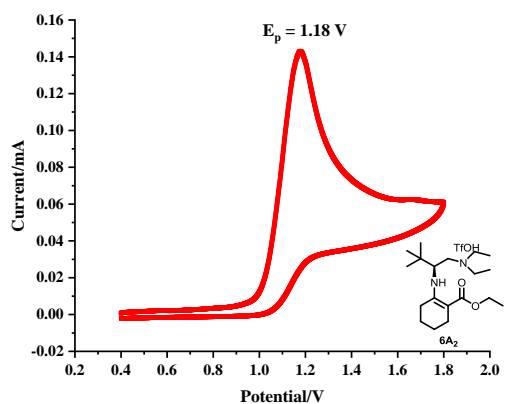


Figure S72. Cyclic voltammogram of $6A_2$.

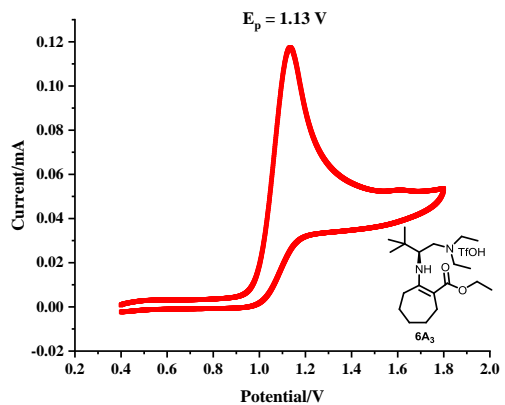


Figure S73. Cyclic voltammogram of 6A_3 .

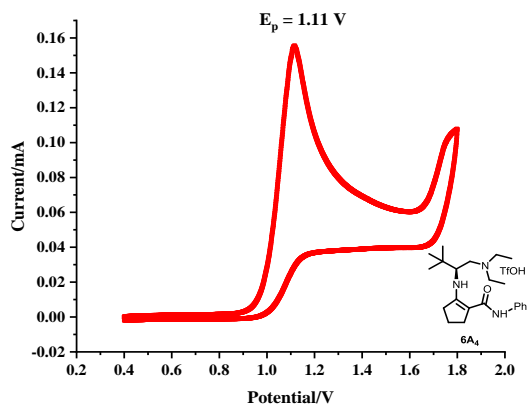


Figure S74. Cyclic voltammogram of 6A_4 .

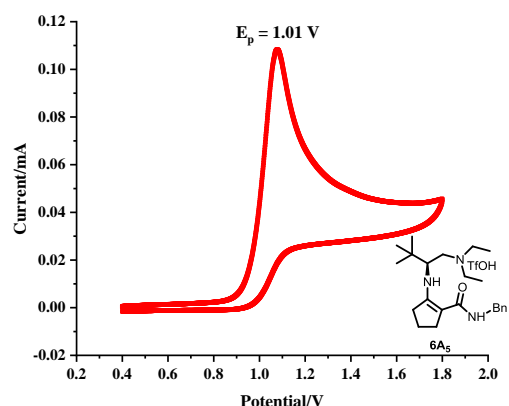


Figure S75. Cyclic voltammogram of 6A_5 .

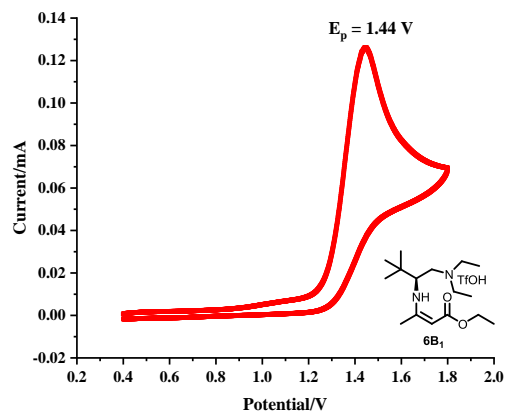


Figure S76. Cyclic voltammogram of **6B₁**.

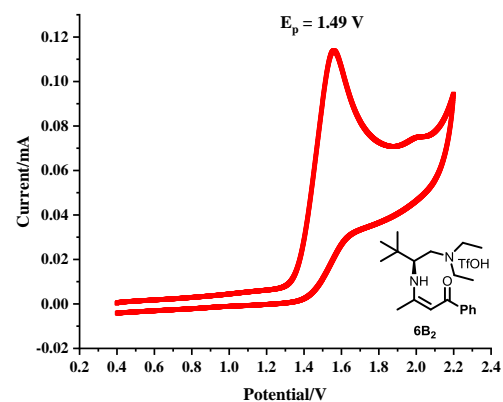


Figure S77. Cyclic voltammogram of **6B₂**.

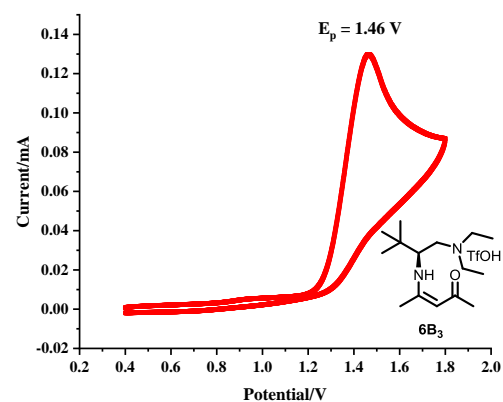


Figure S78. Cyclic voltammogram of **6B₃**.

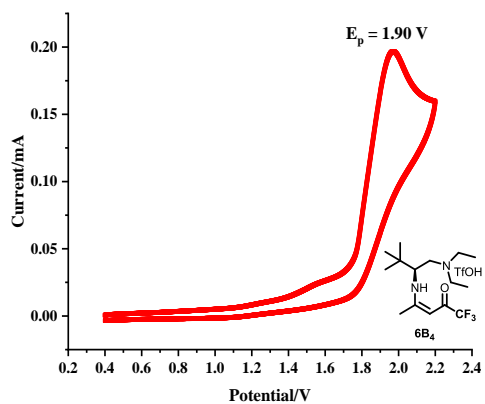


Figure S79. Cyclic voltammogram of **6B₄**.

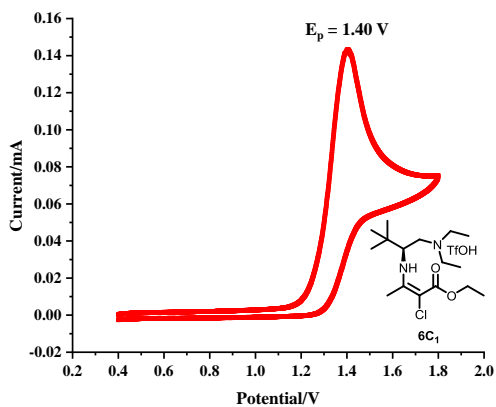


Figure S80. Cyclic voltammogram of **6C₁**.

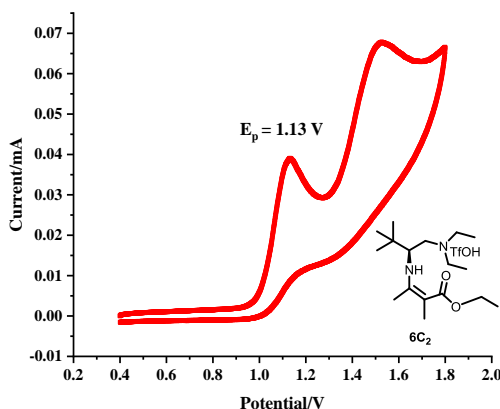


Figure S81. Cyclic voltammogram of **6C₂**.

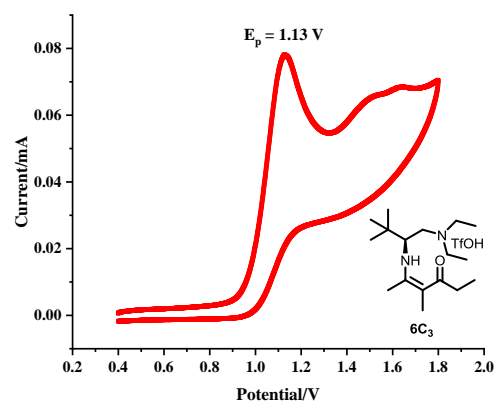
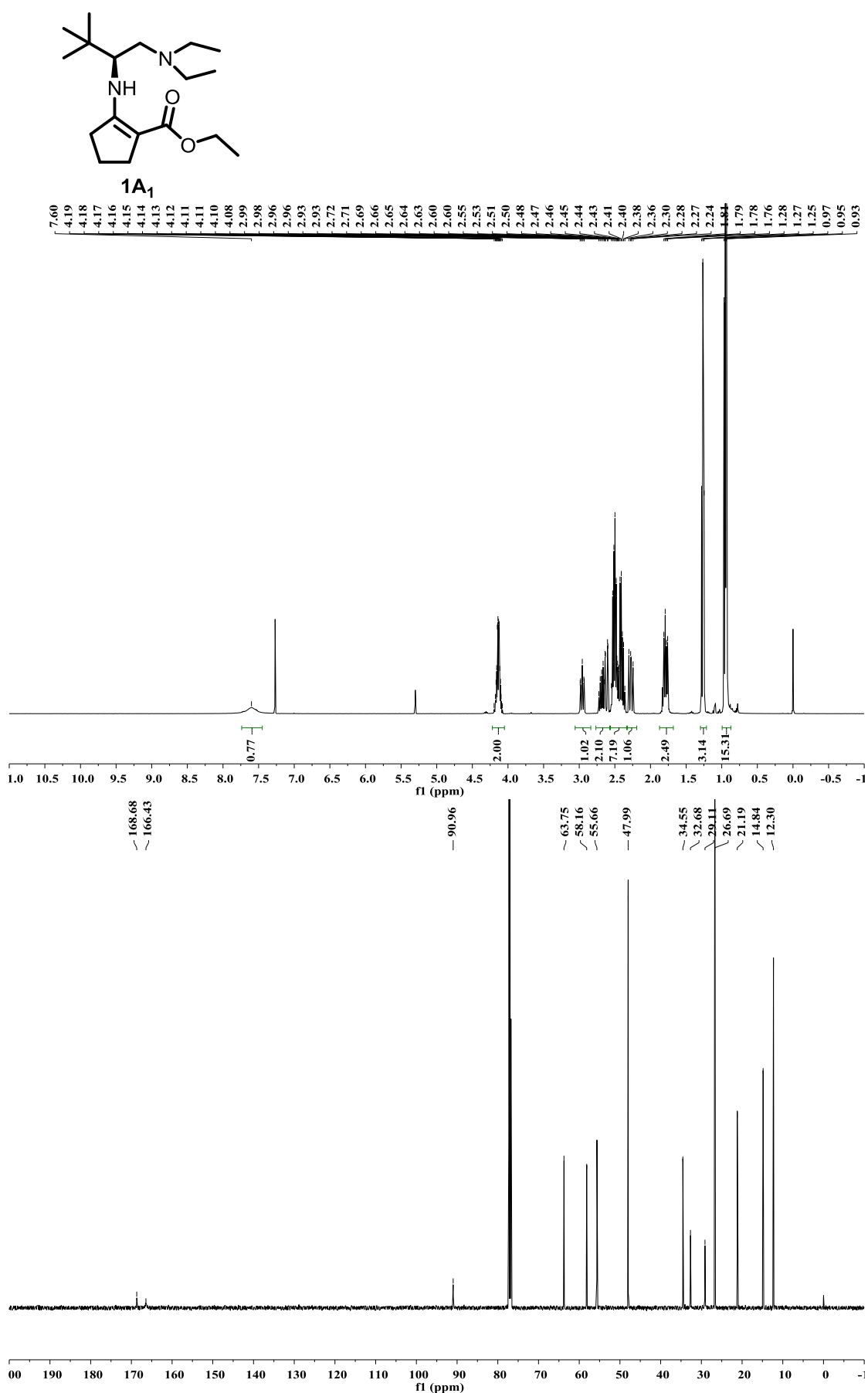
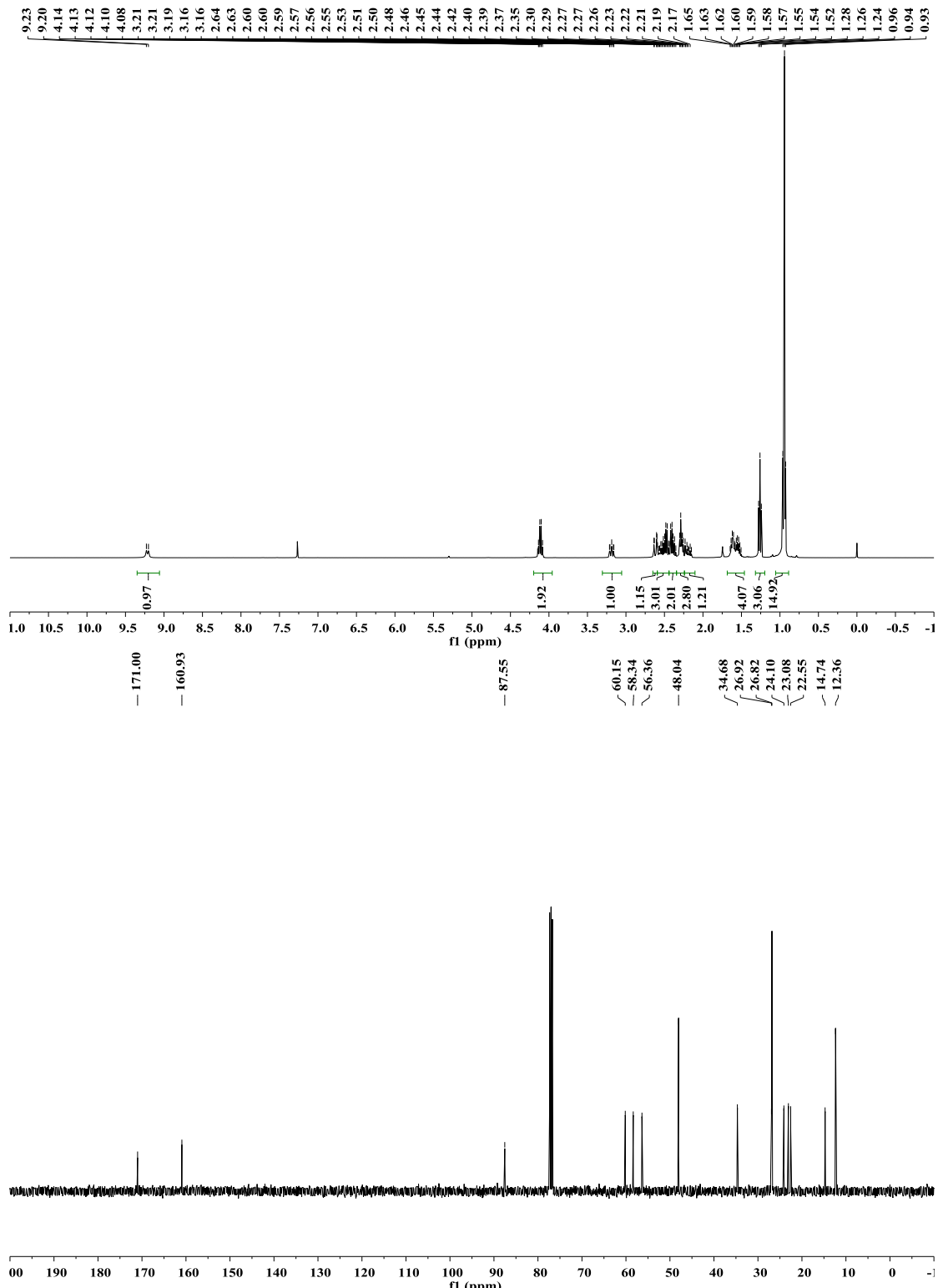
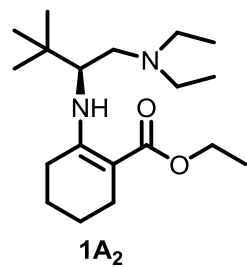
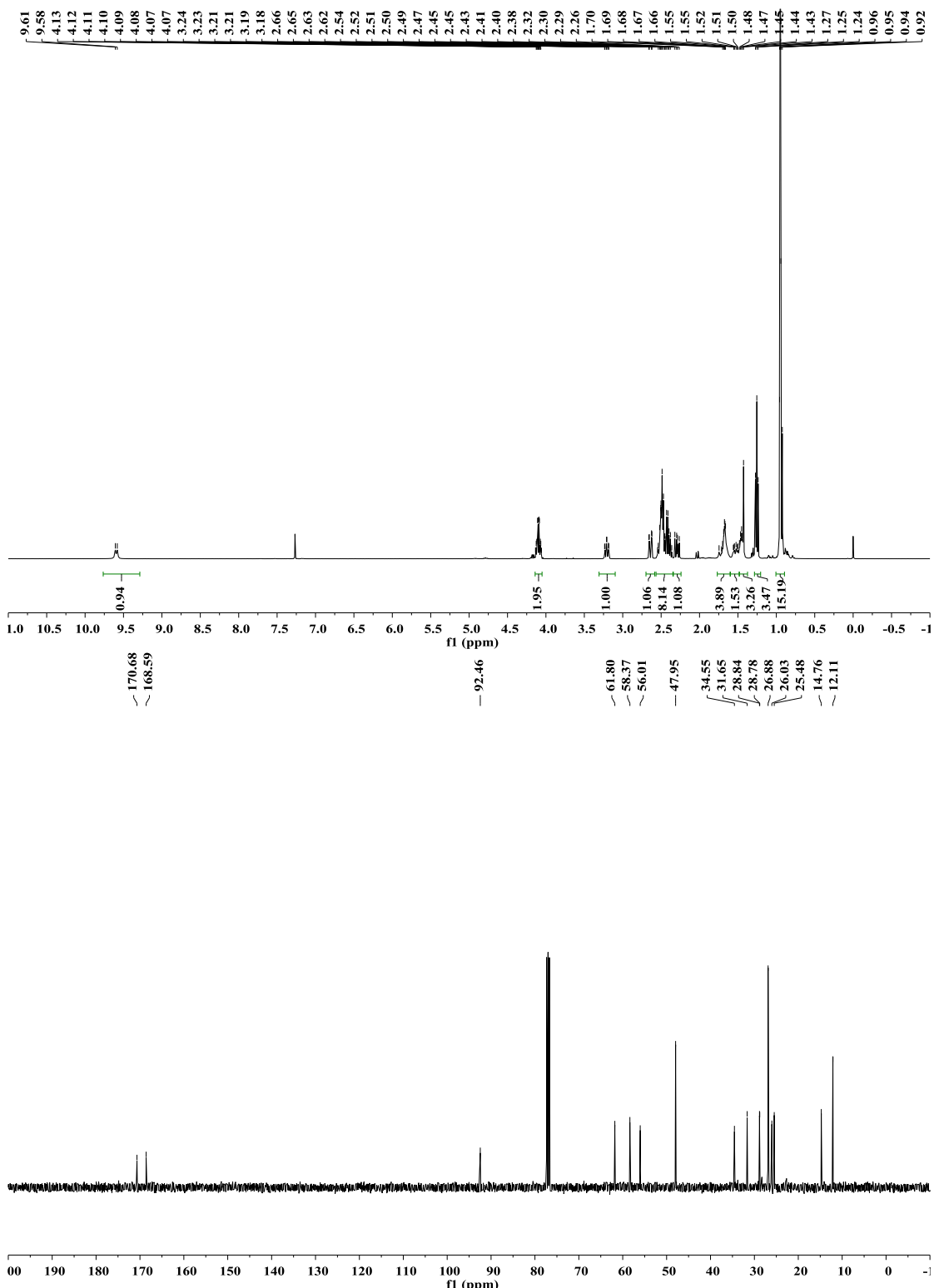
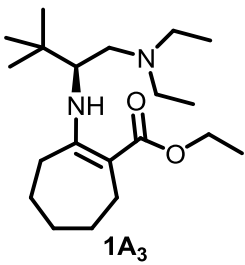


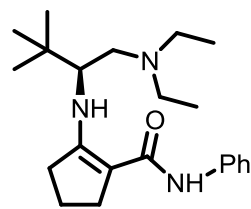
Figure S82. Cyclic voltammogram of $6C_3$.

2. NMR spectra of enamines

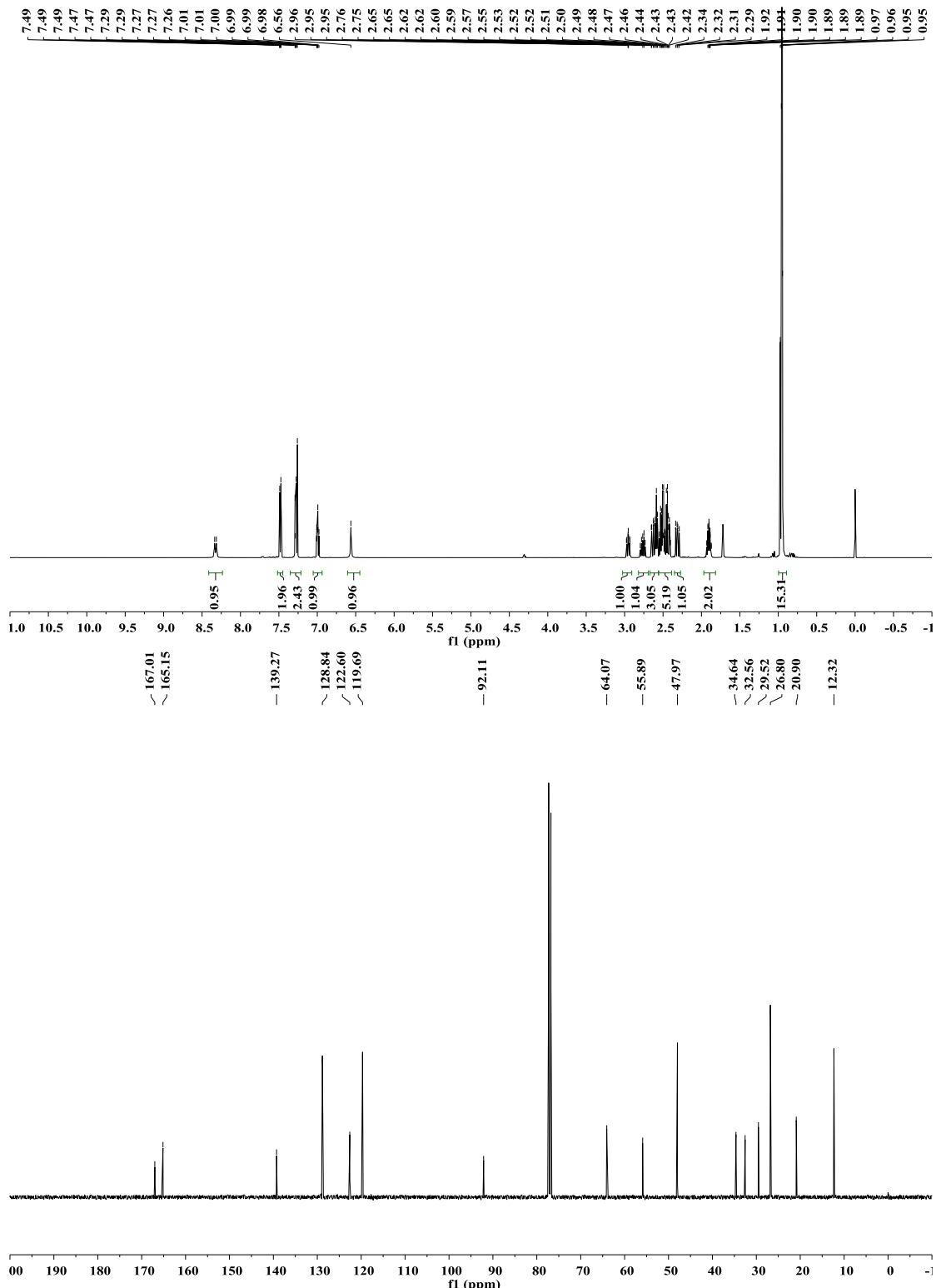


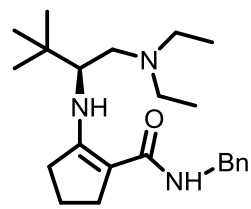




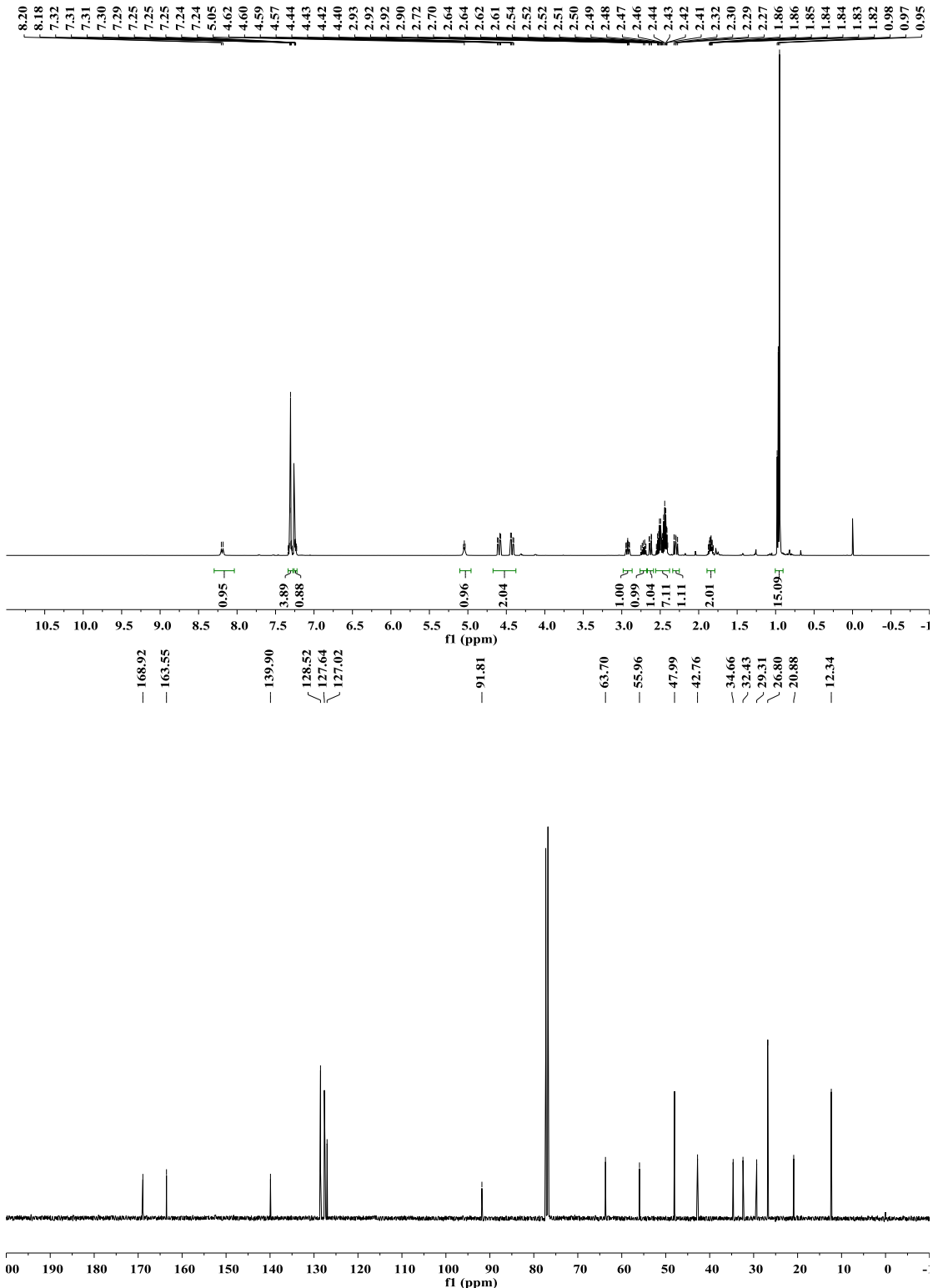


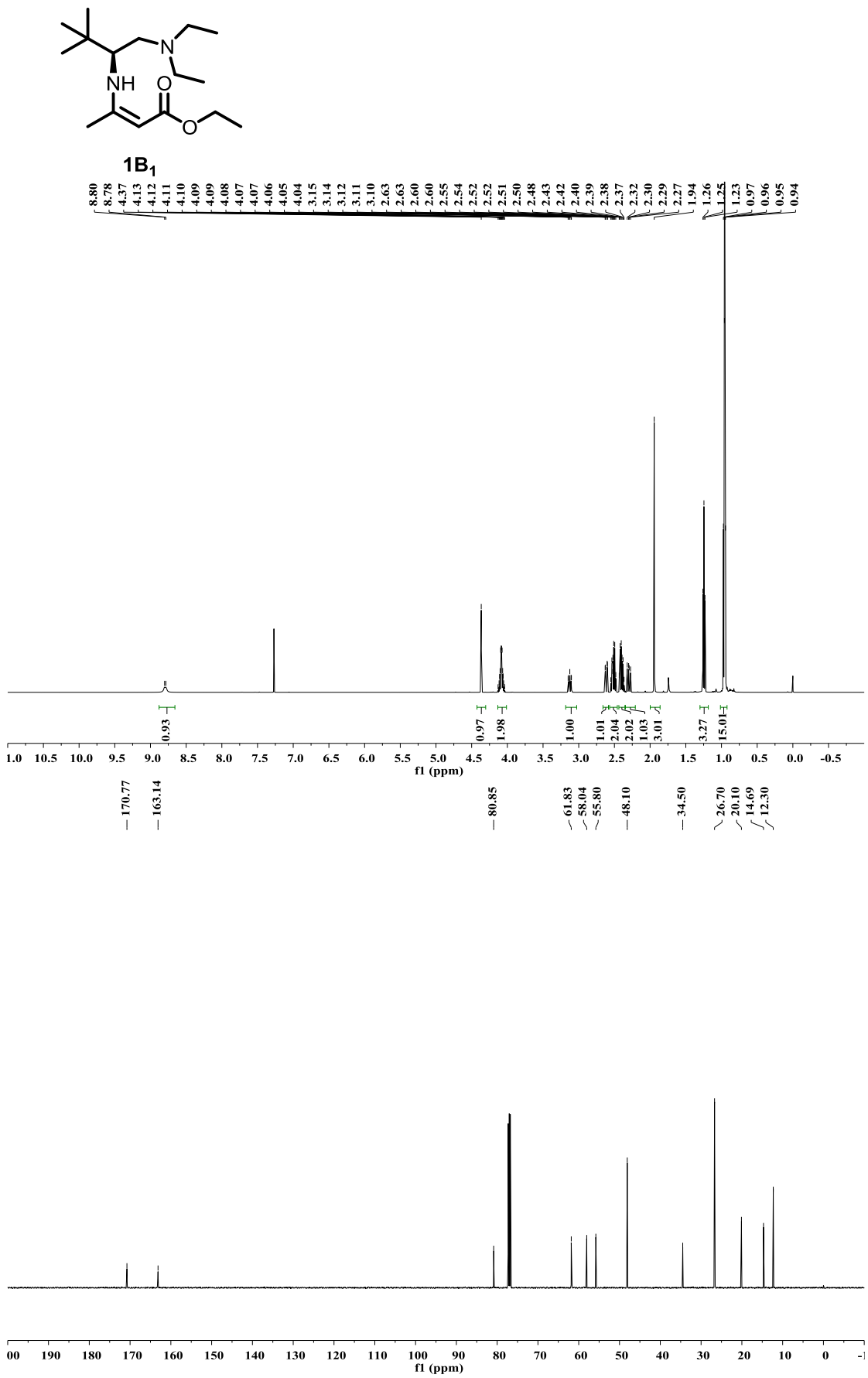
1A₄

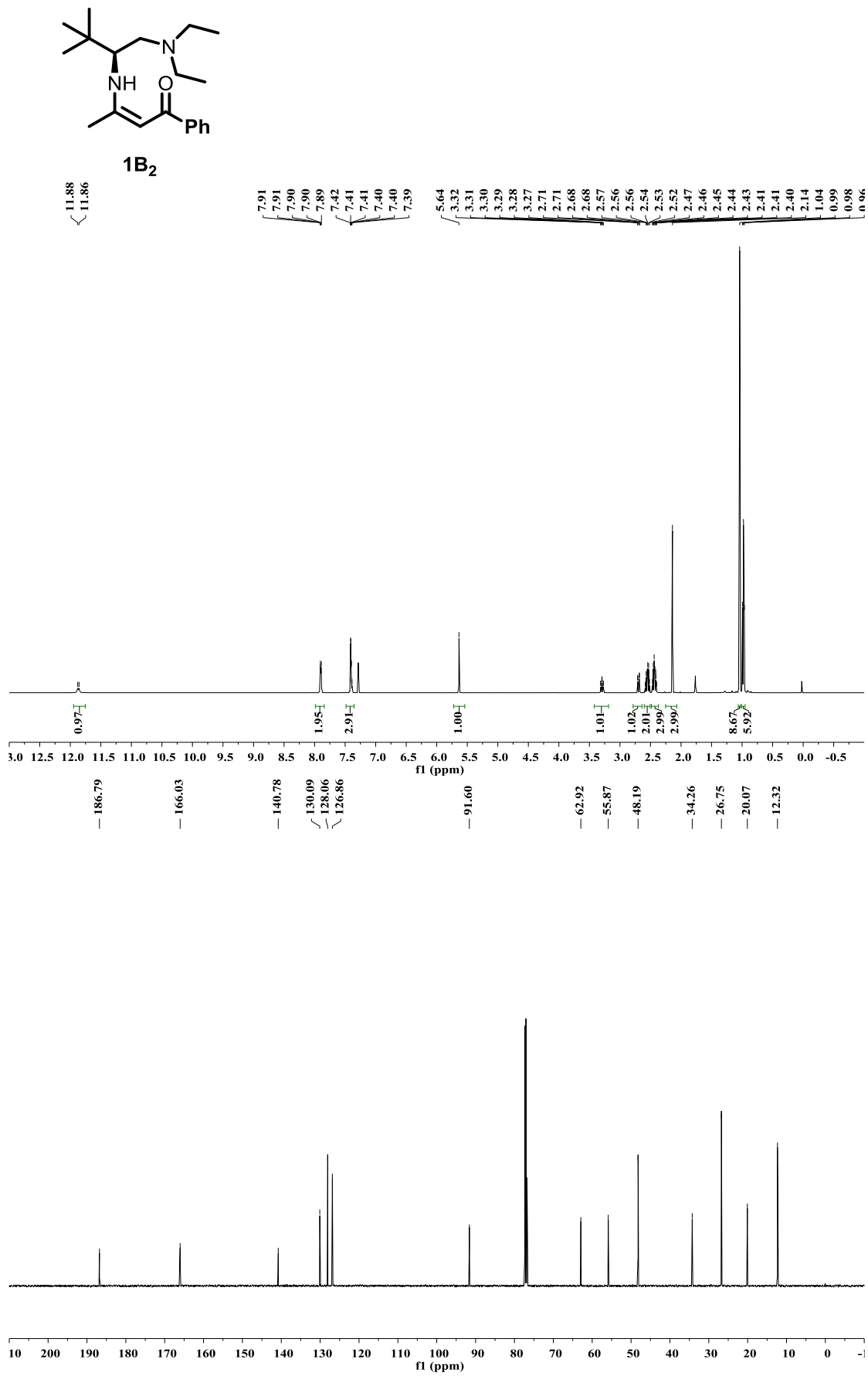


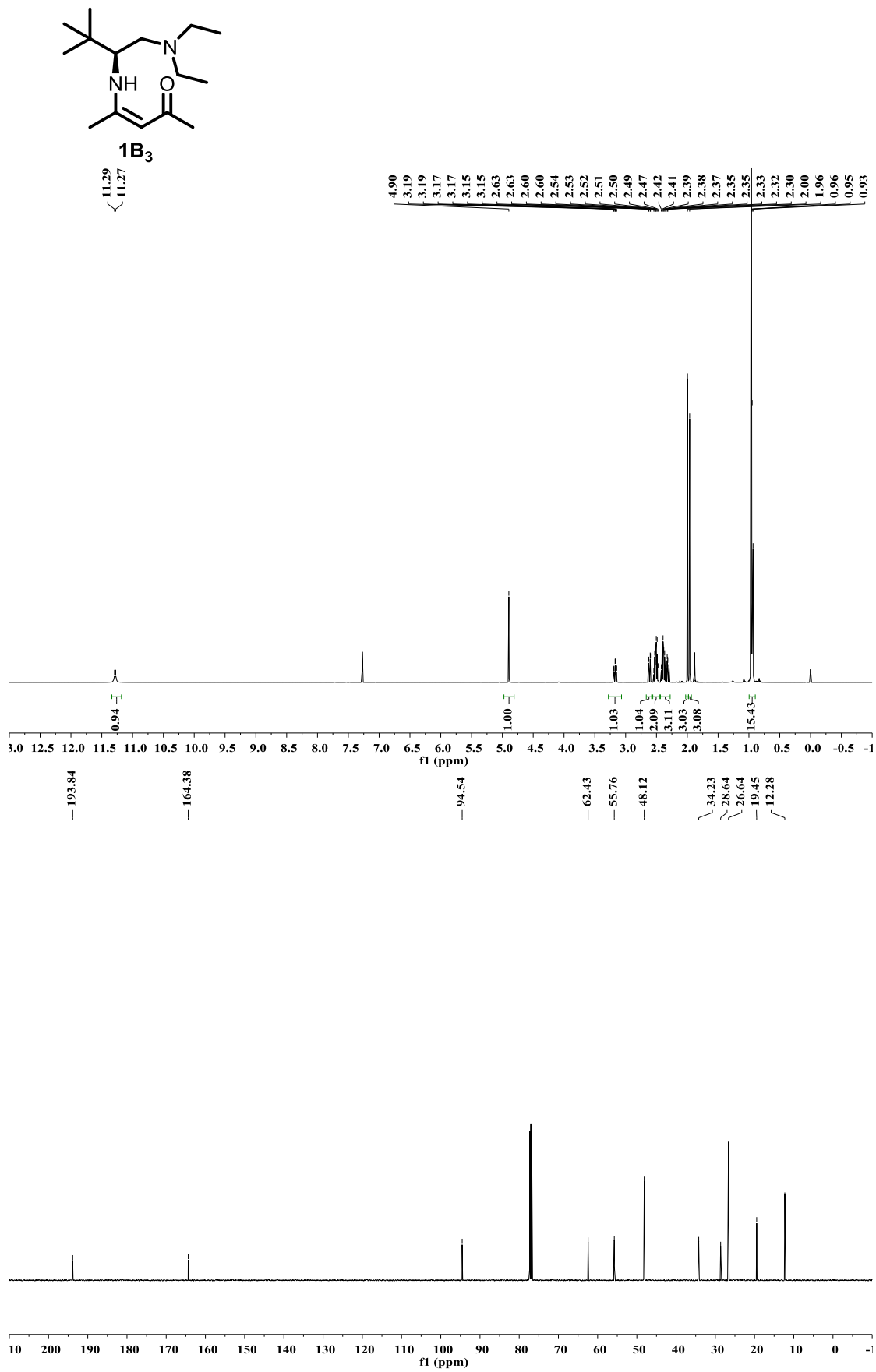


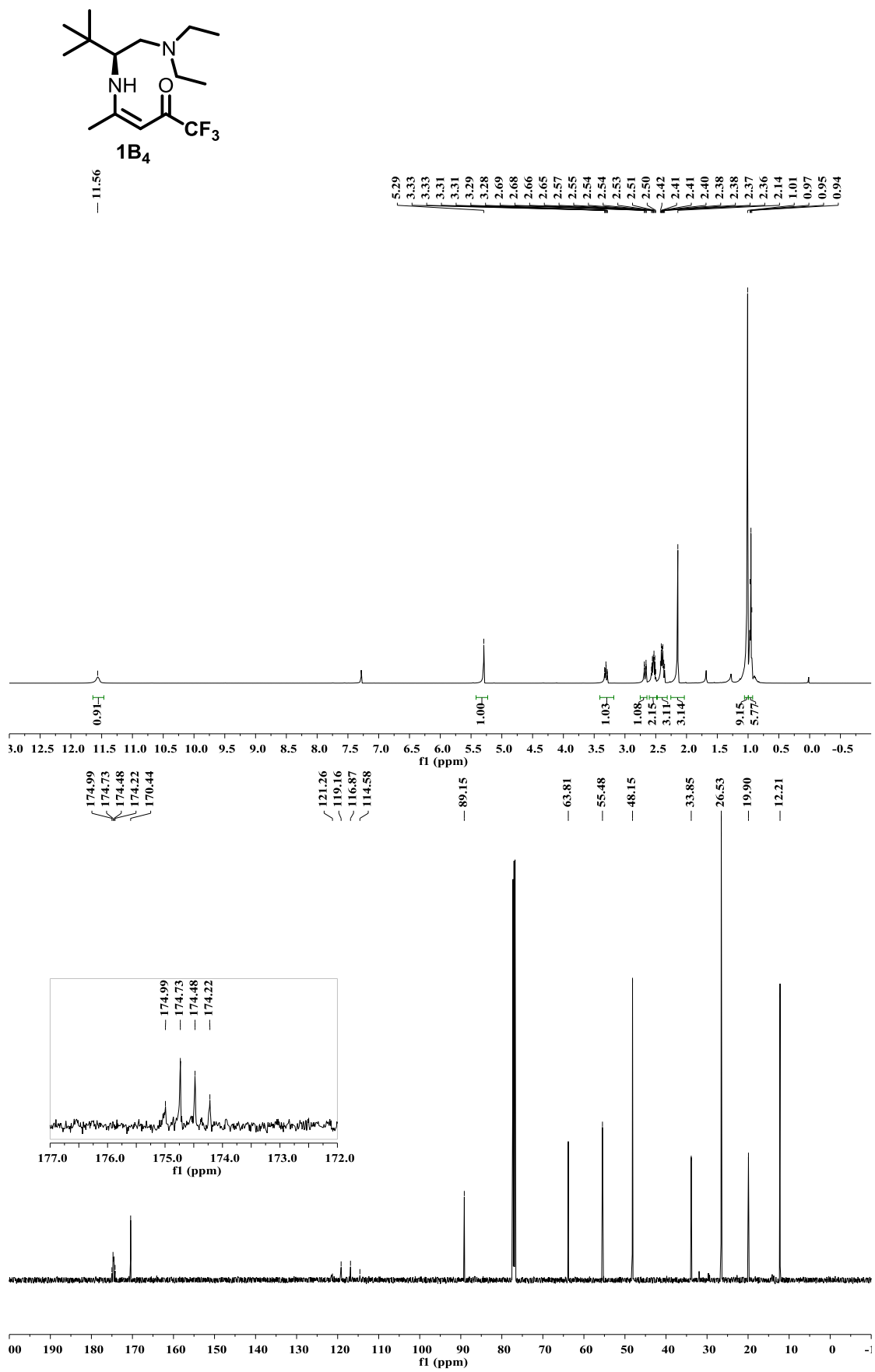
1A₅

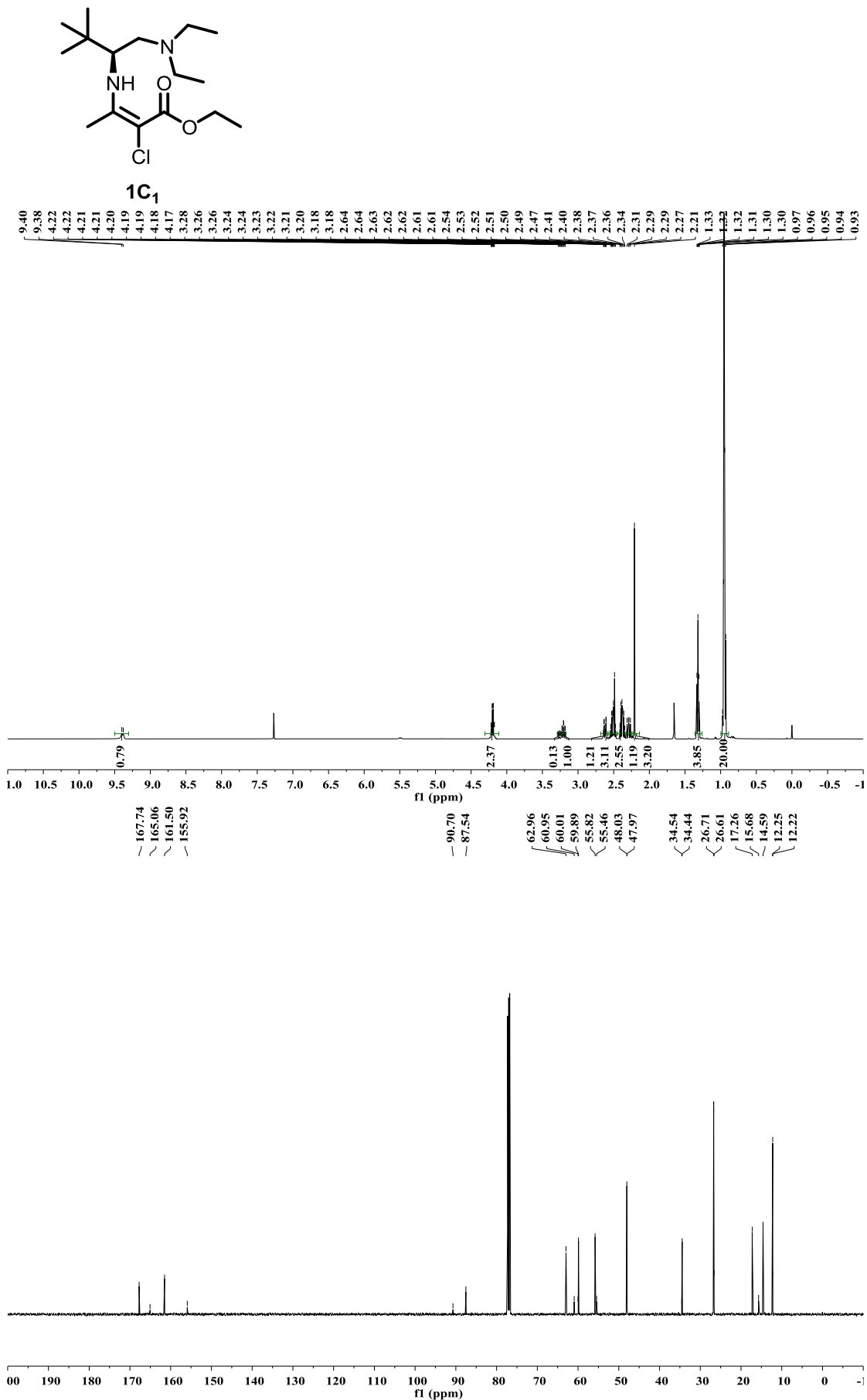


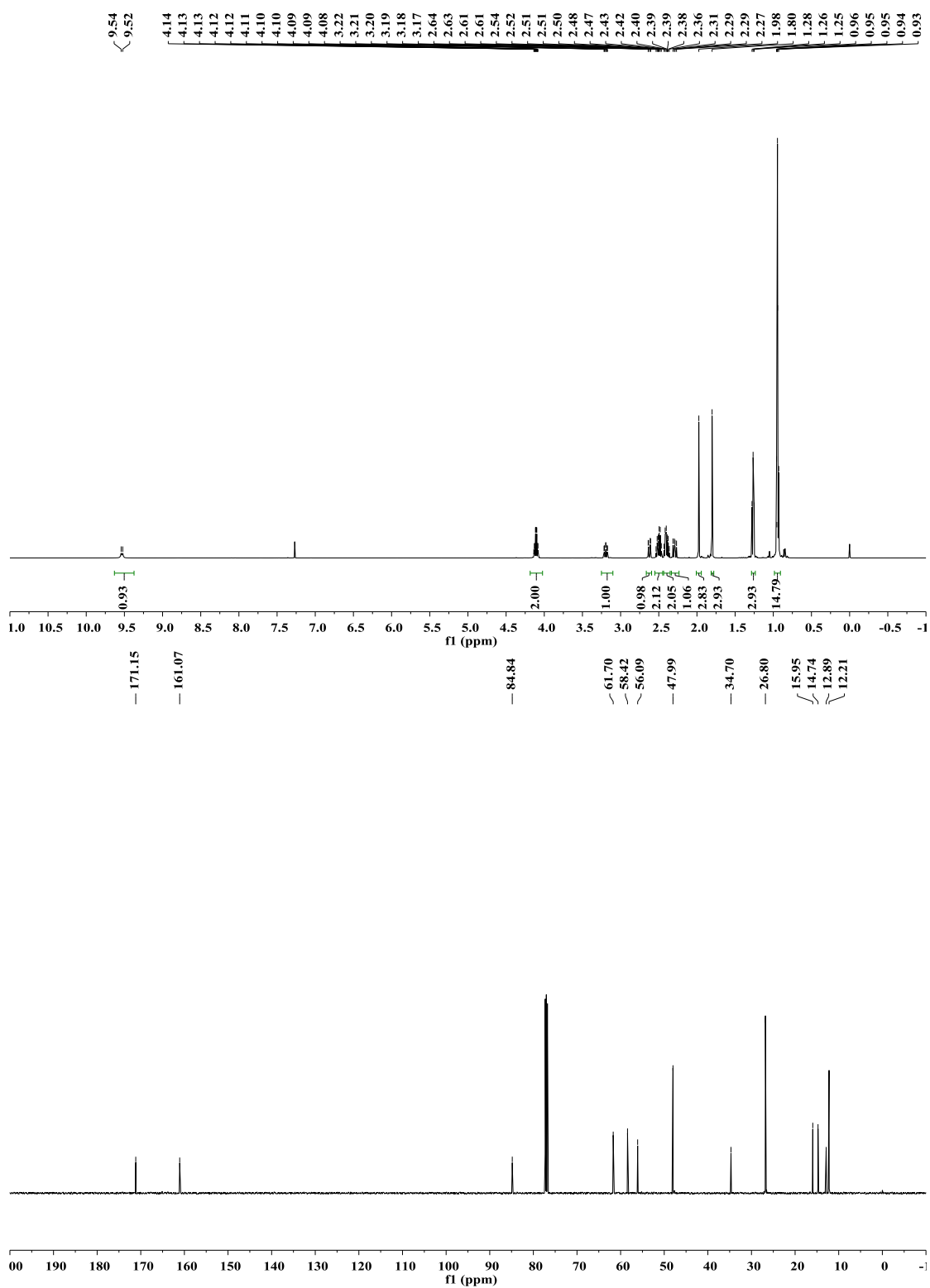
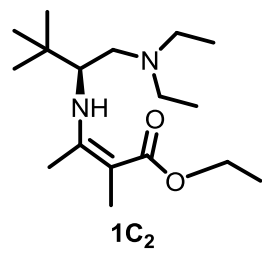


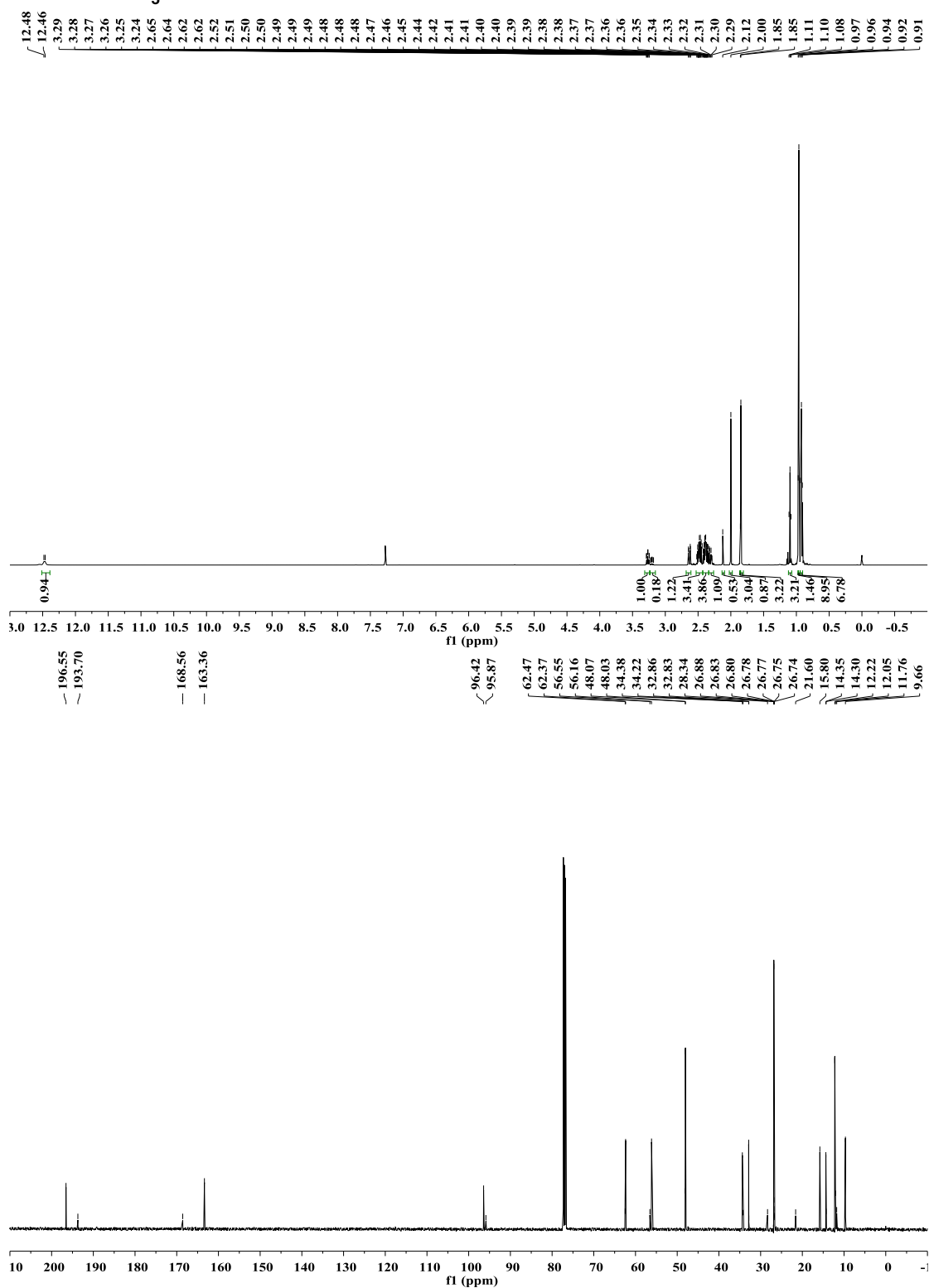
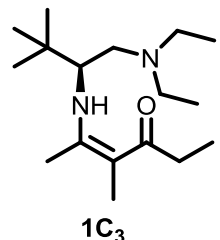


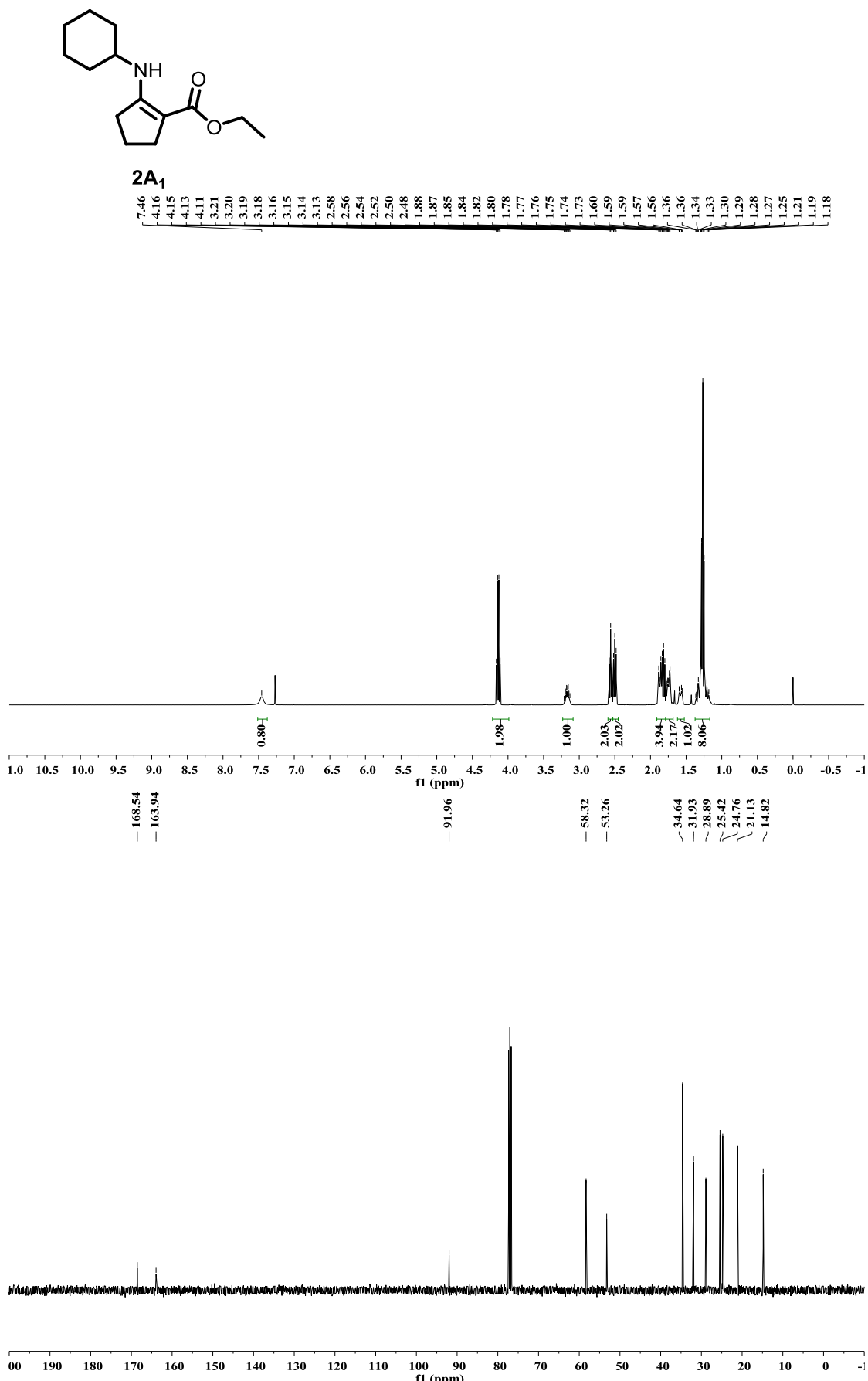


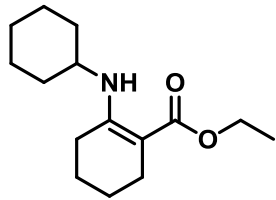




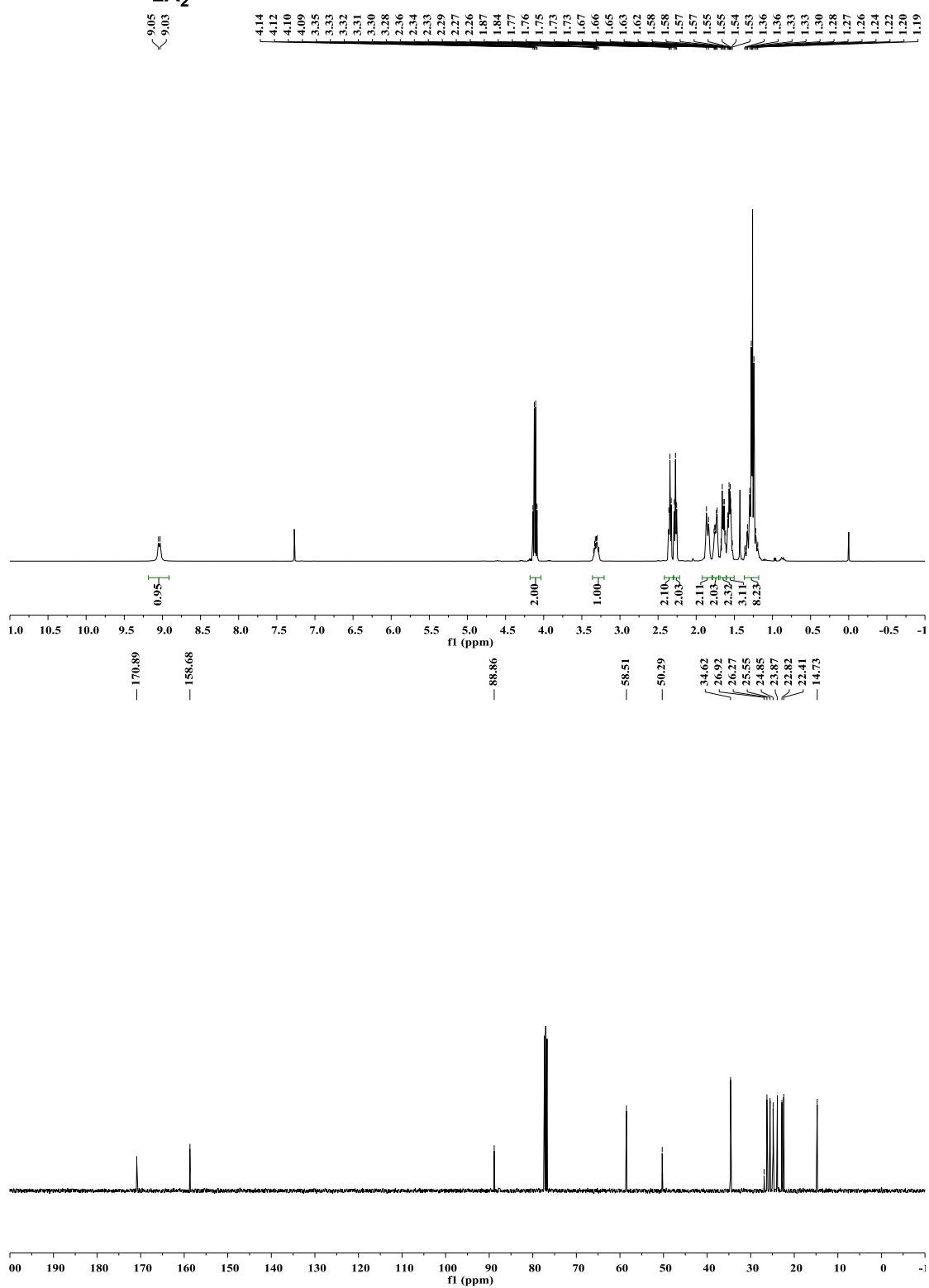


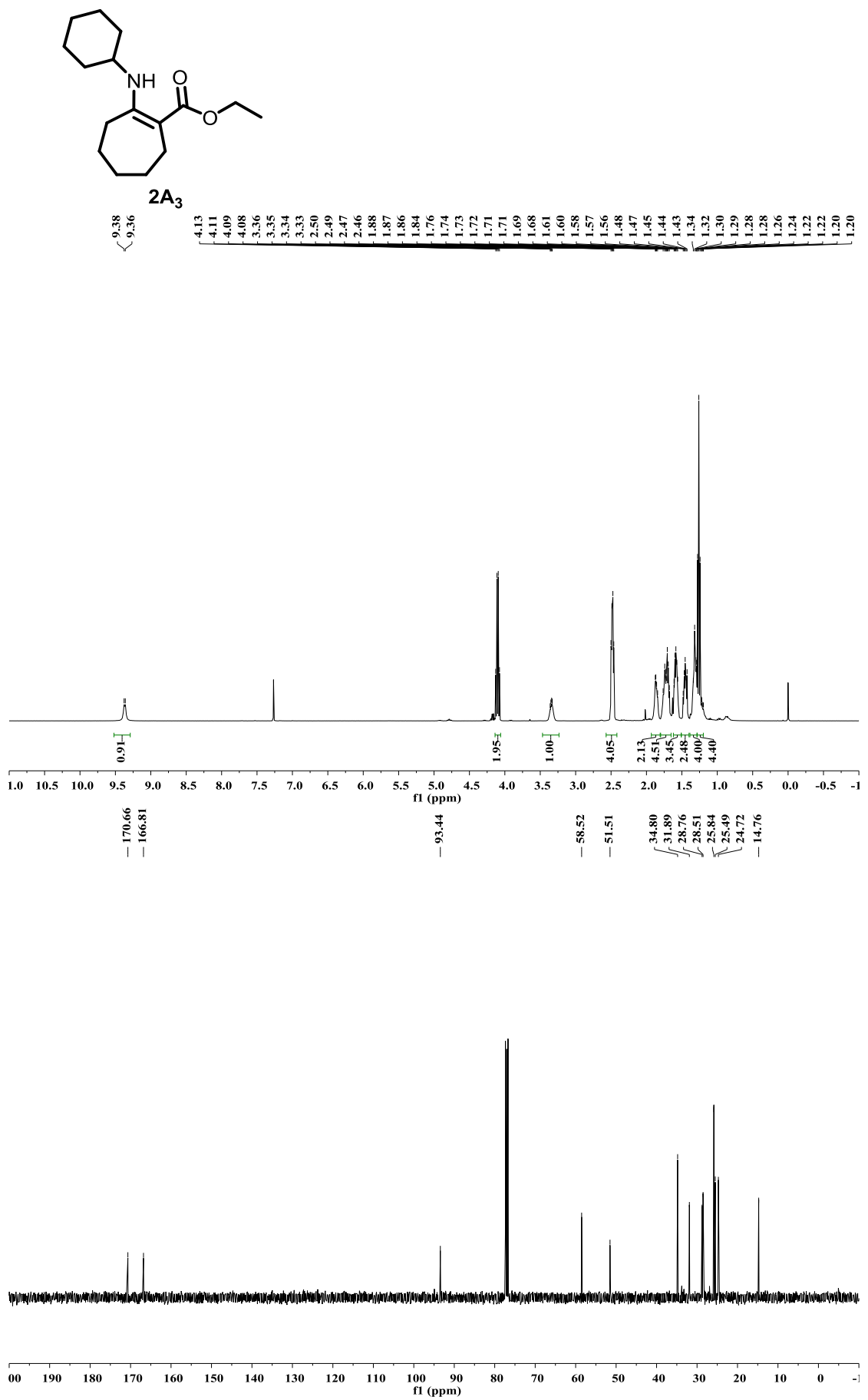


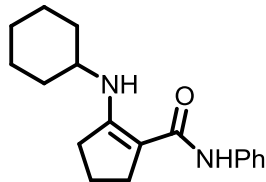




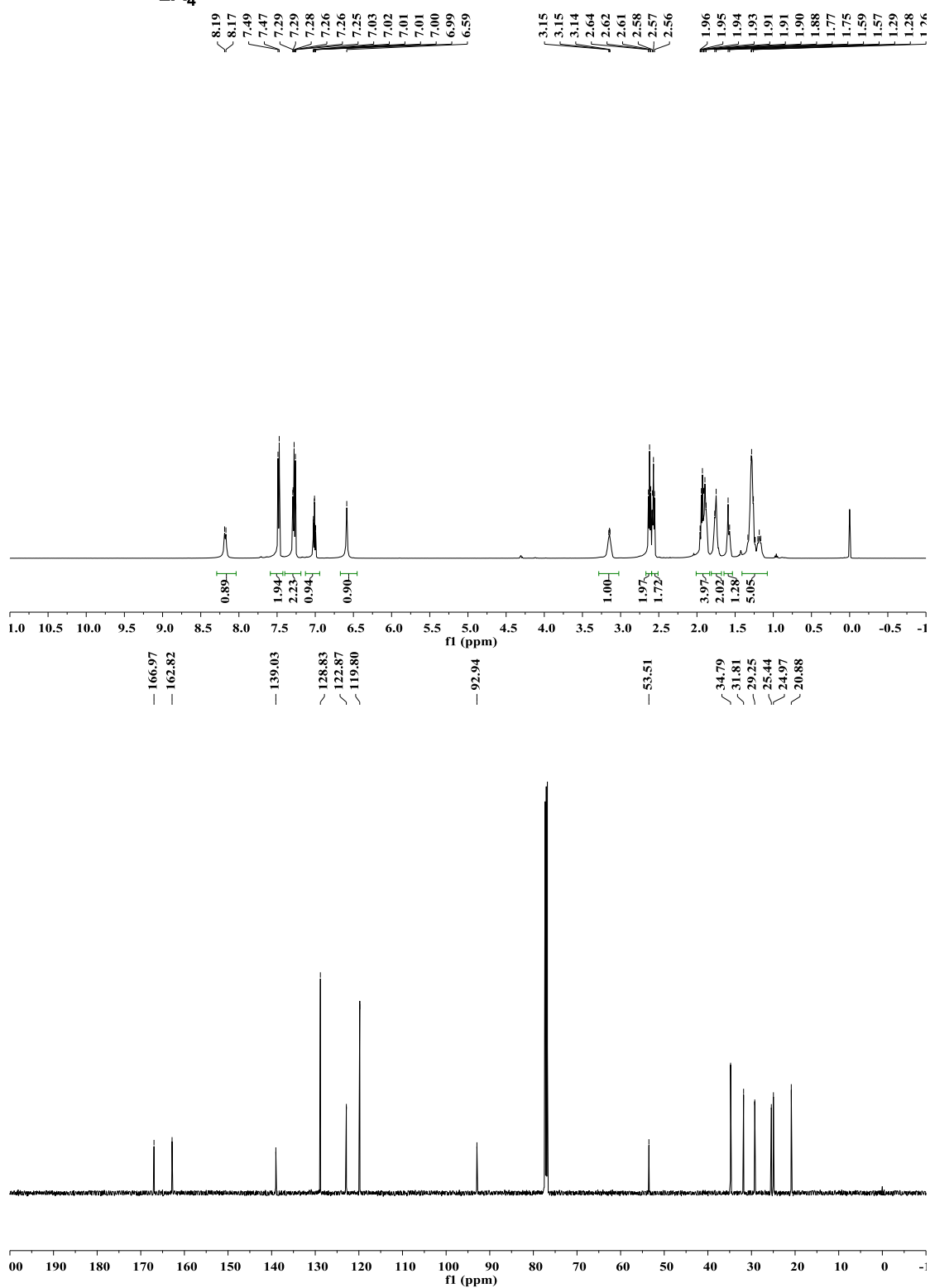
2A₂

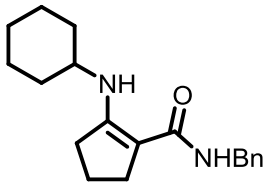




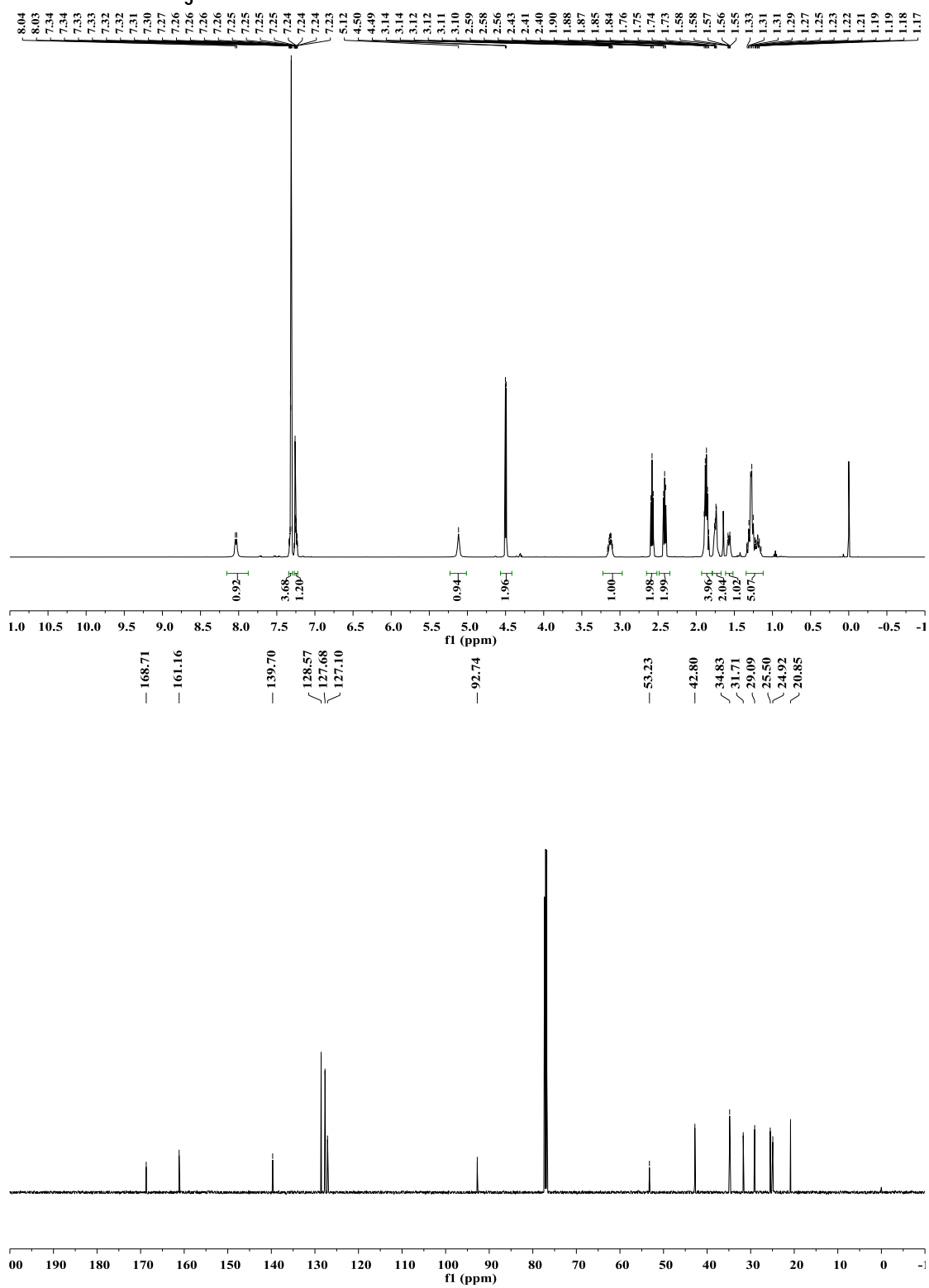


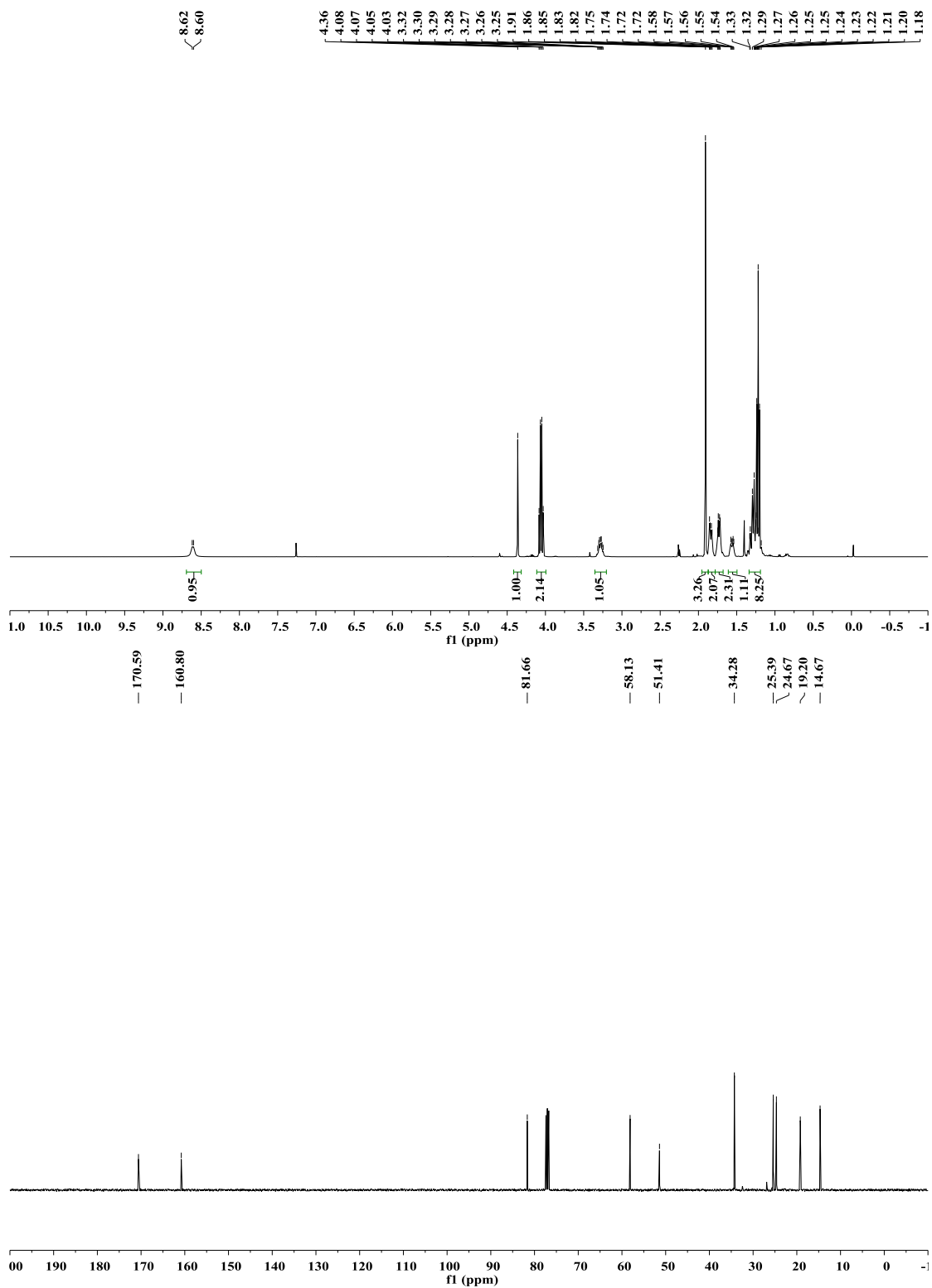
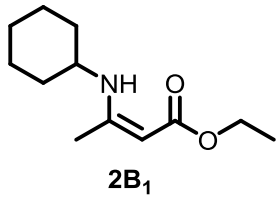
2A₄

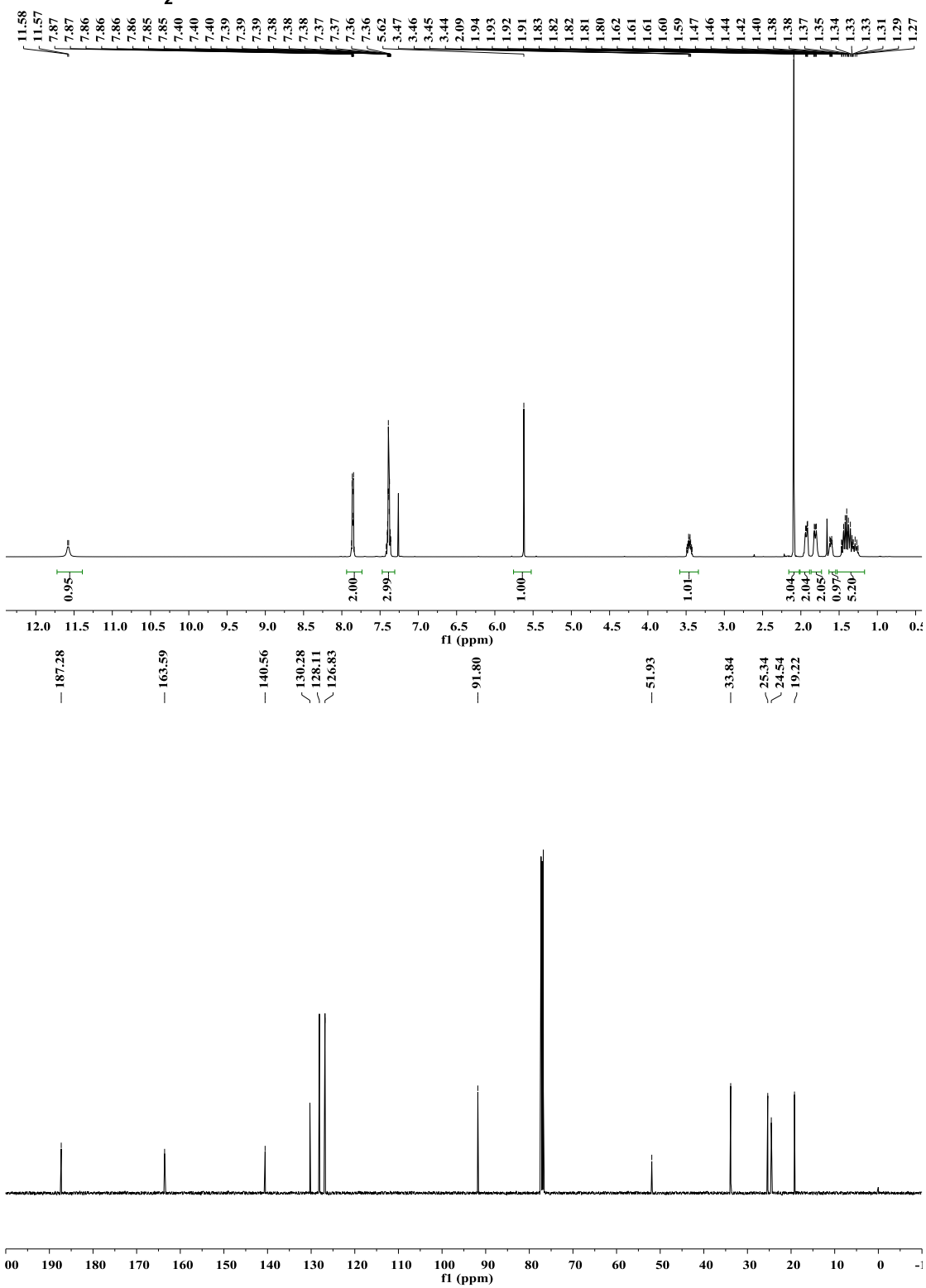
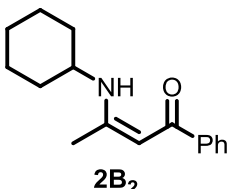


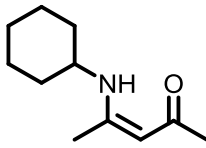


2A₅

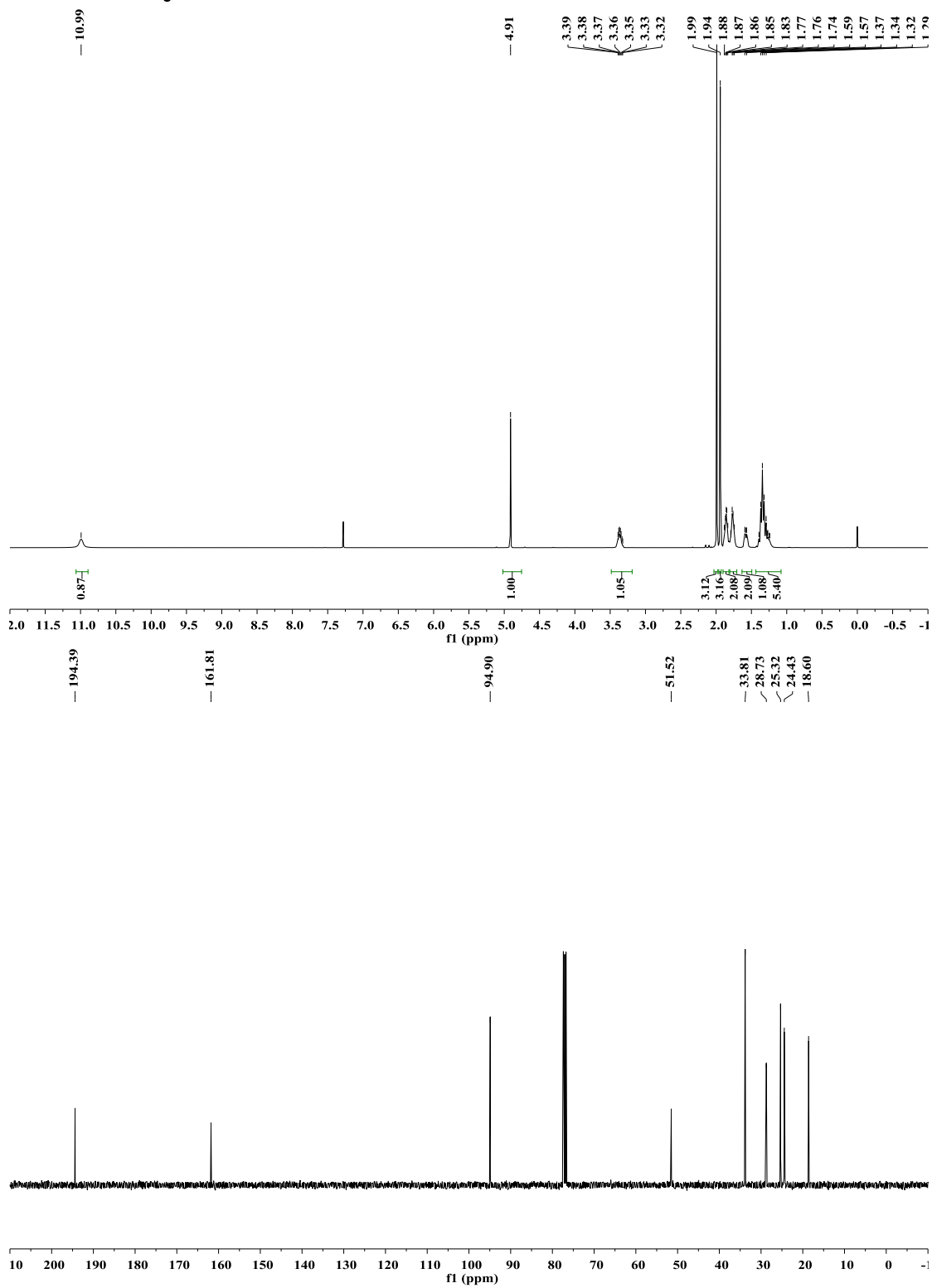


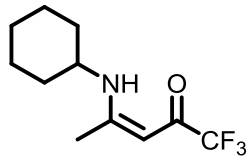




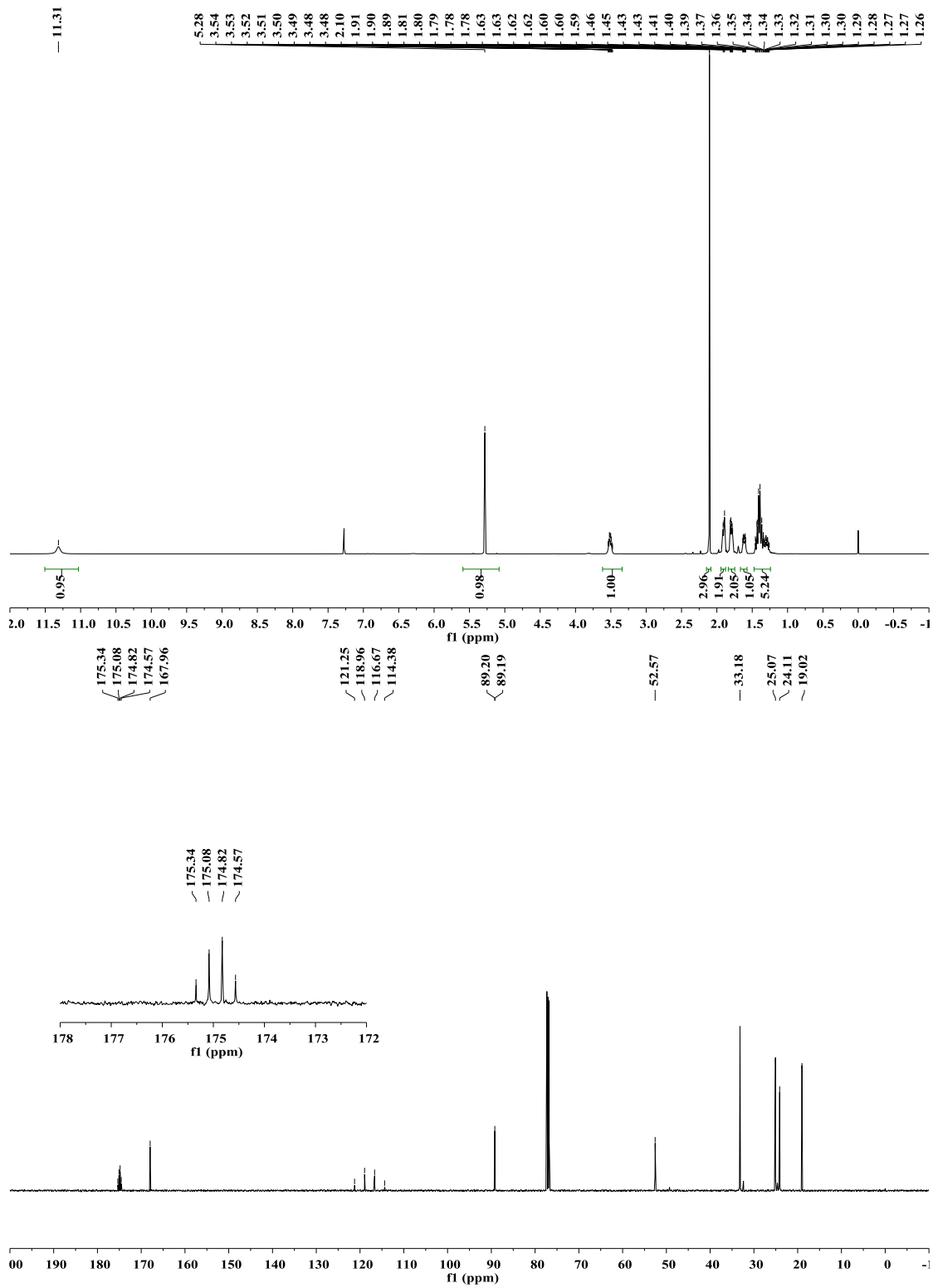


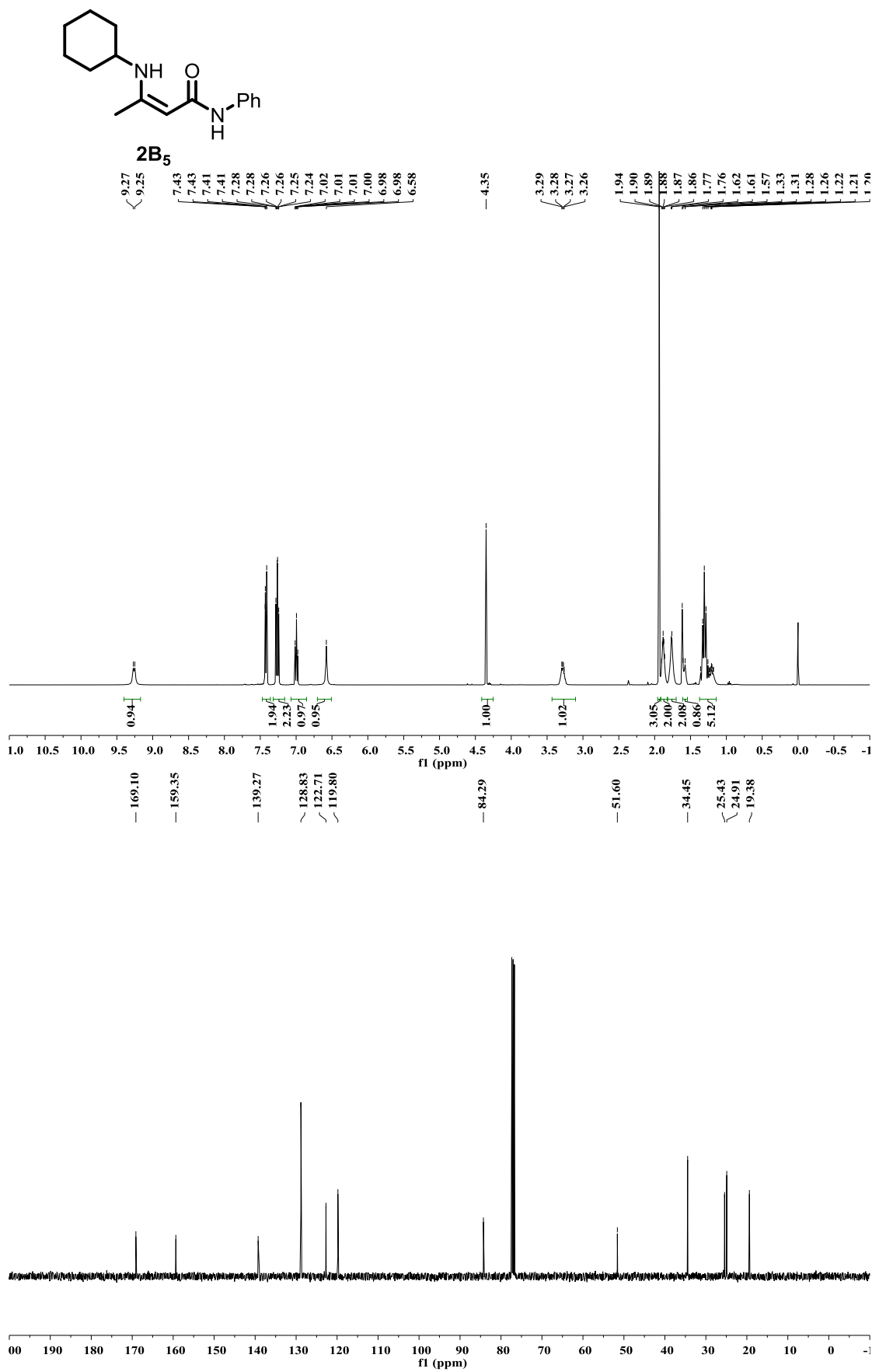
2B₃

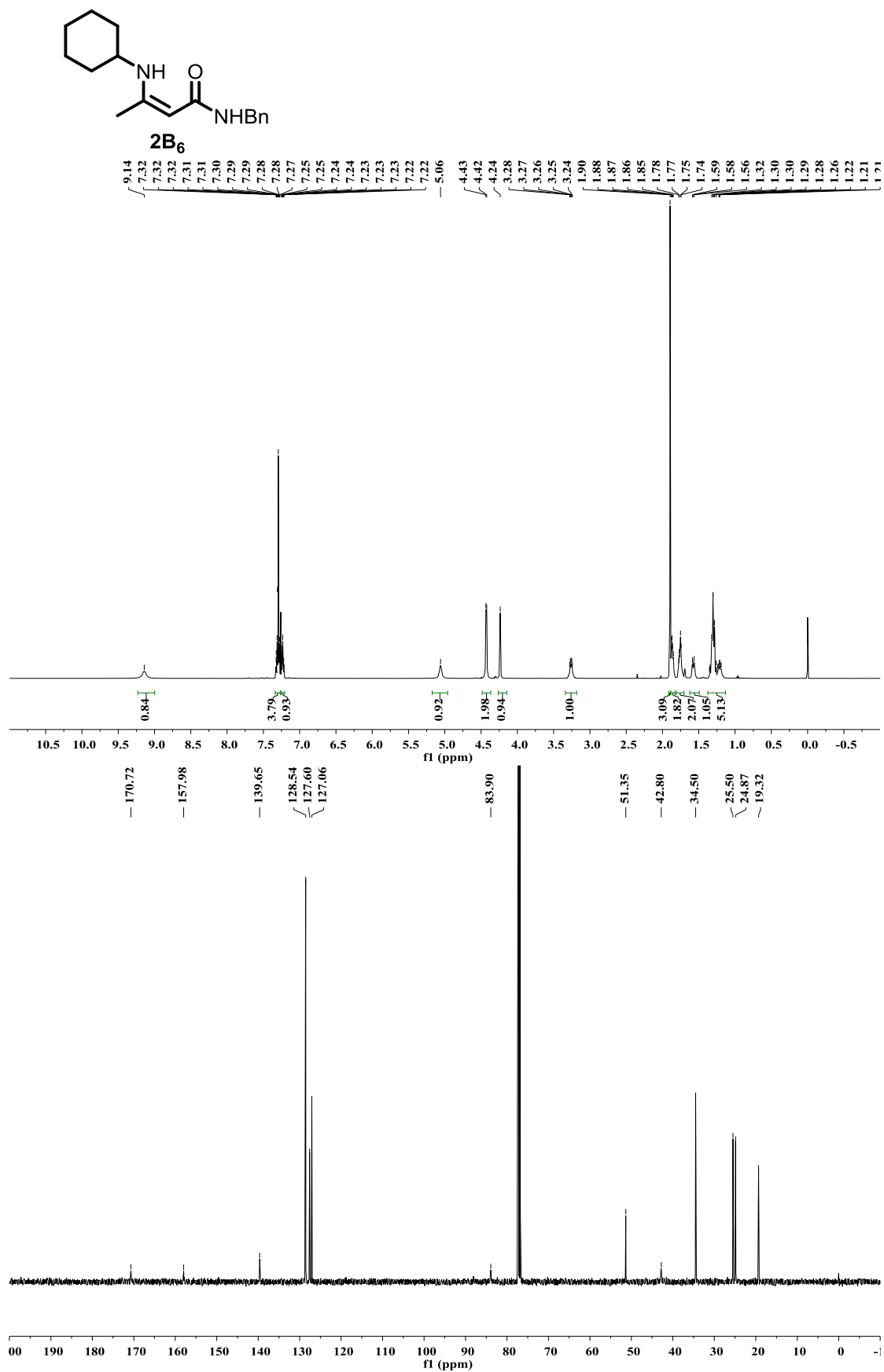


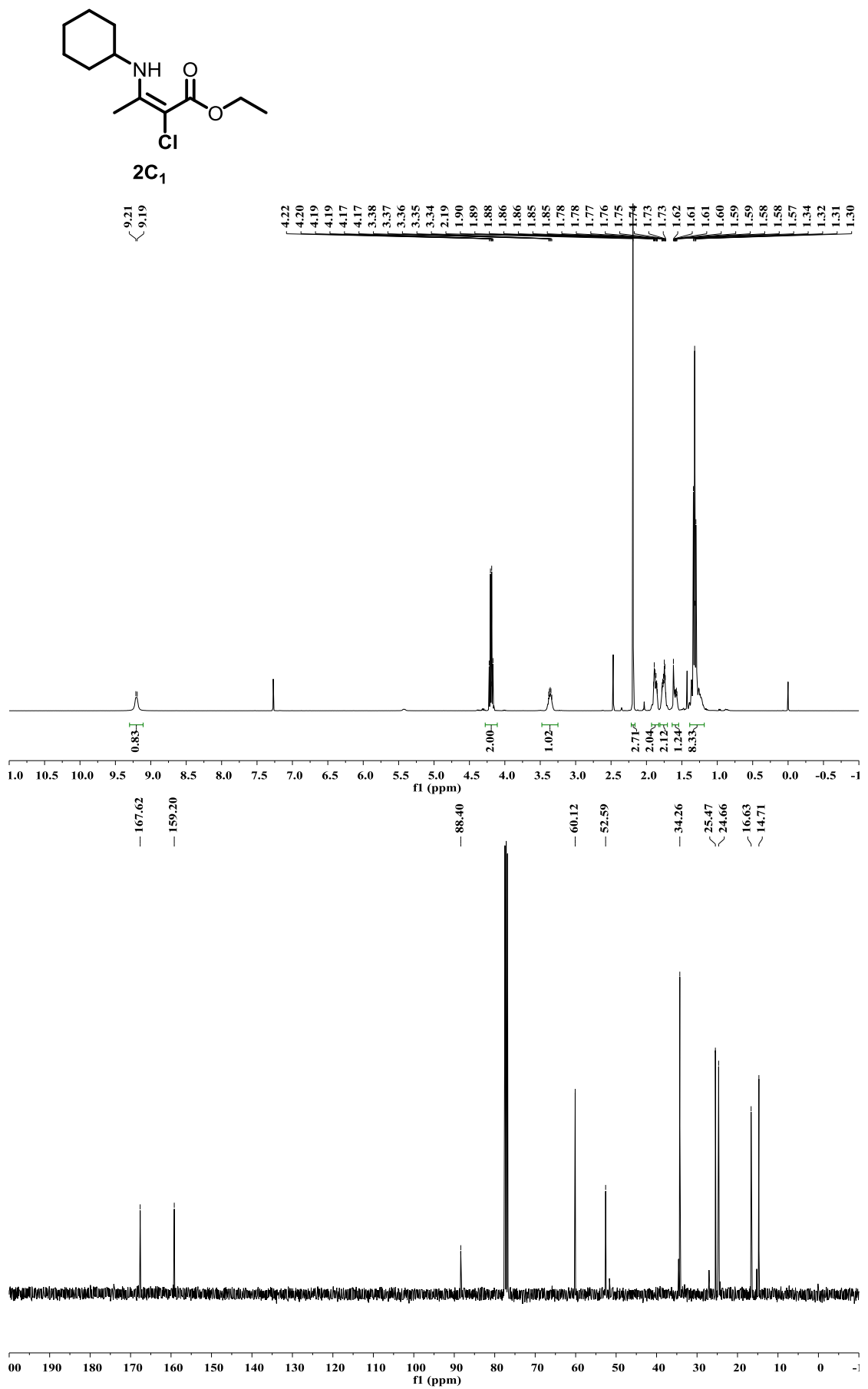


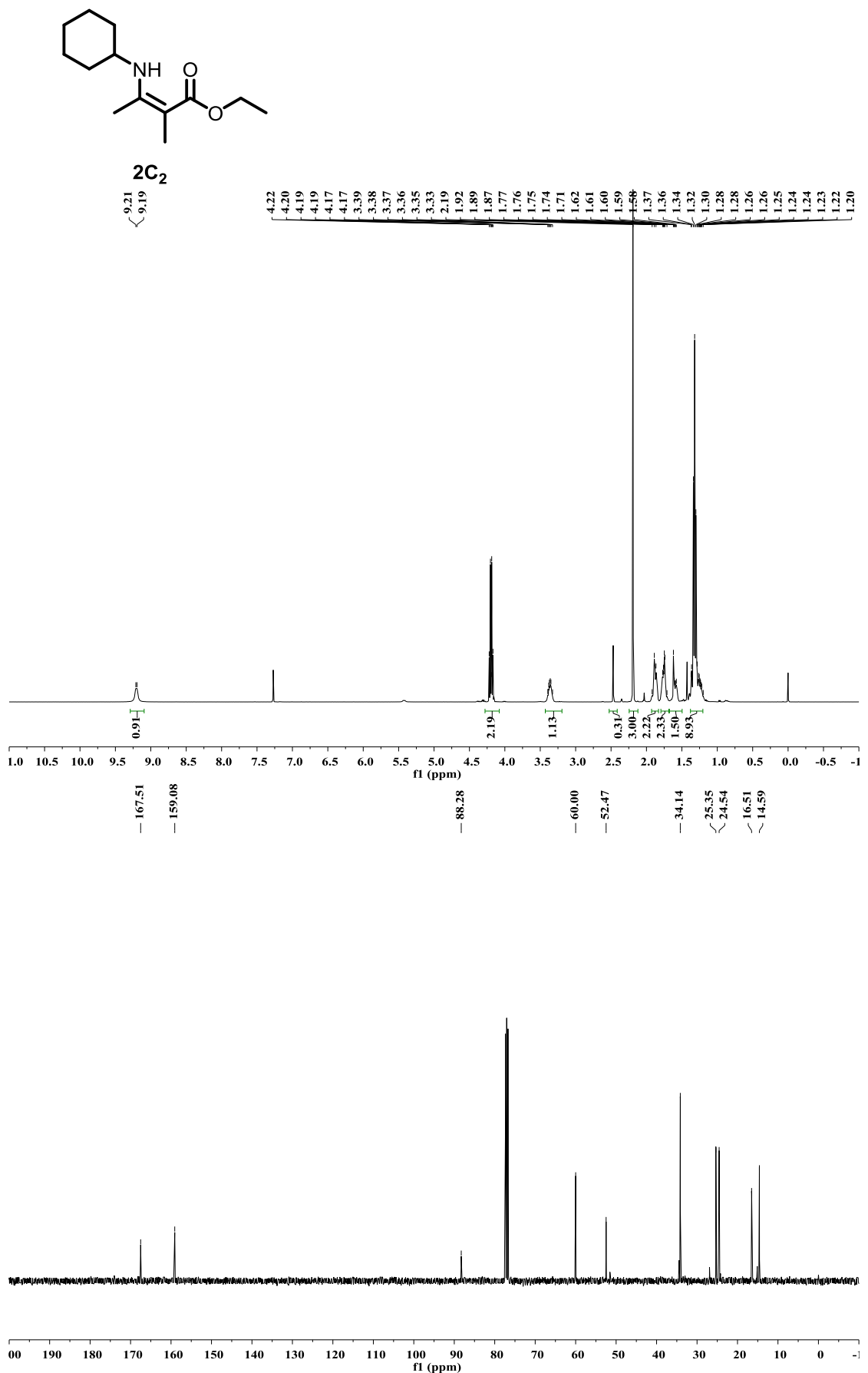
2B₄

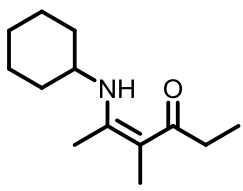




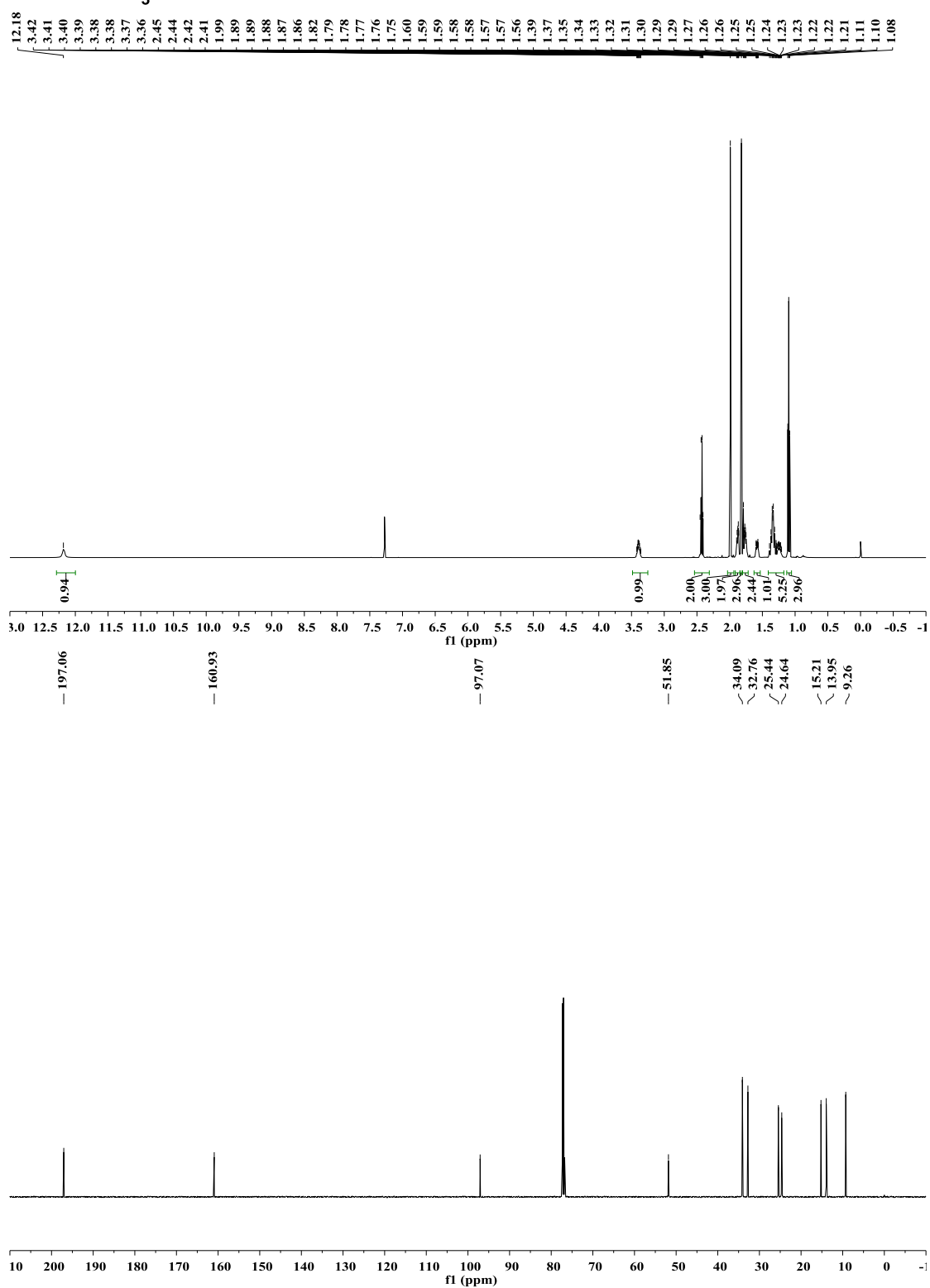


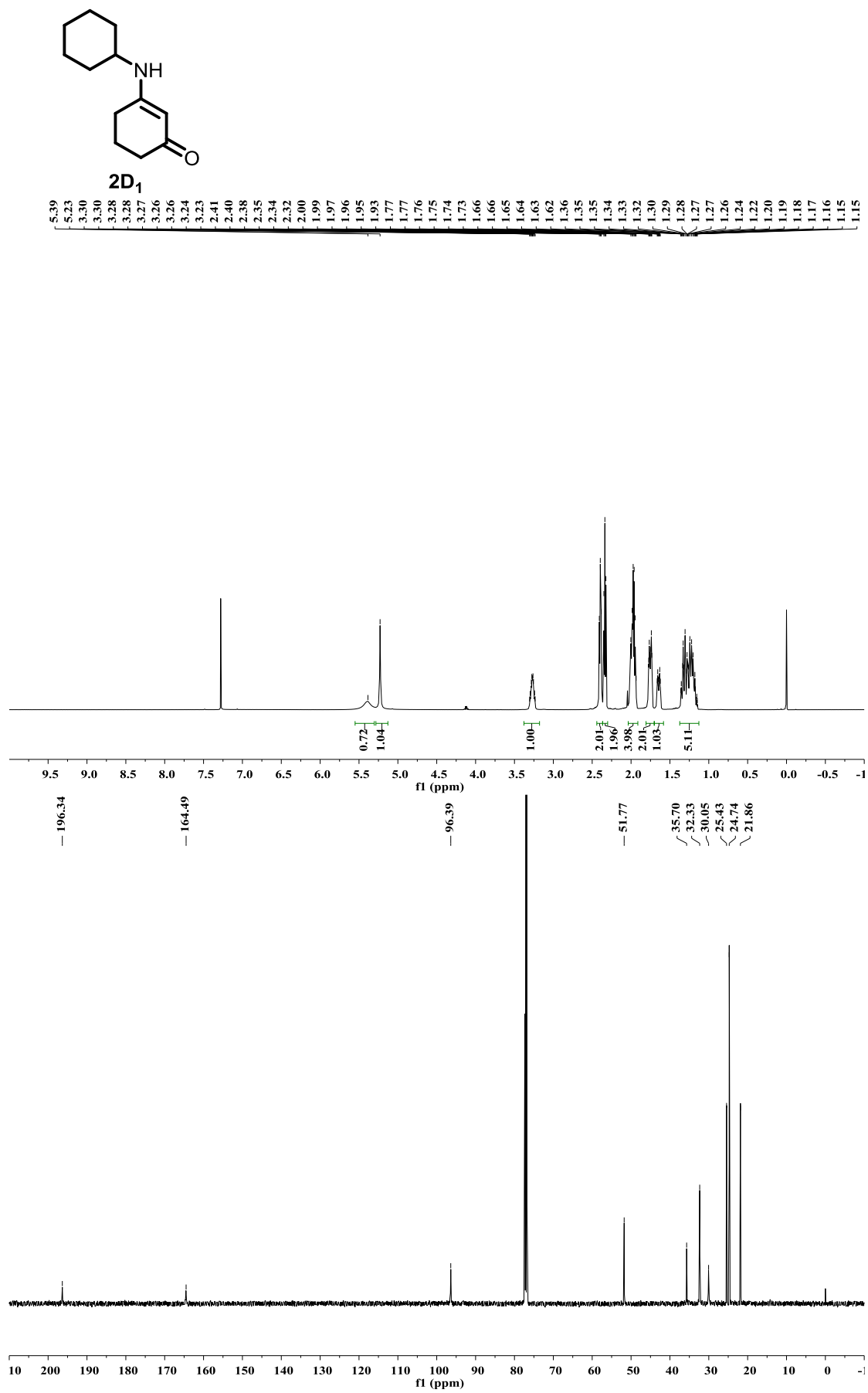


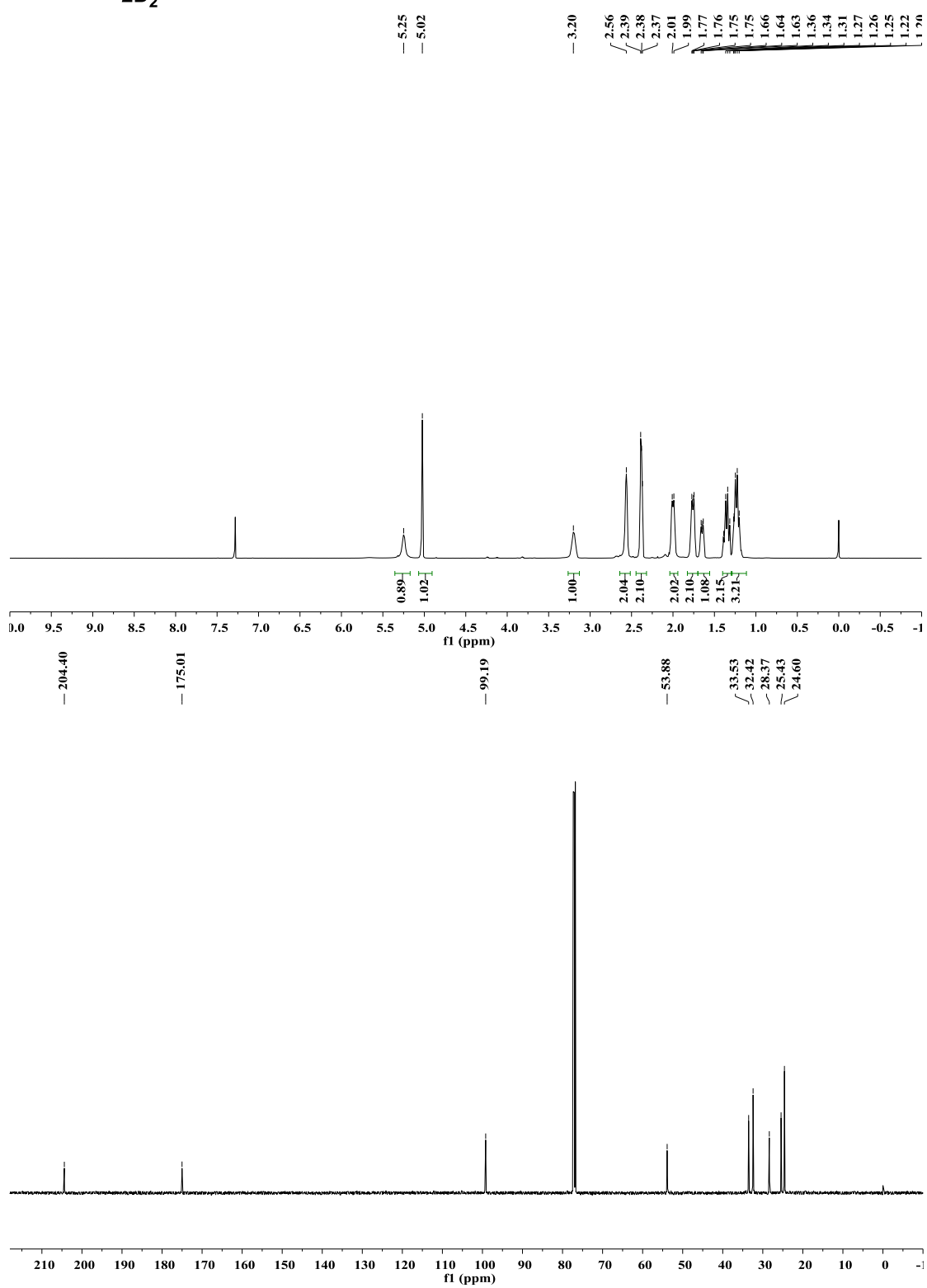
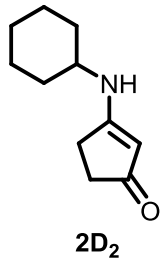


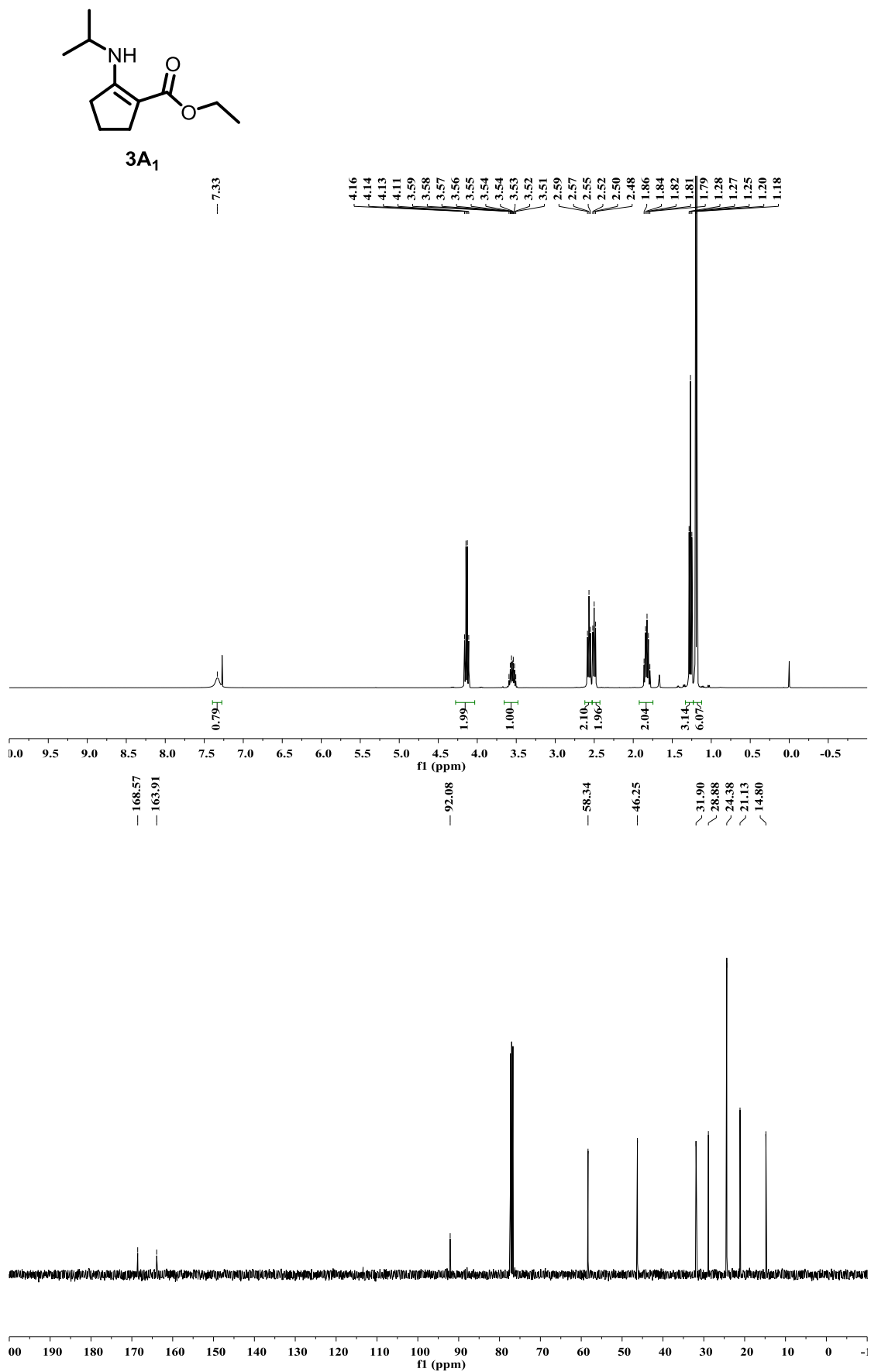


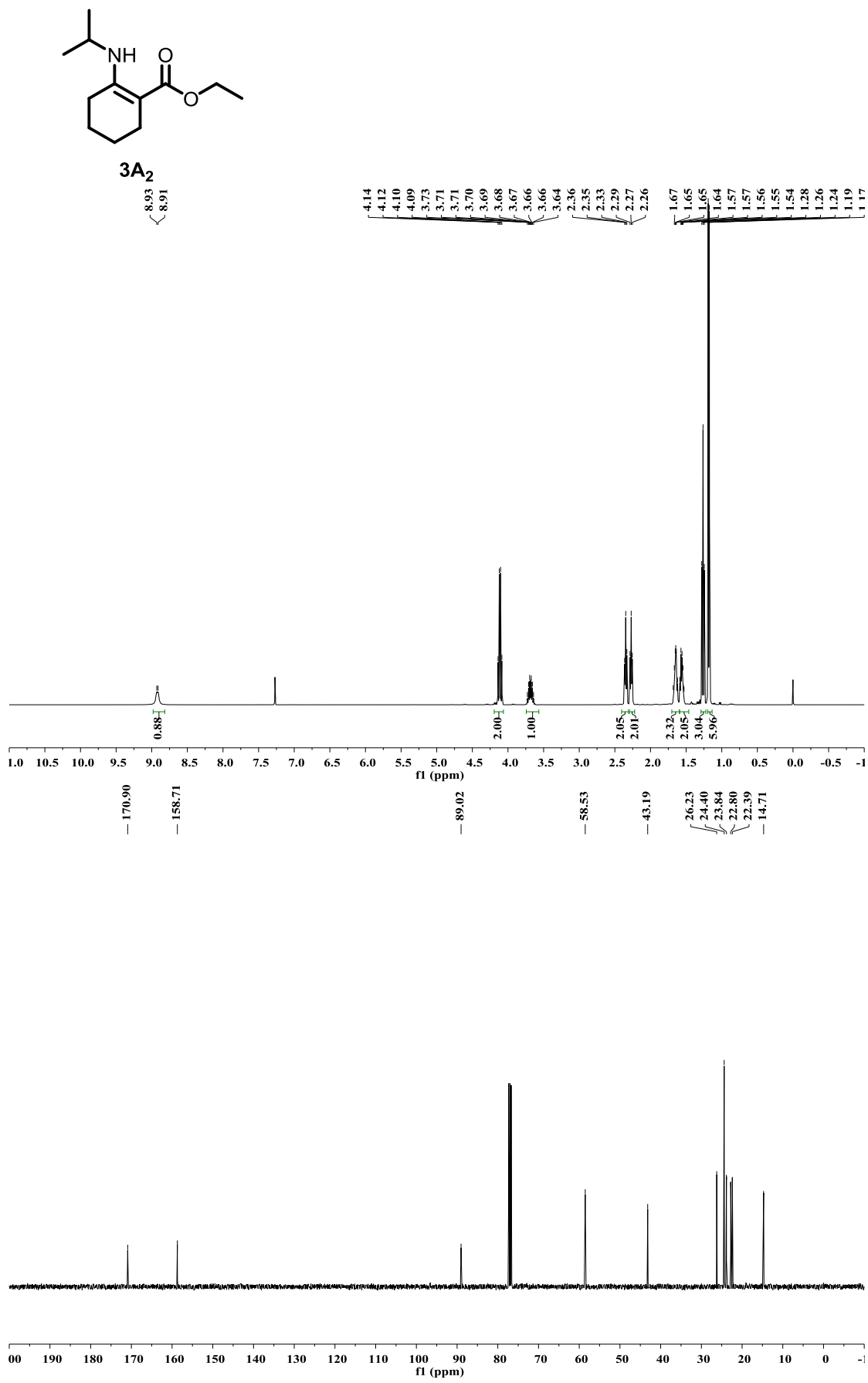
2C₃

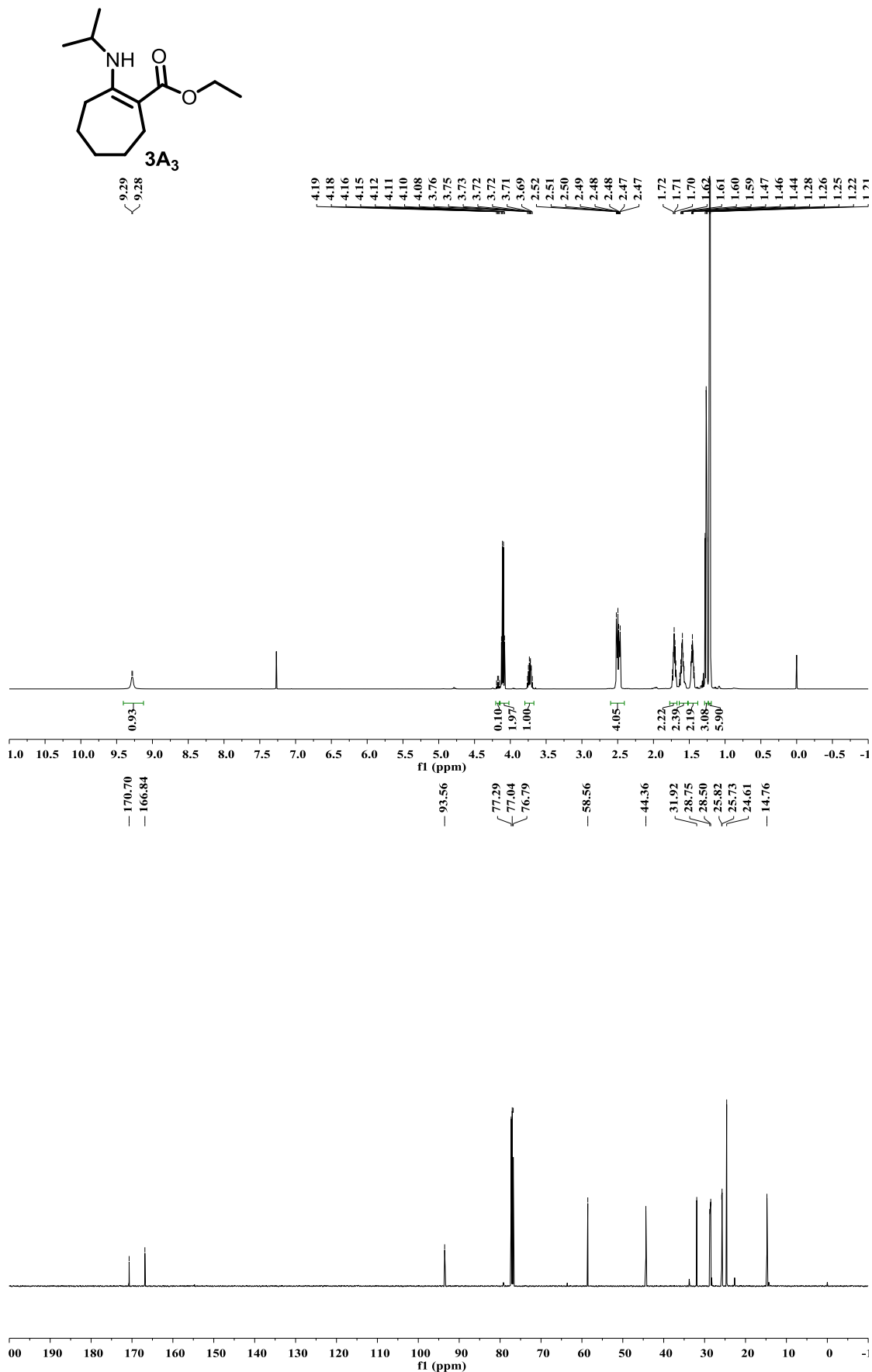


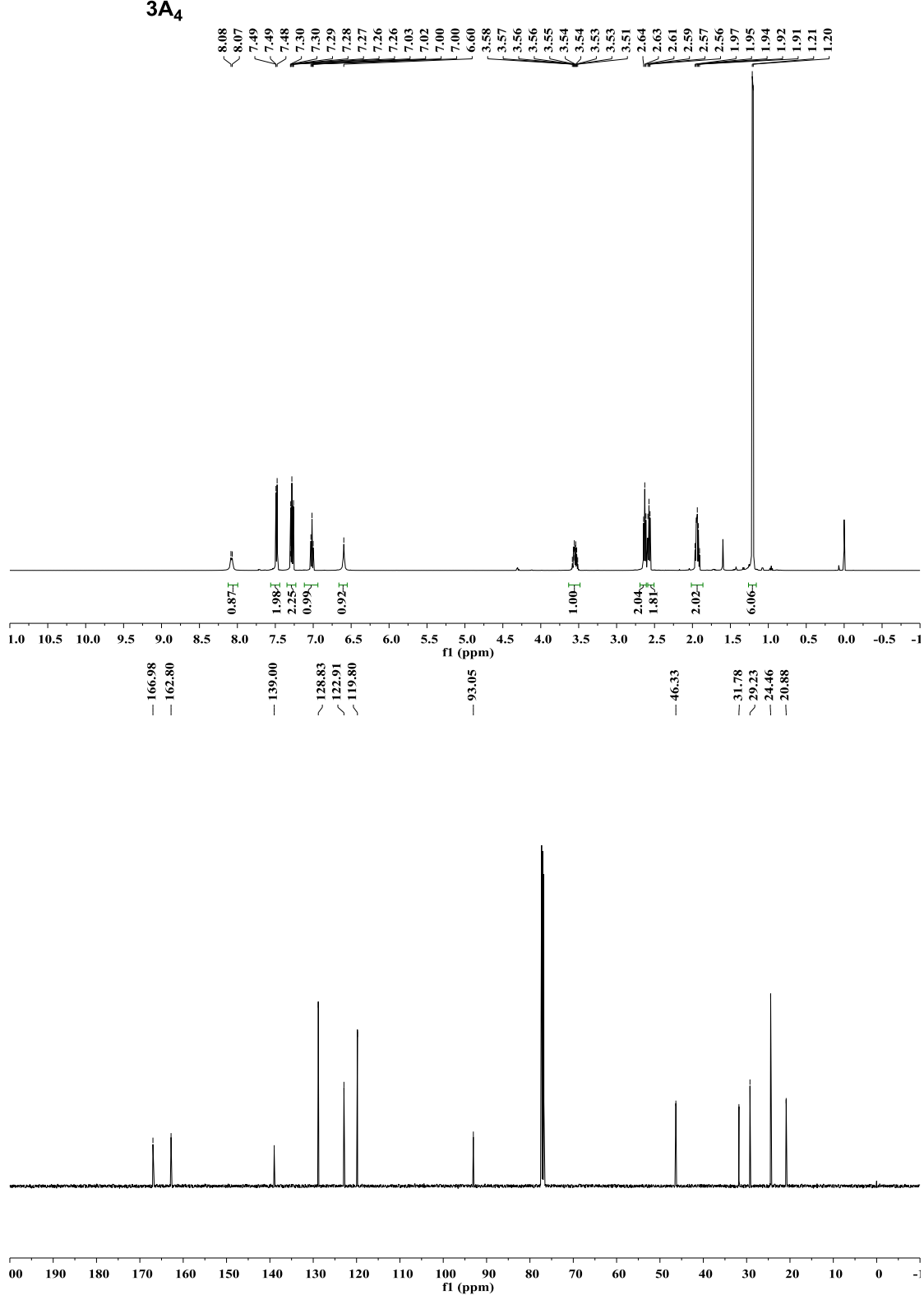
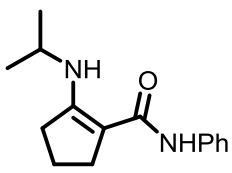


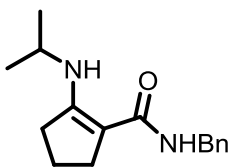




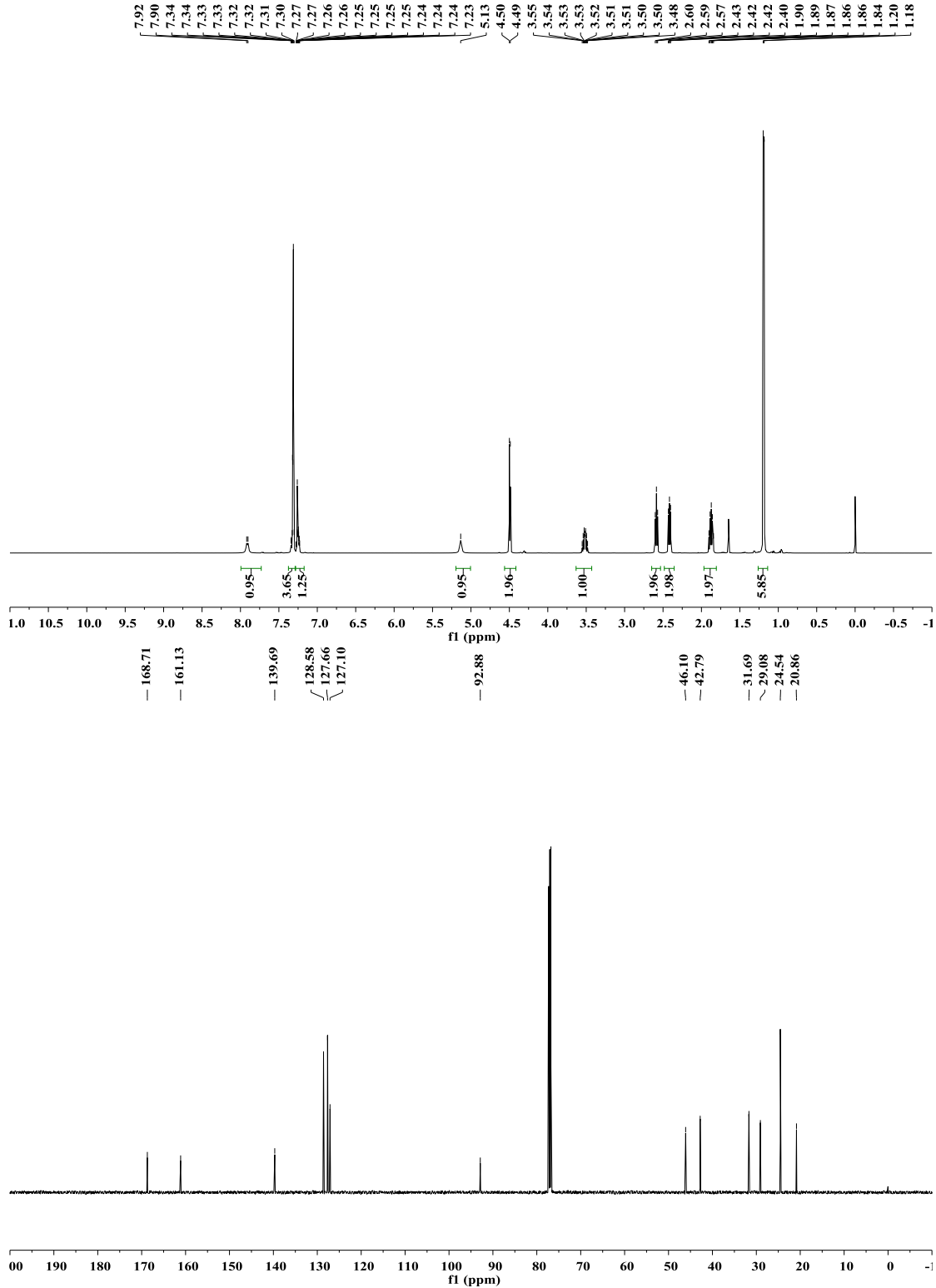


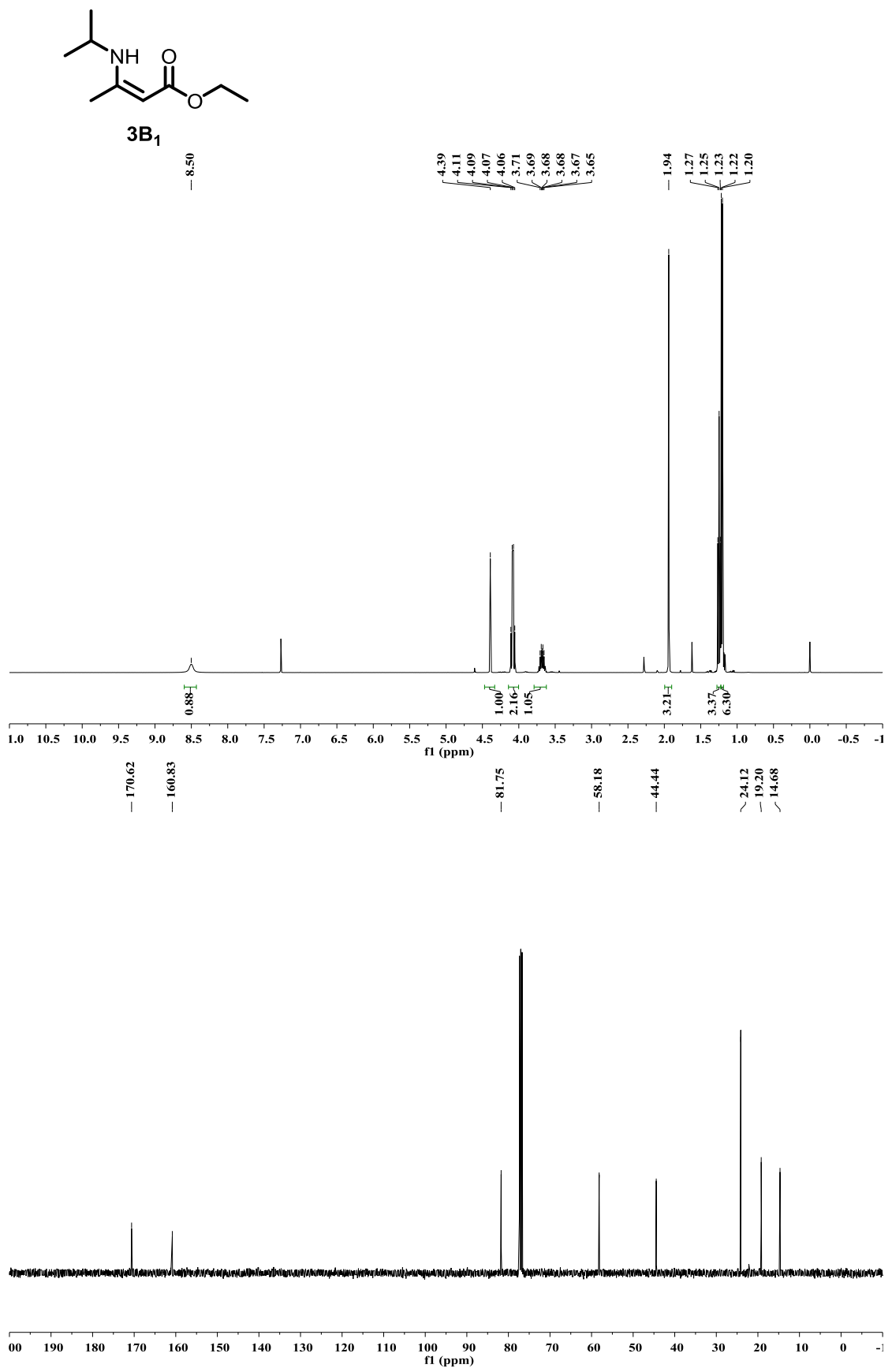


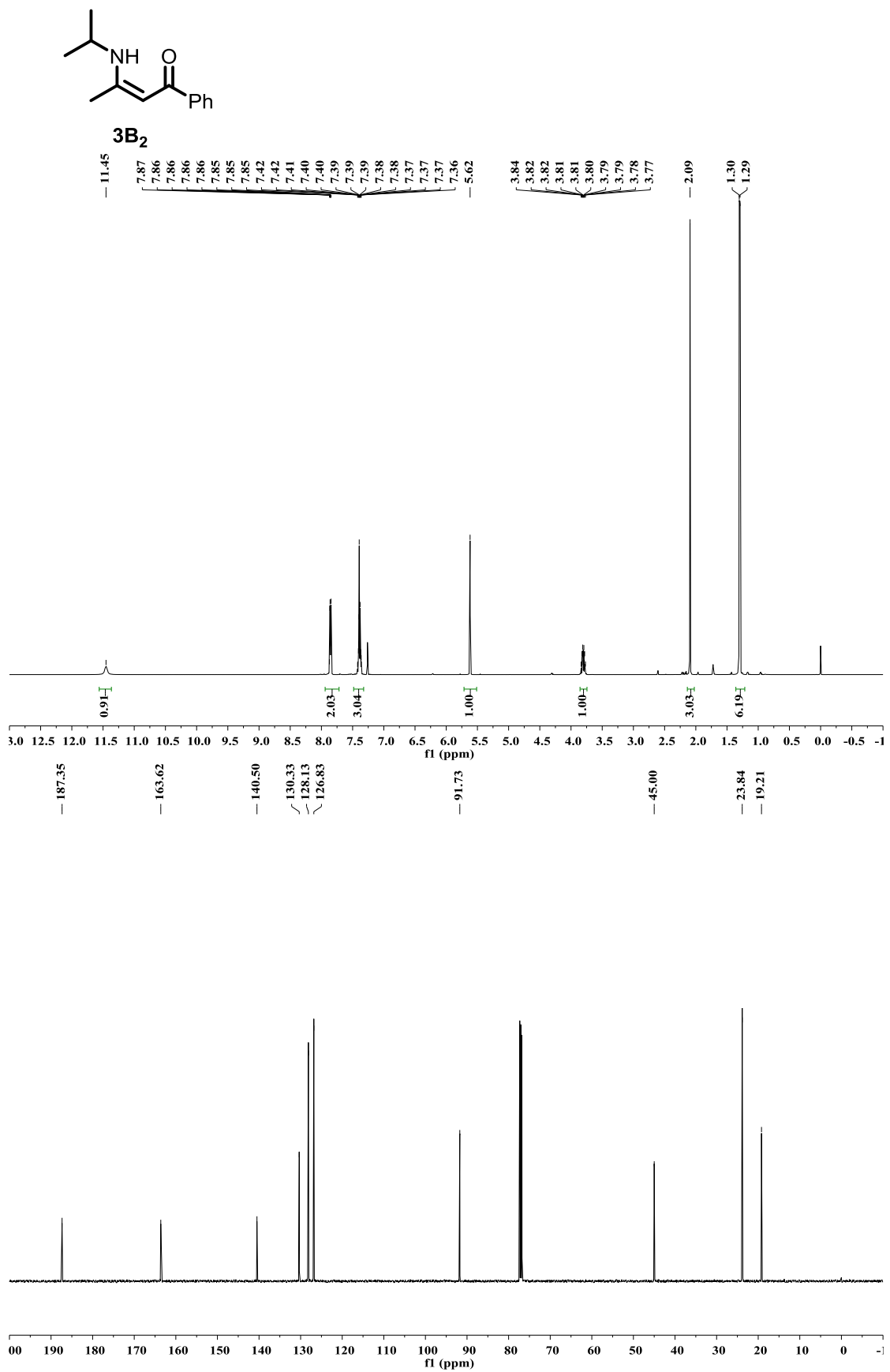


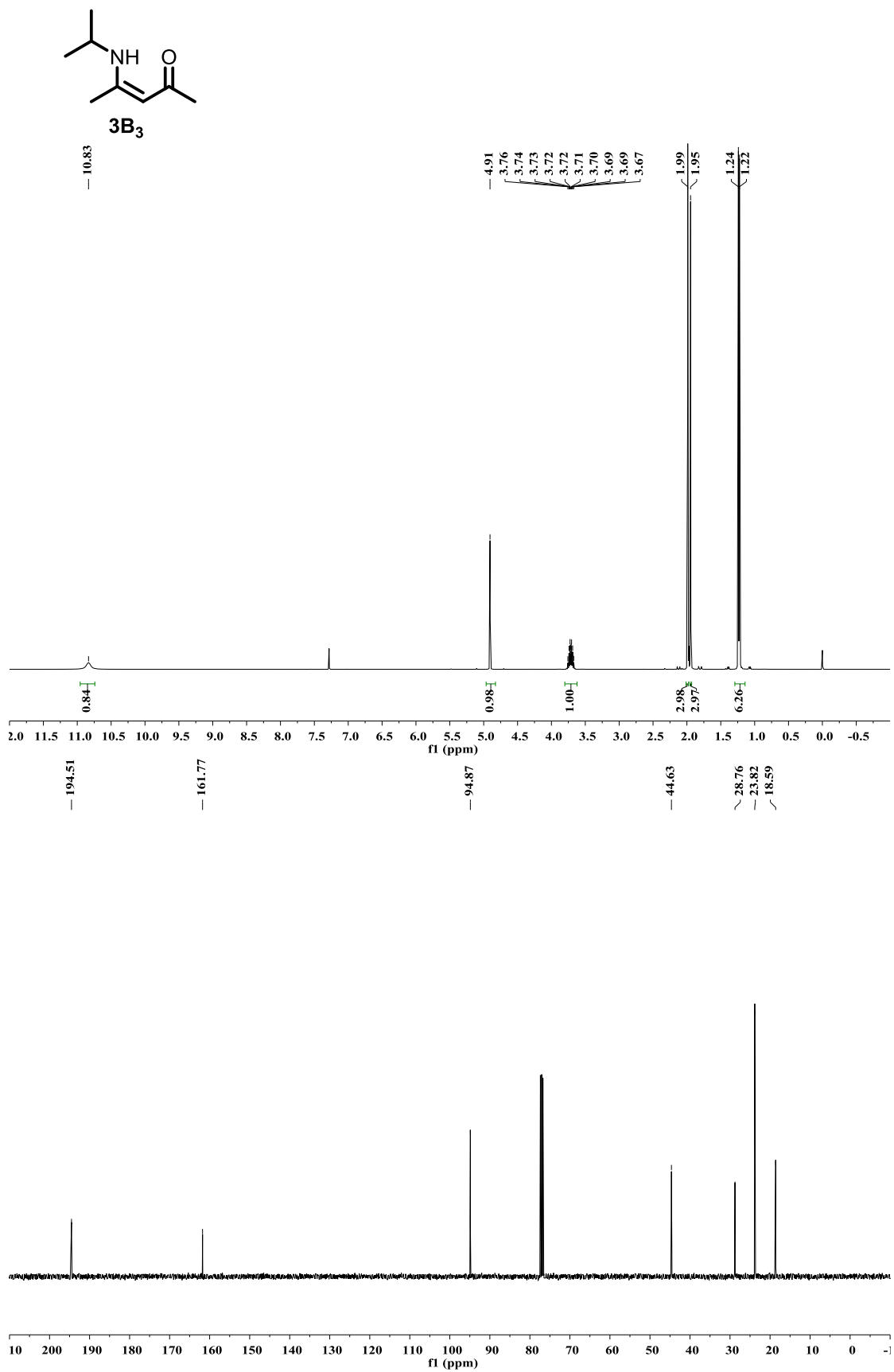


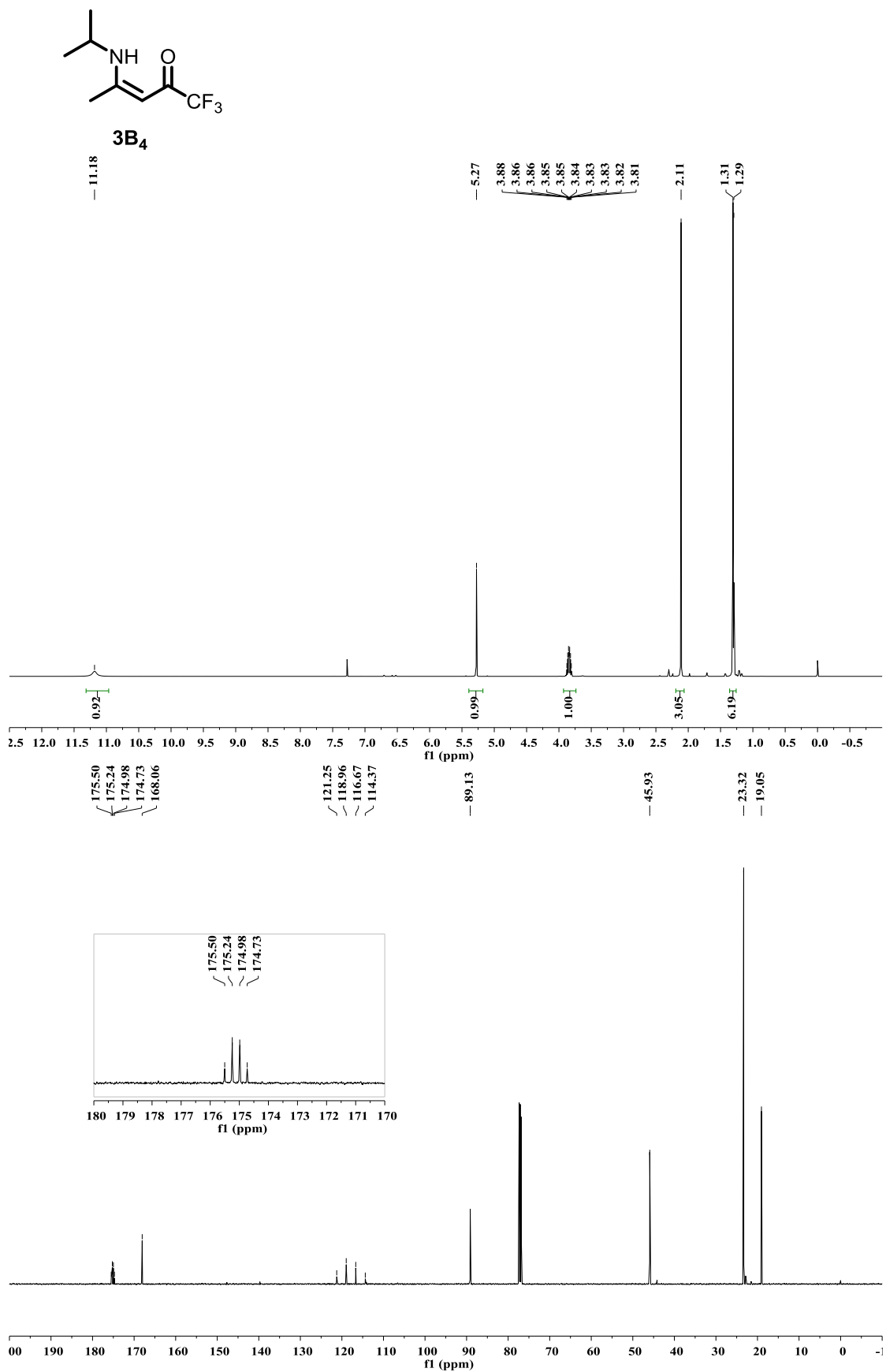
3A₅

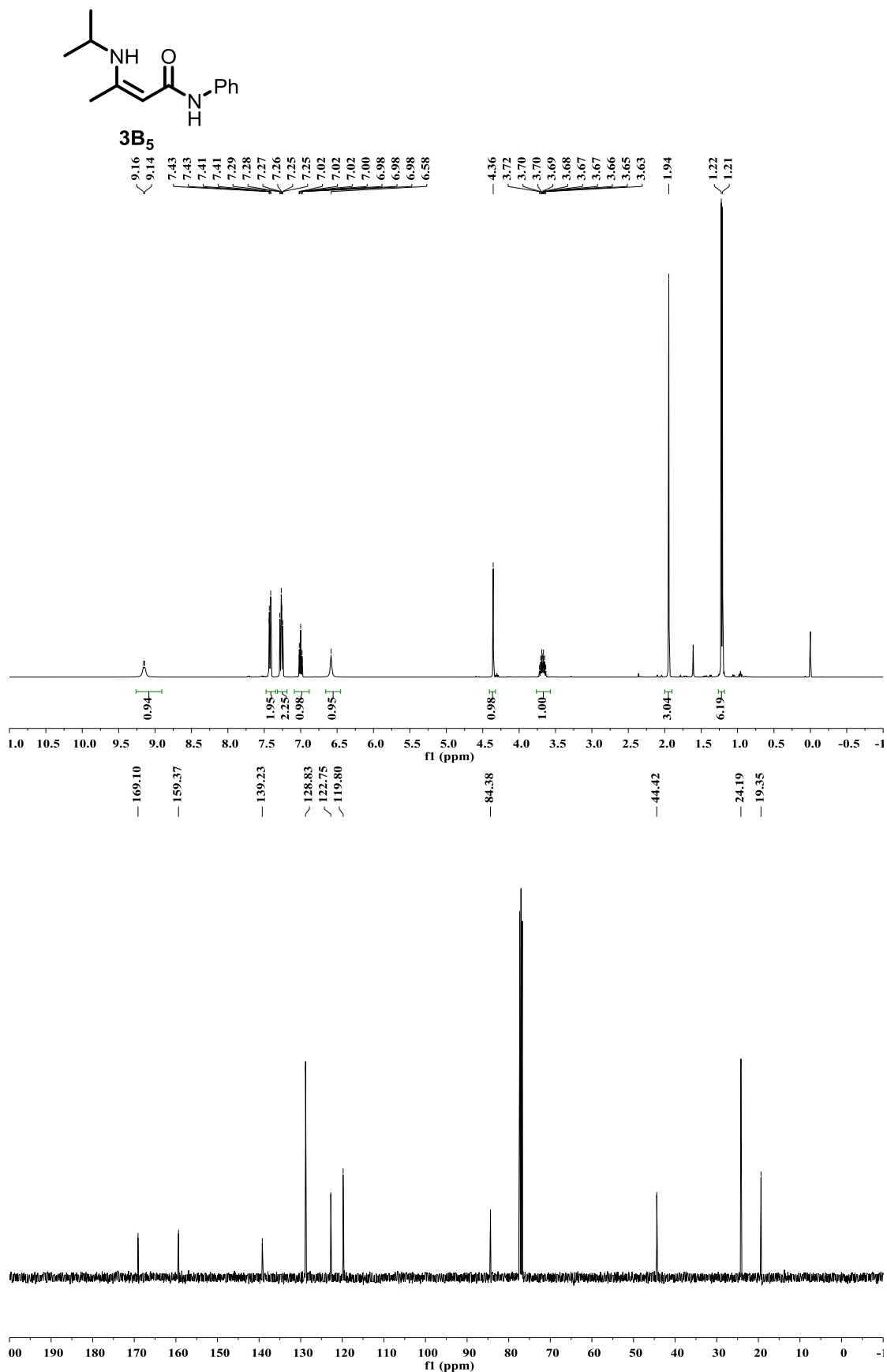


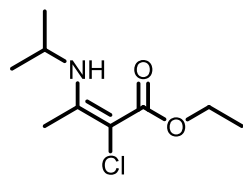




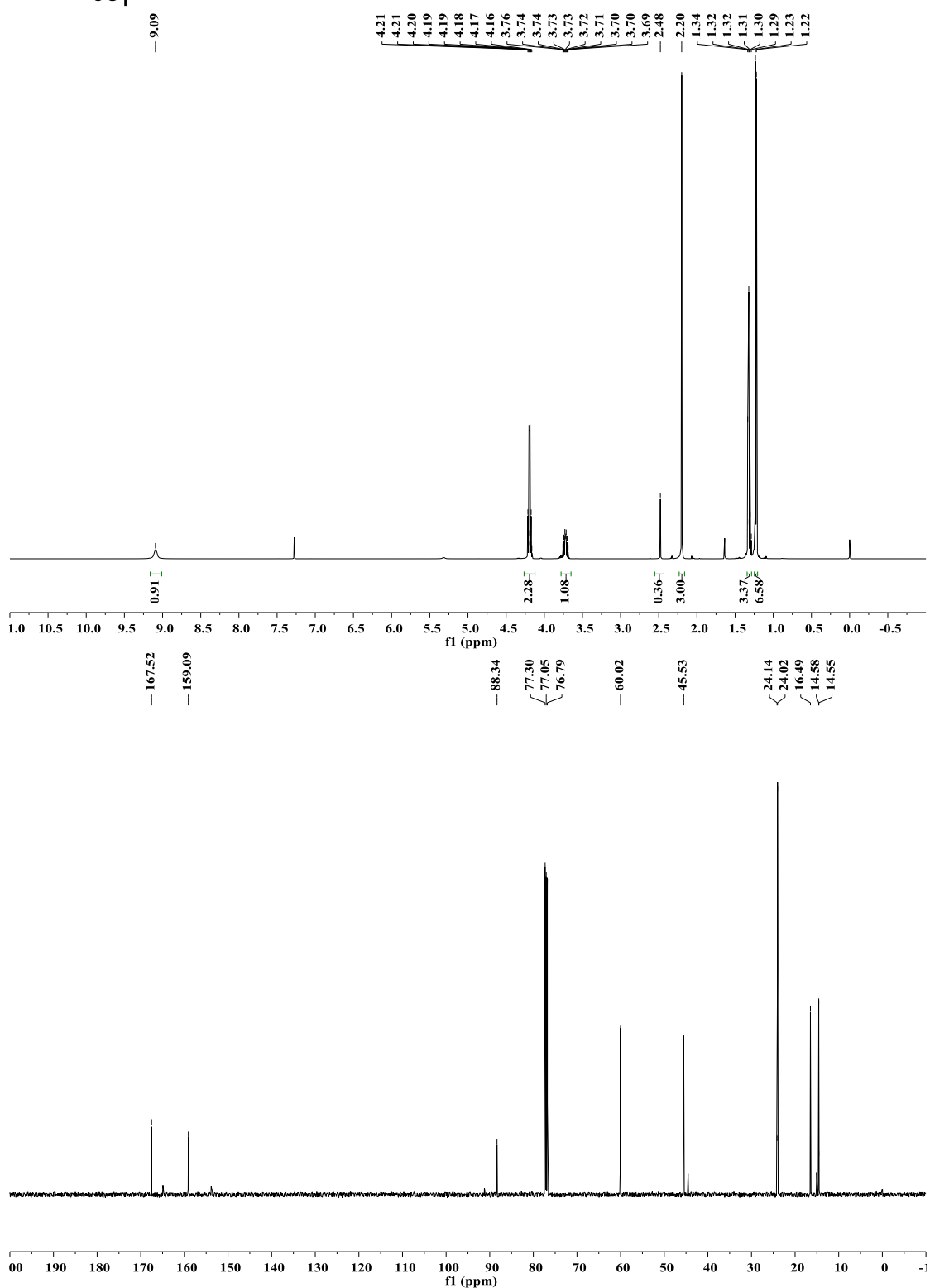


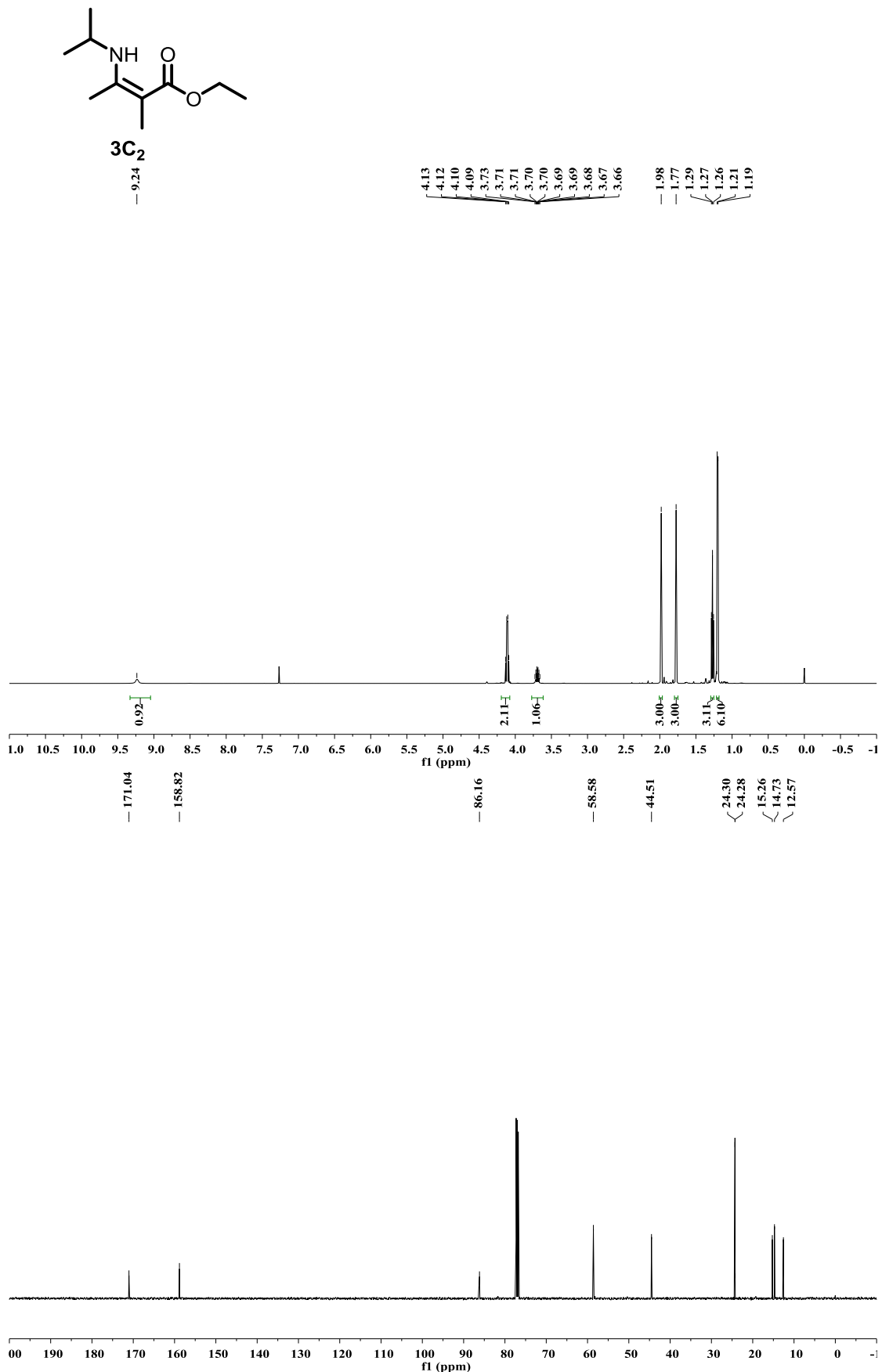


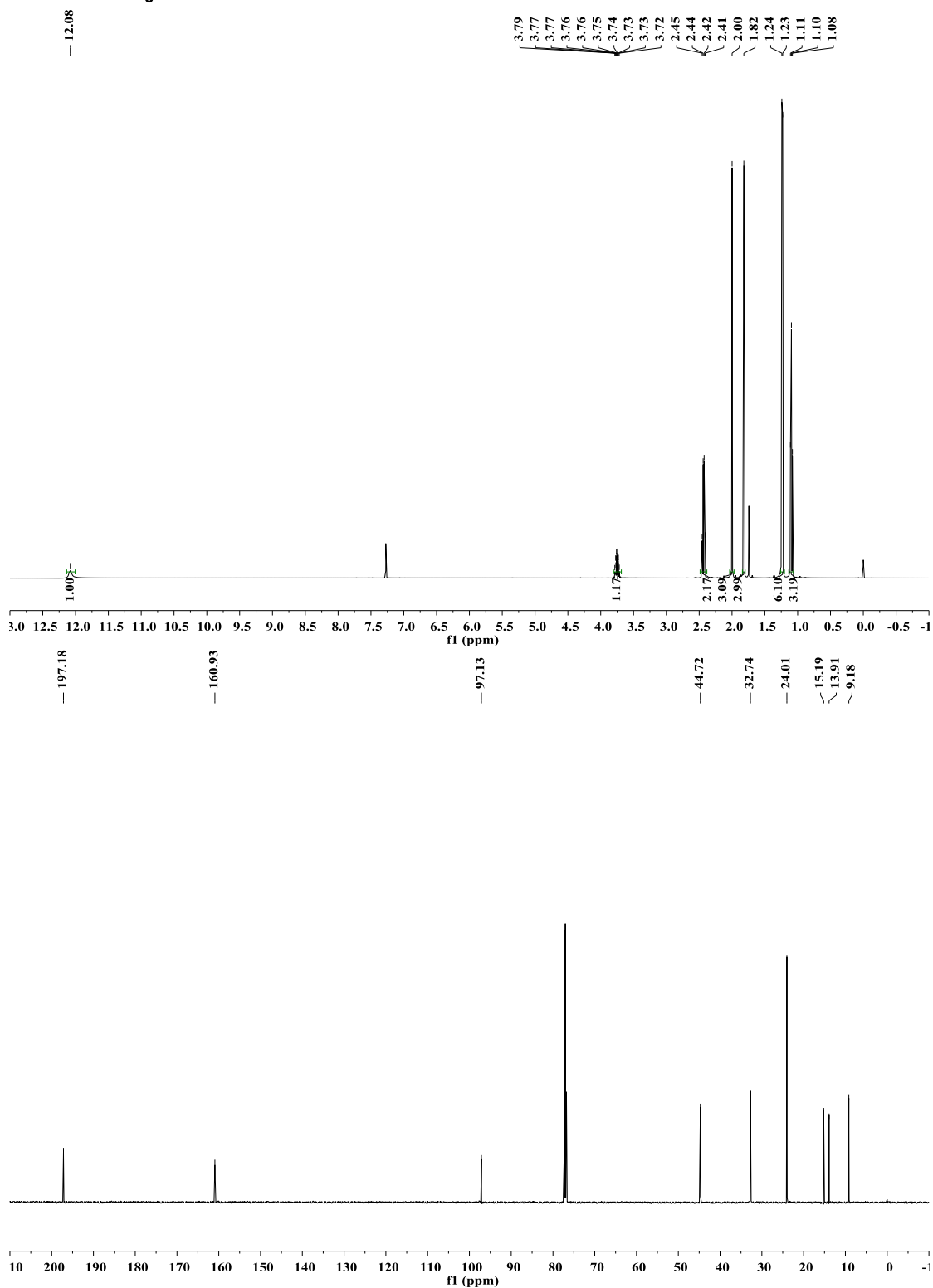
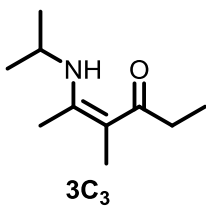


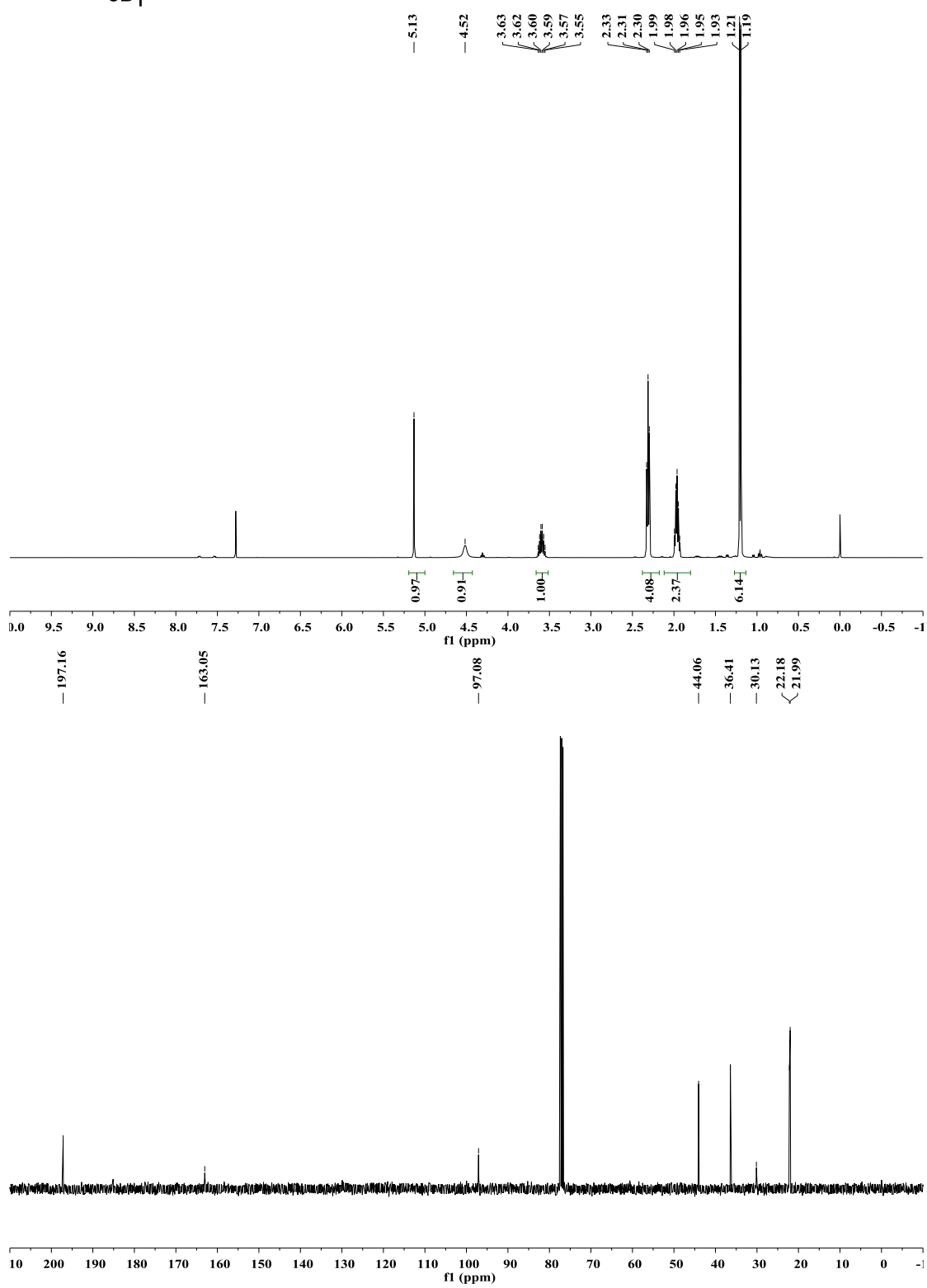
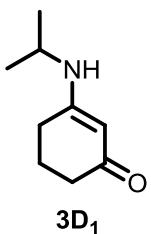


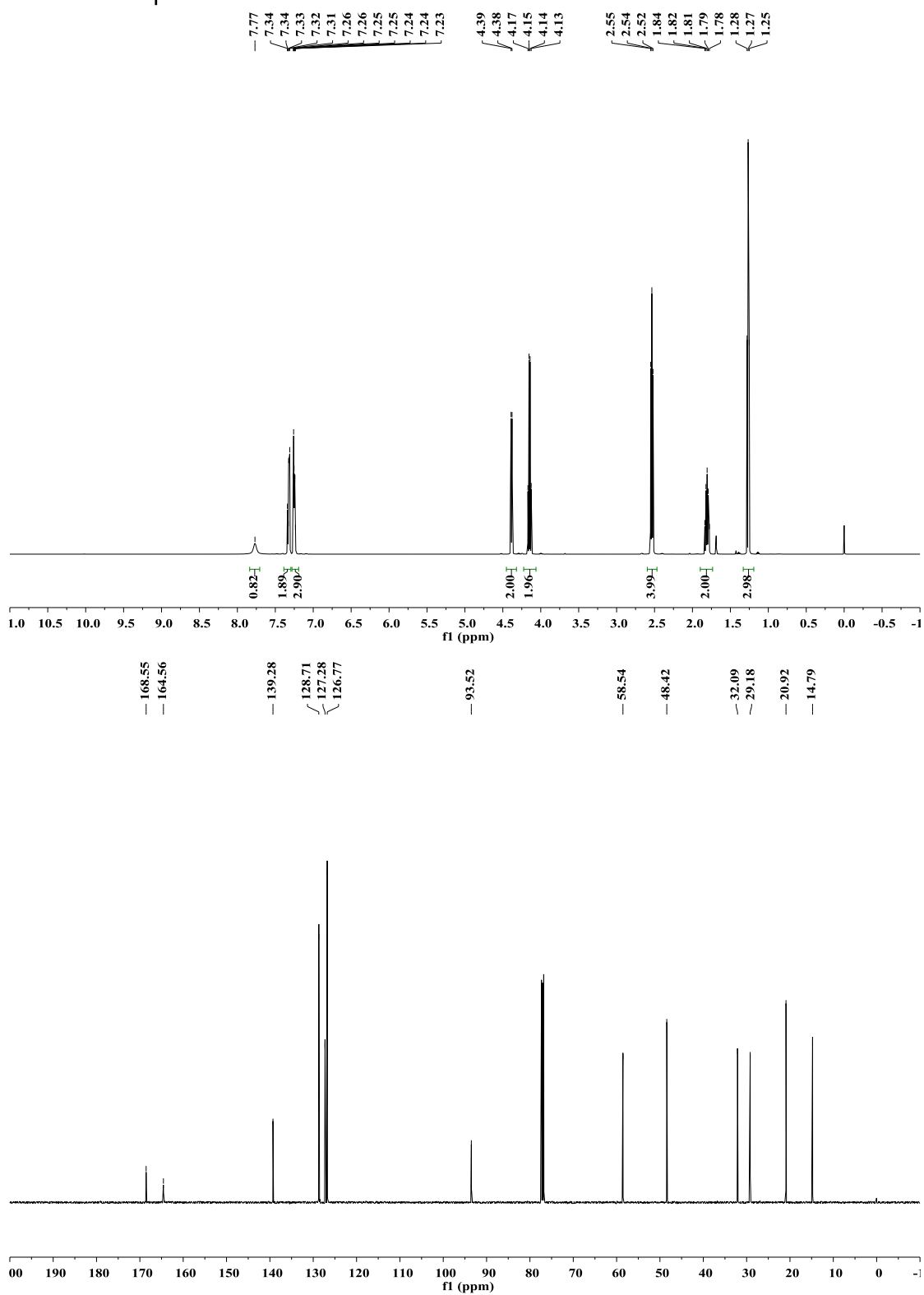
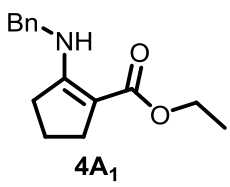
3C₁

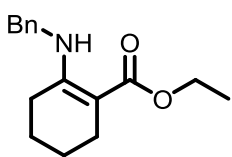




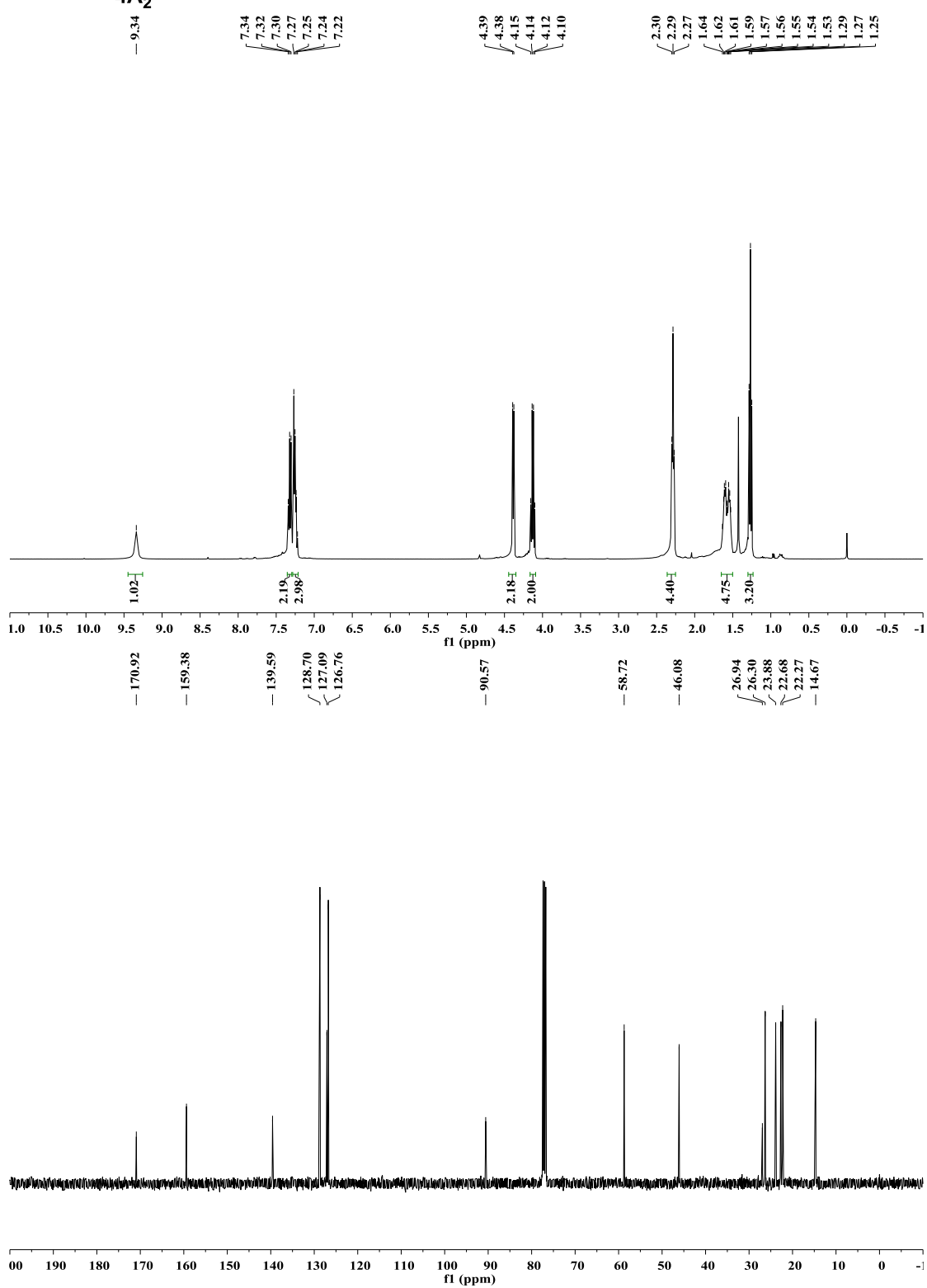


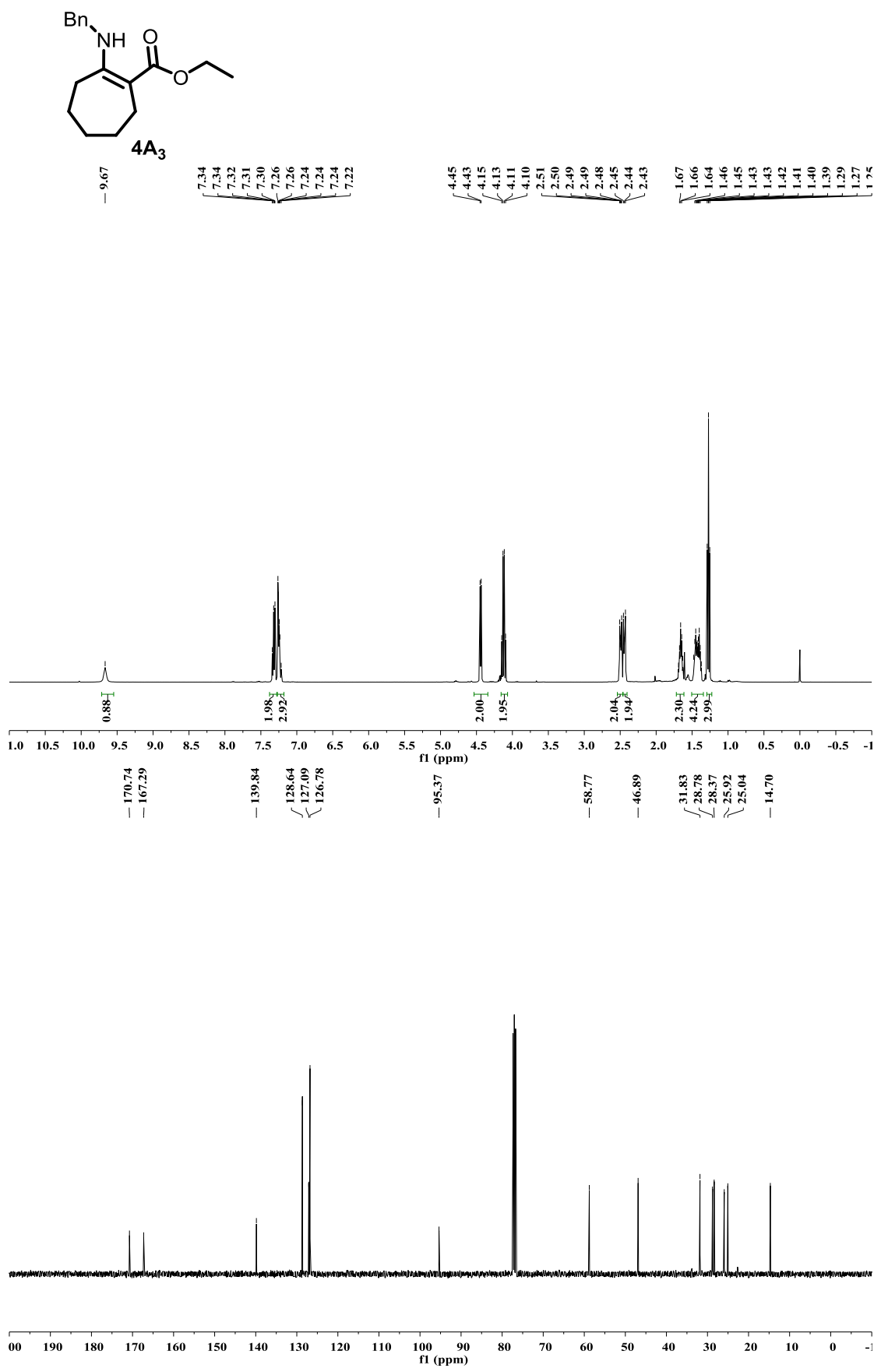


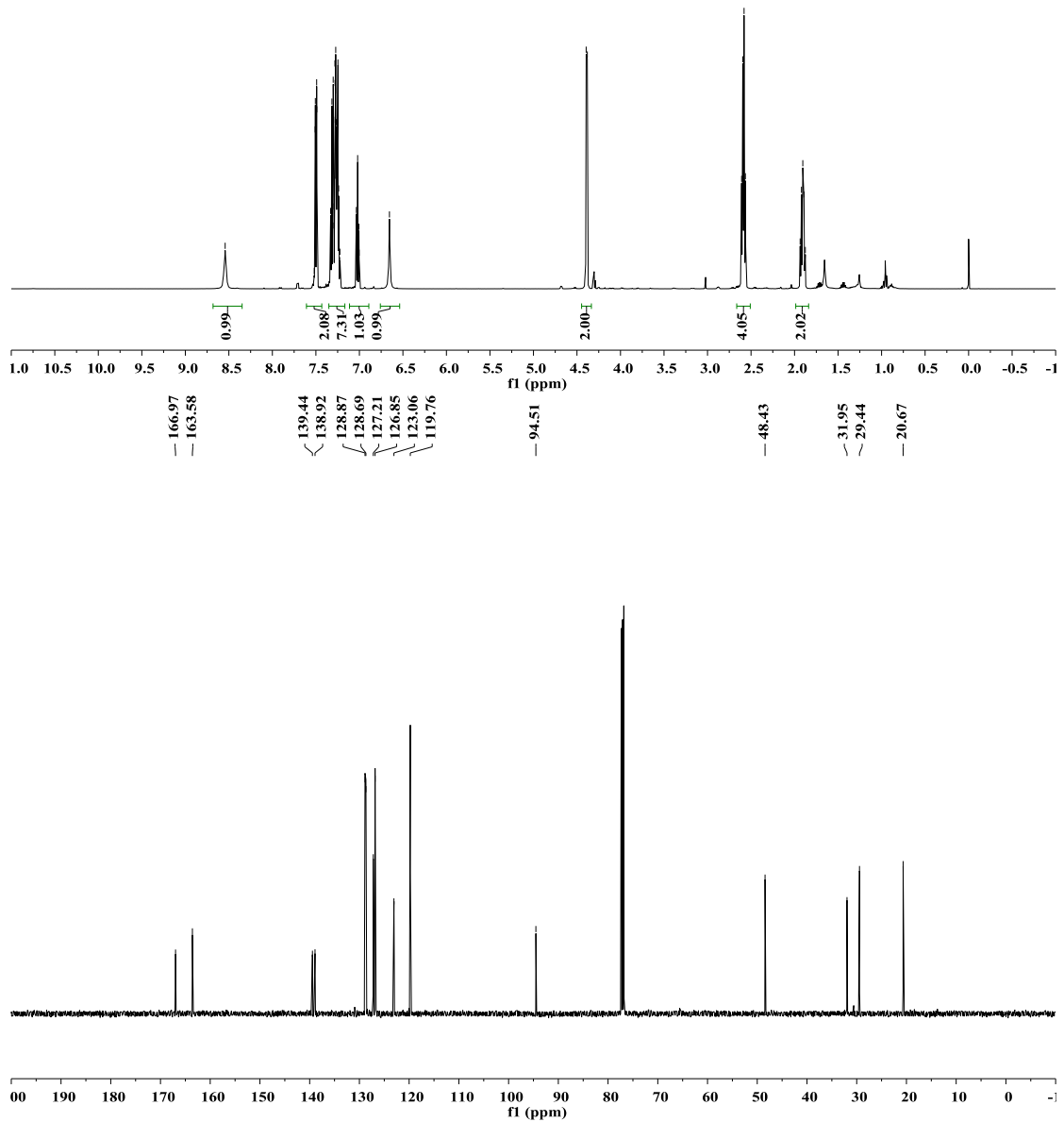
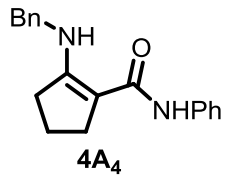


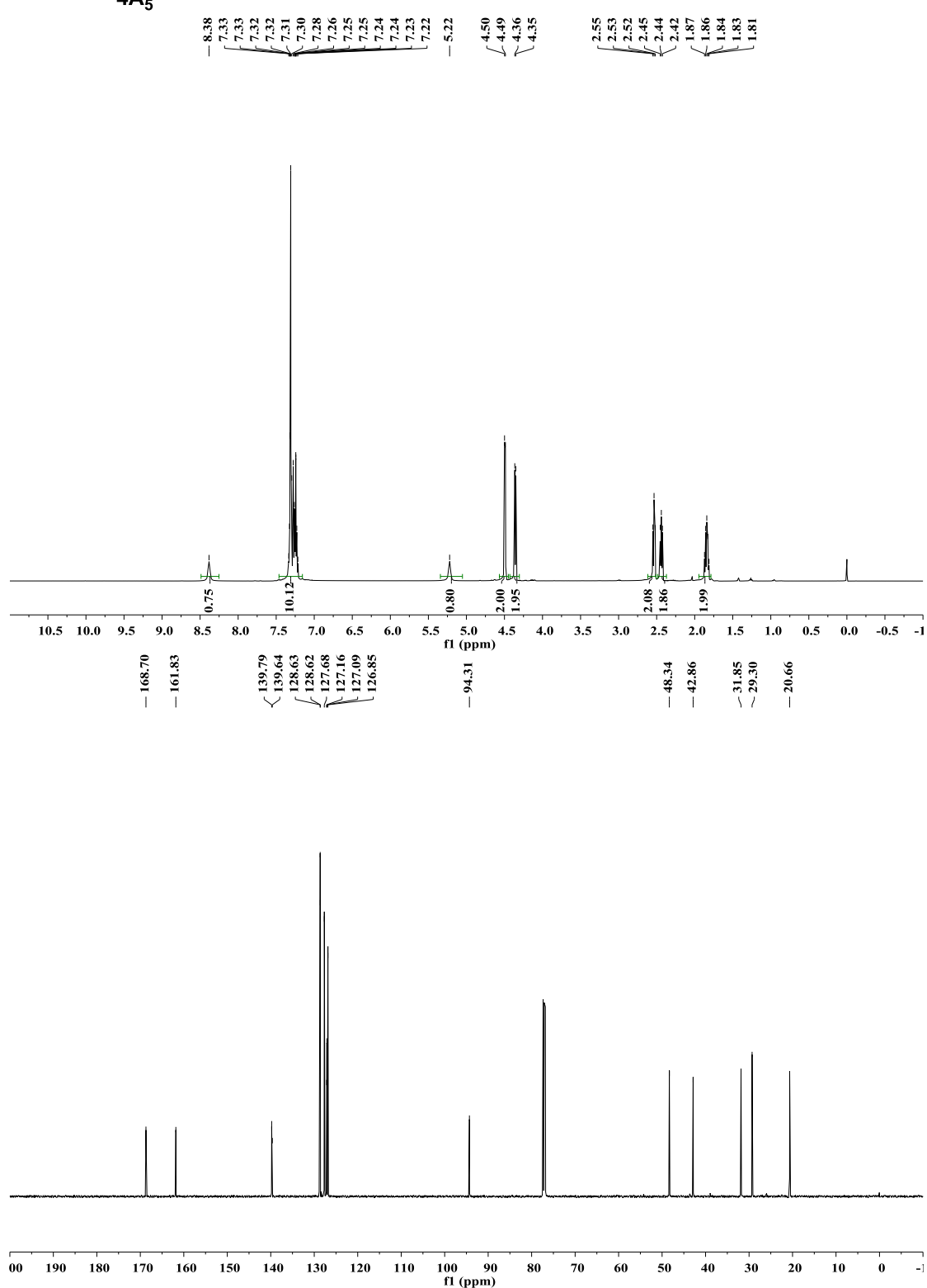
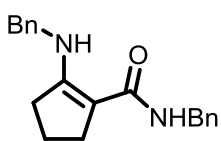


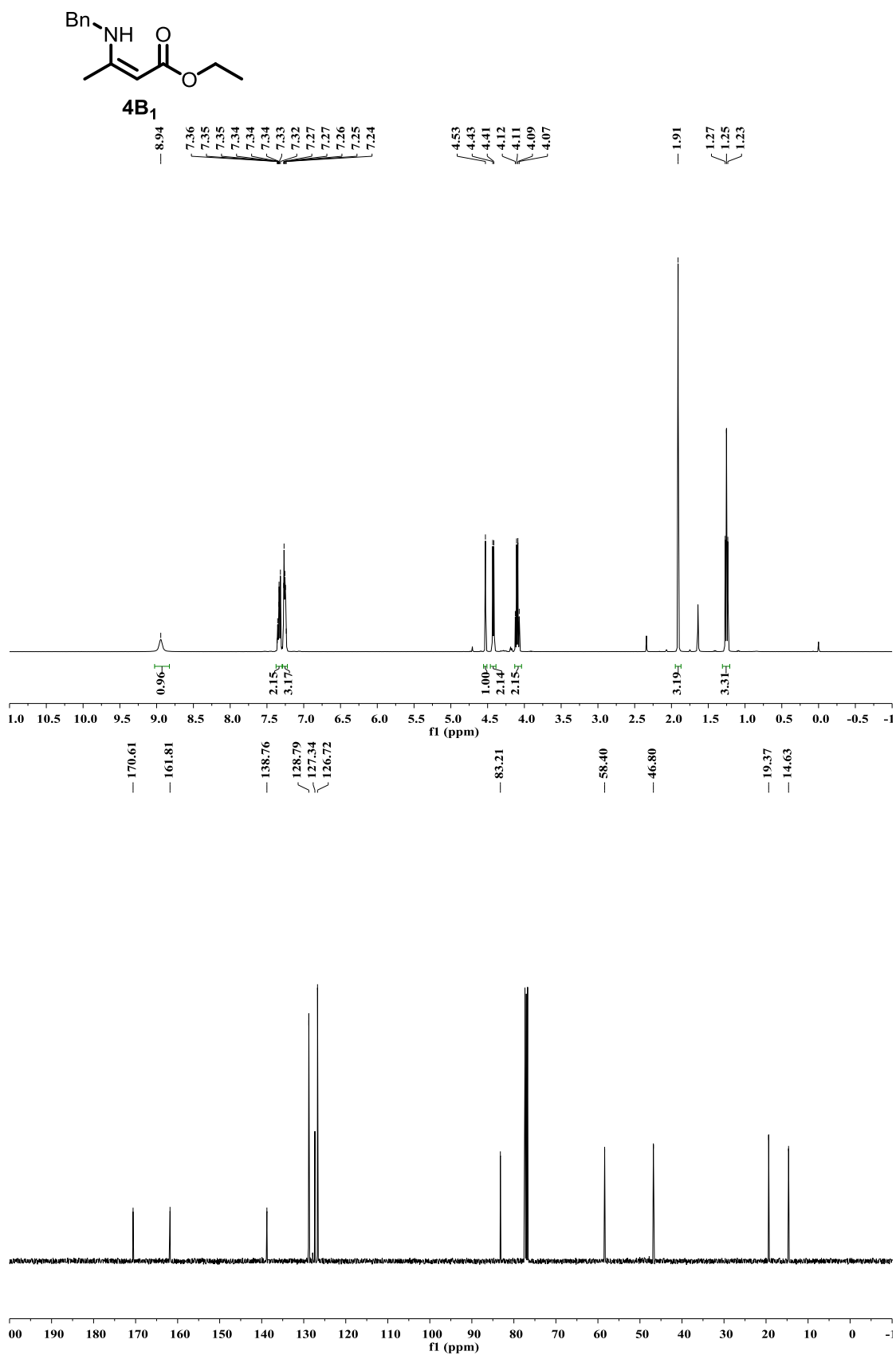
4A₂

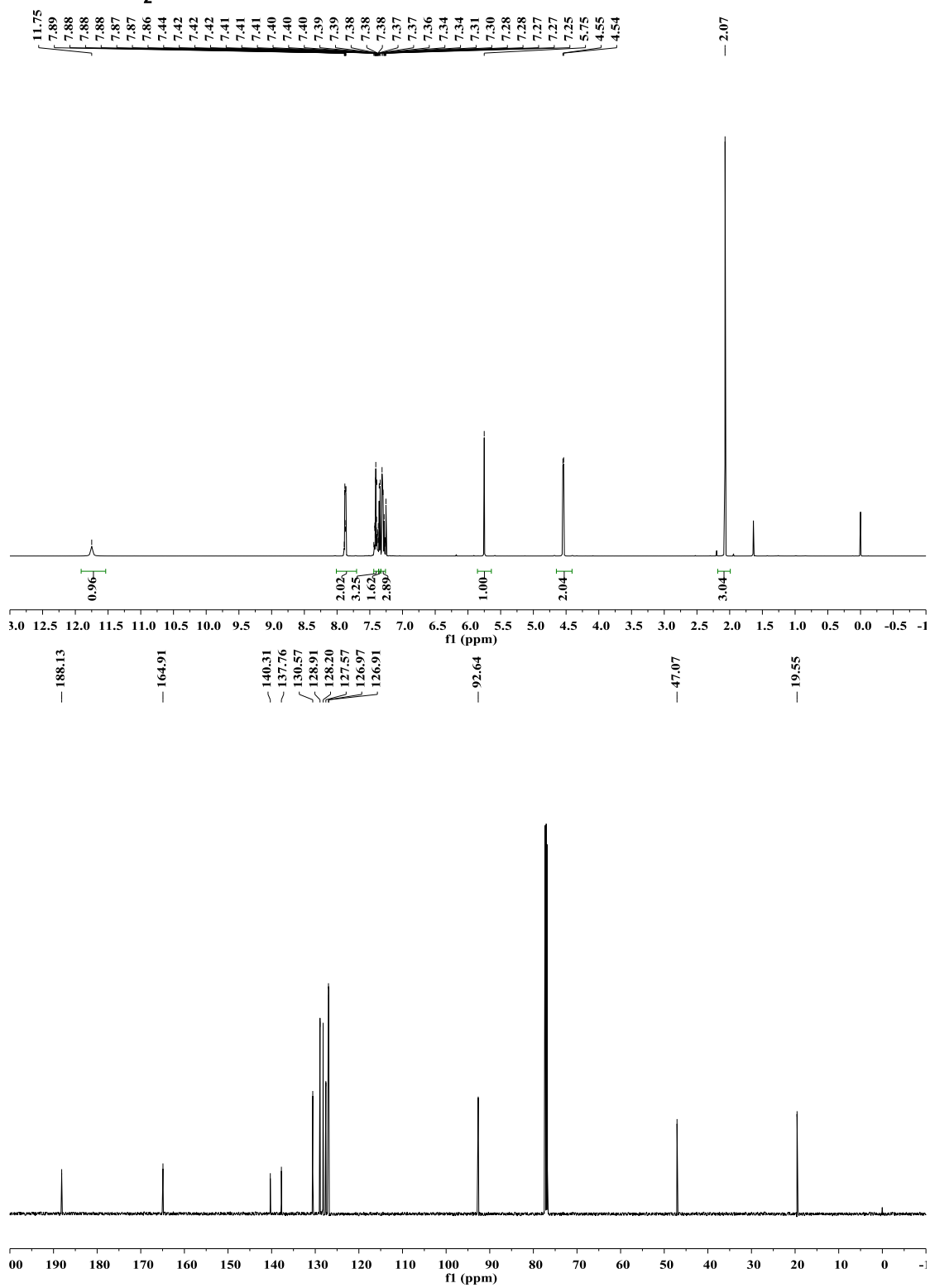
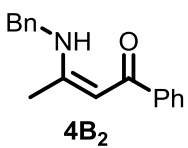


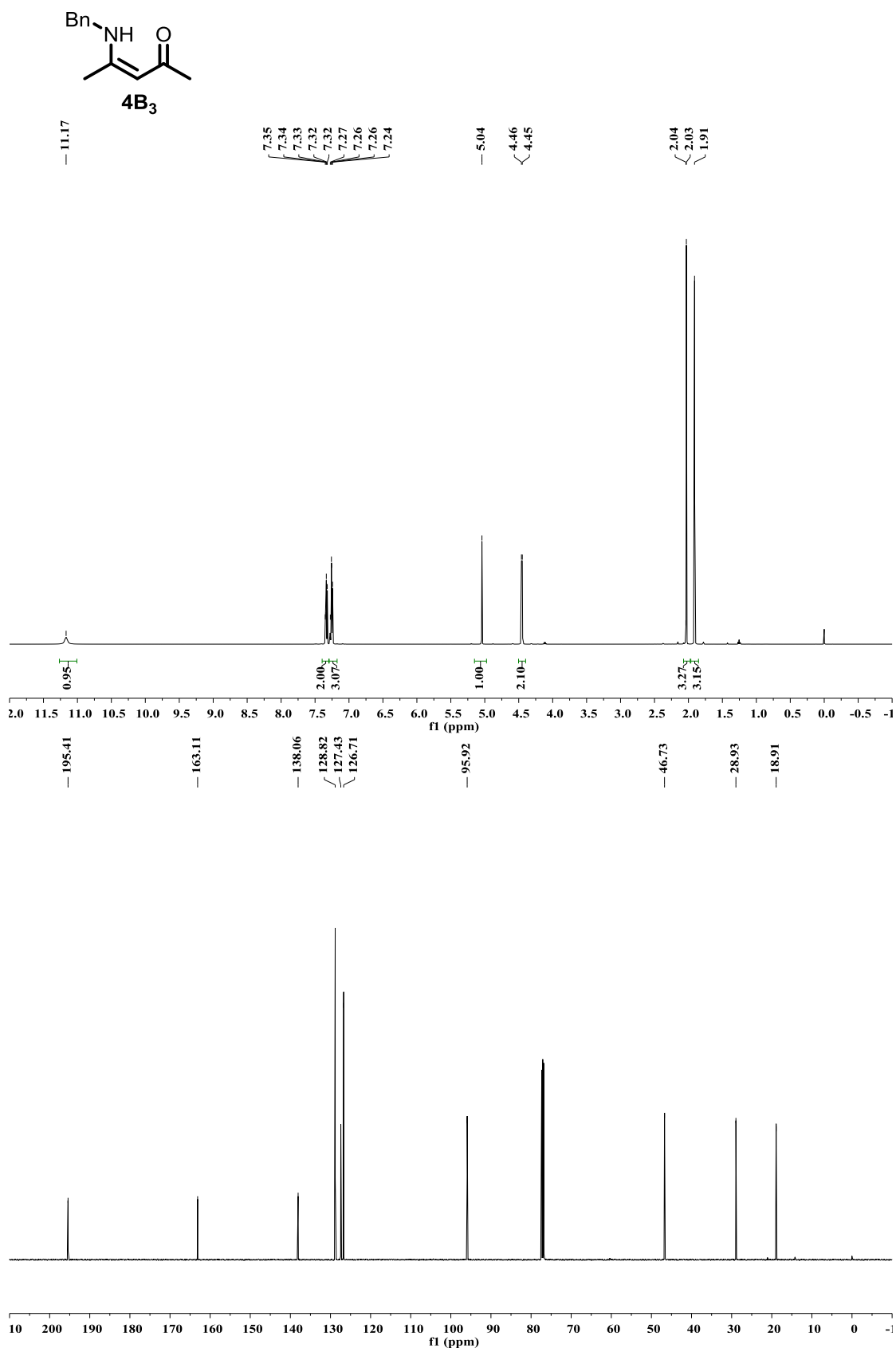


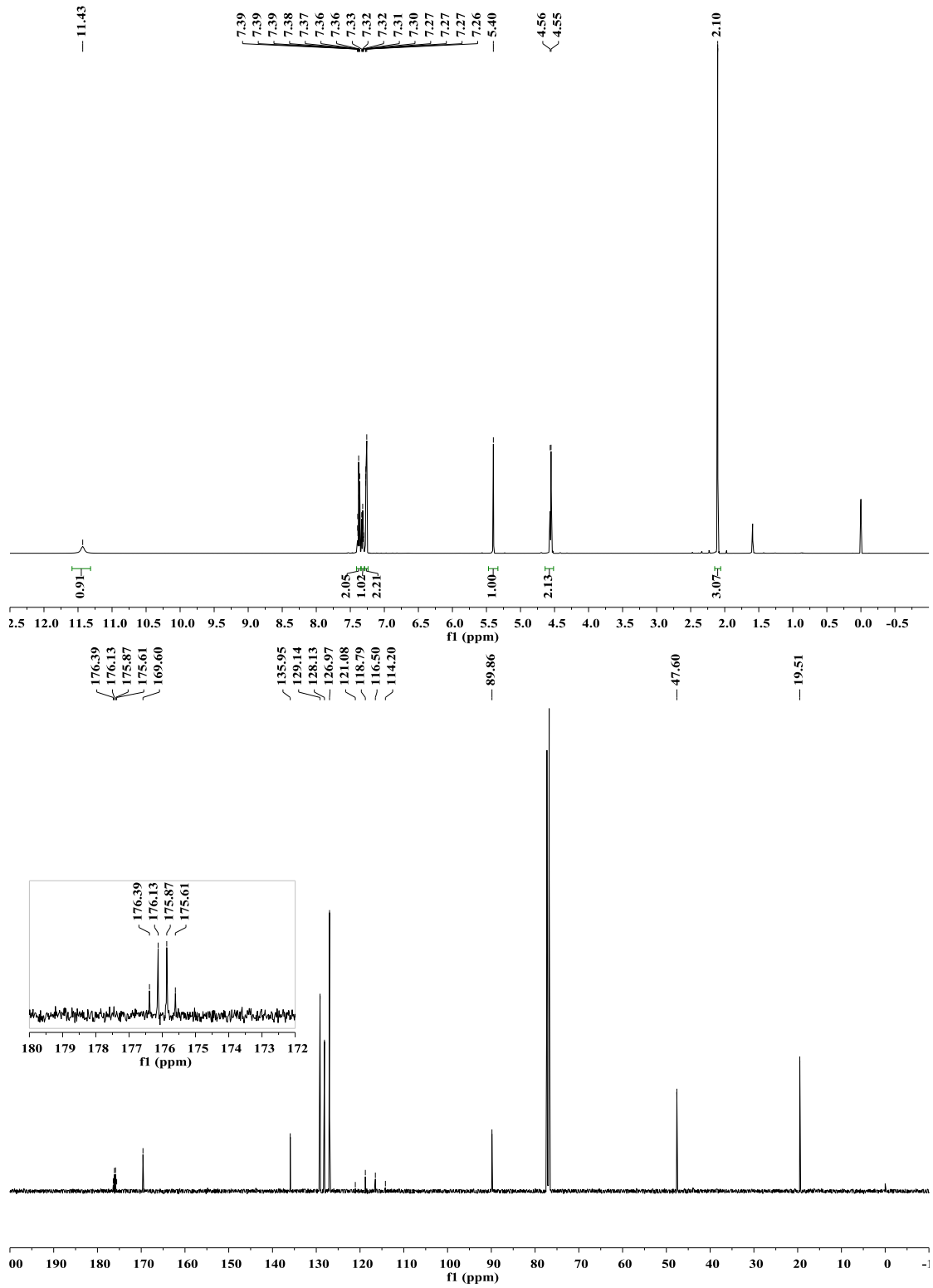
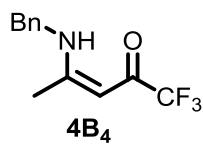


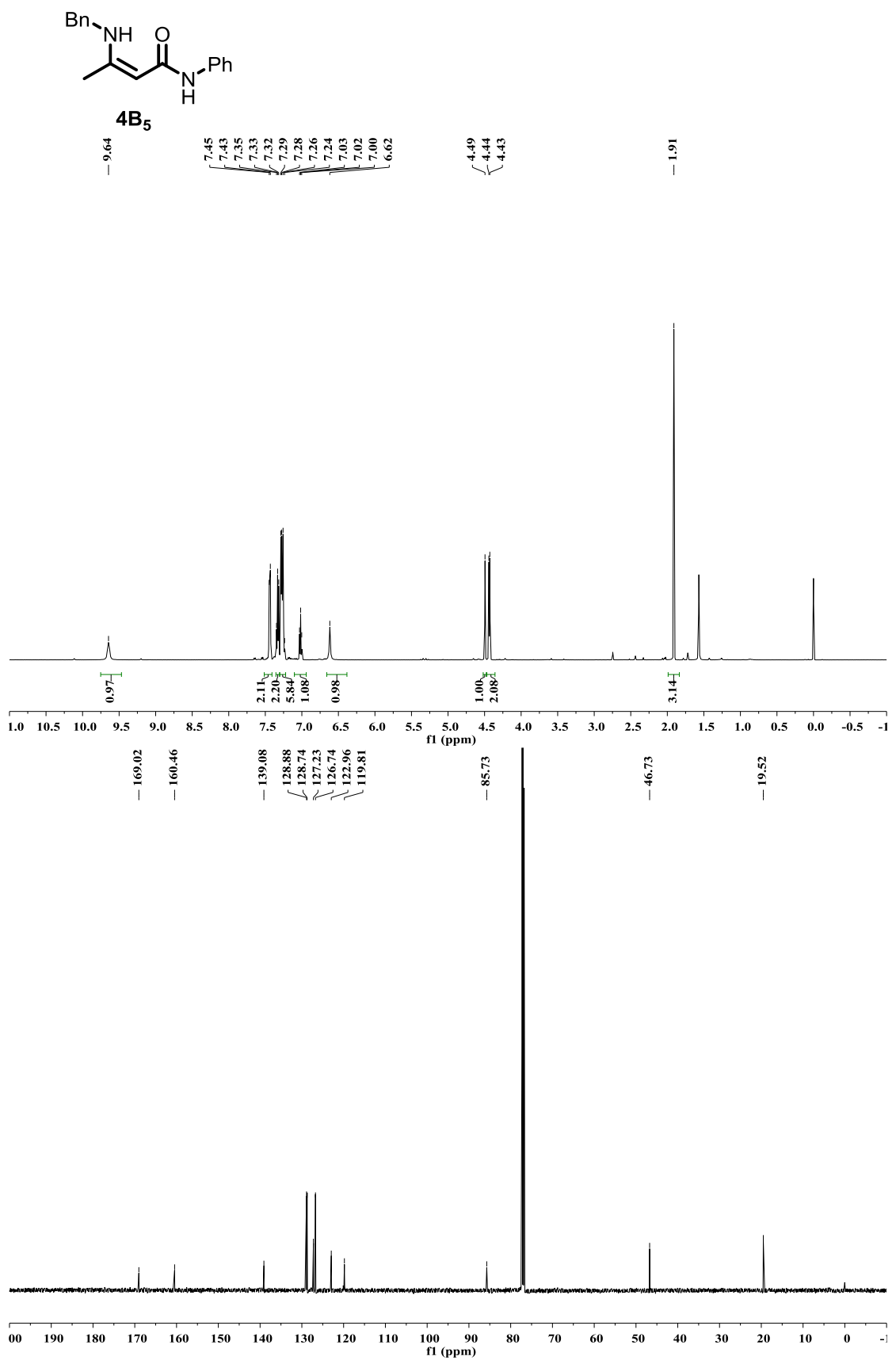


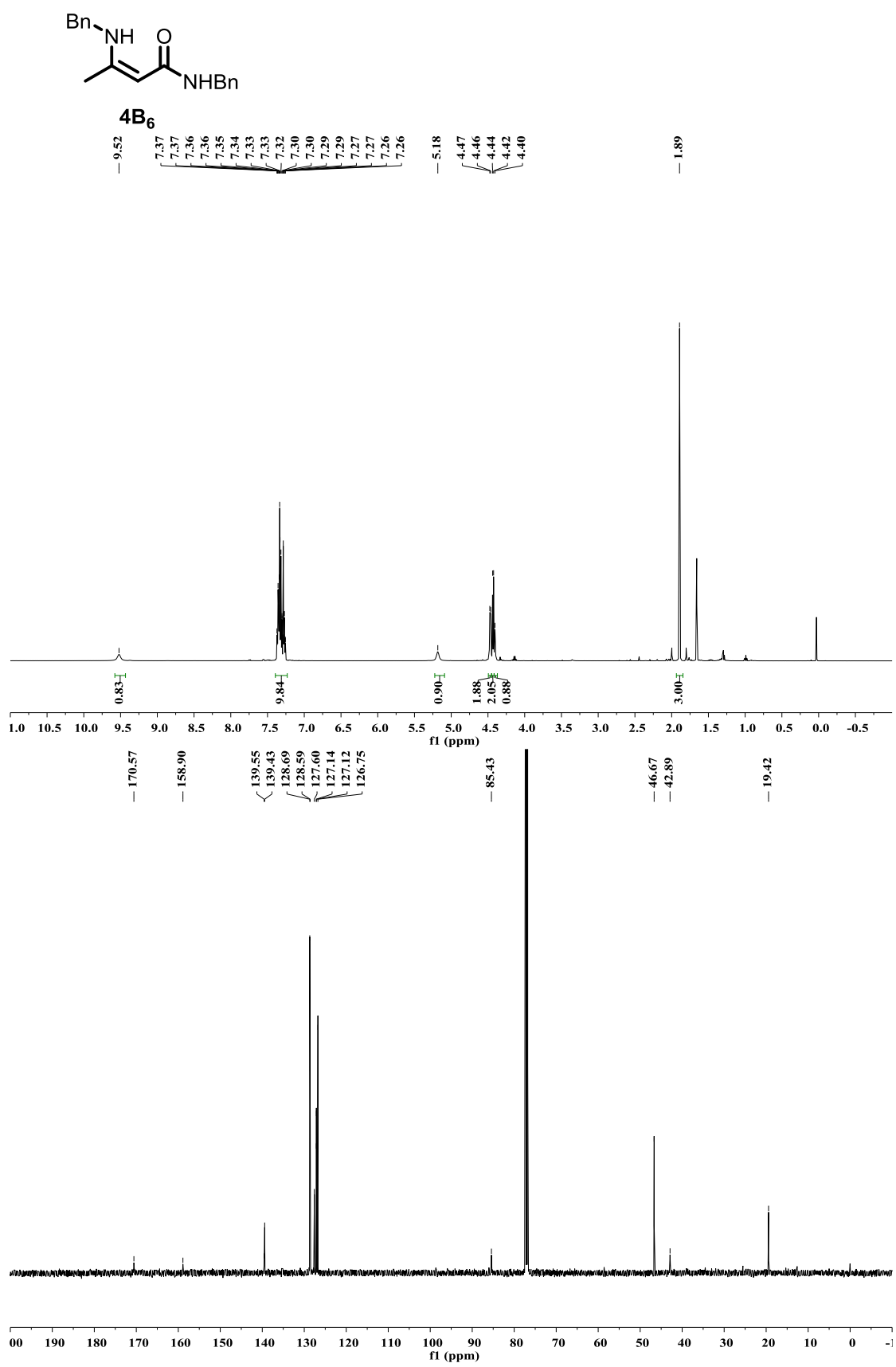


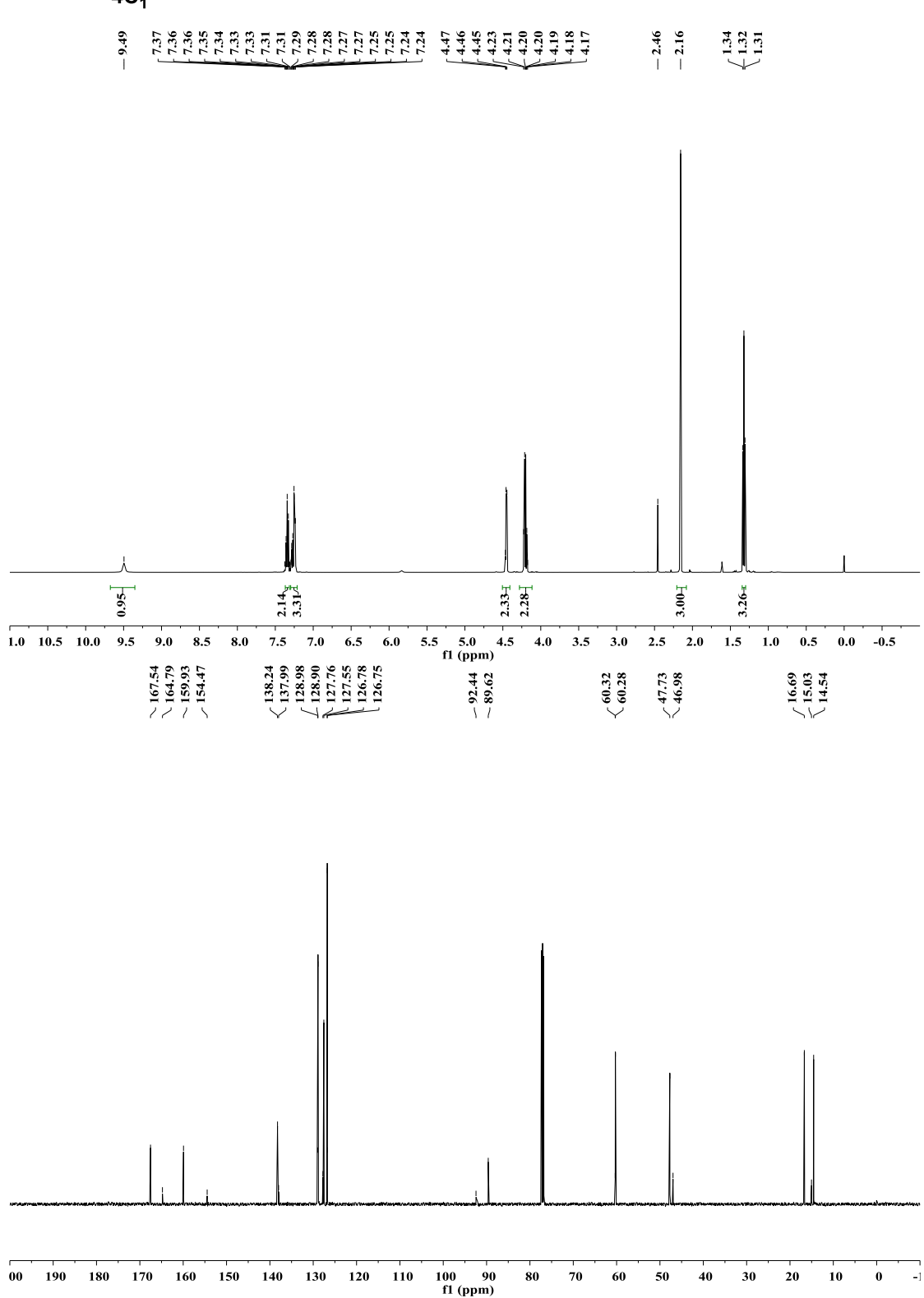
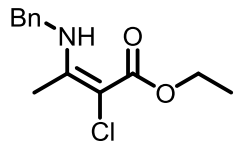


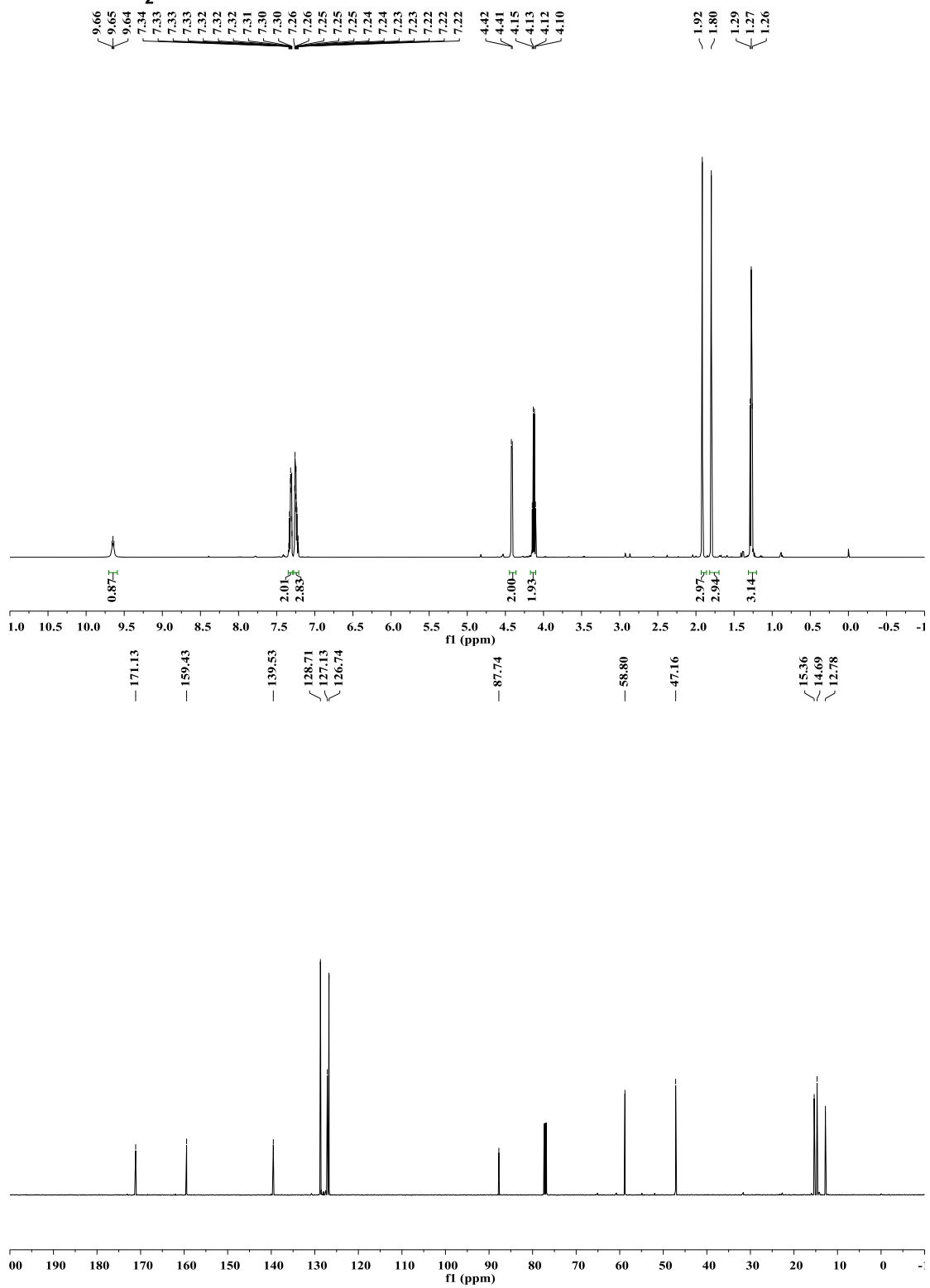
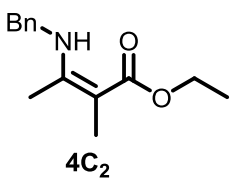


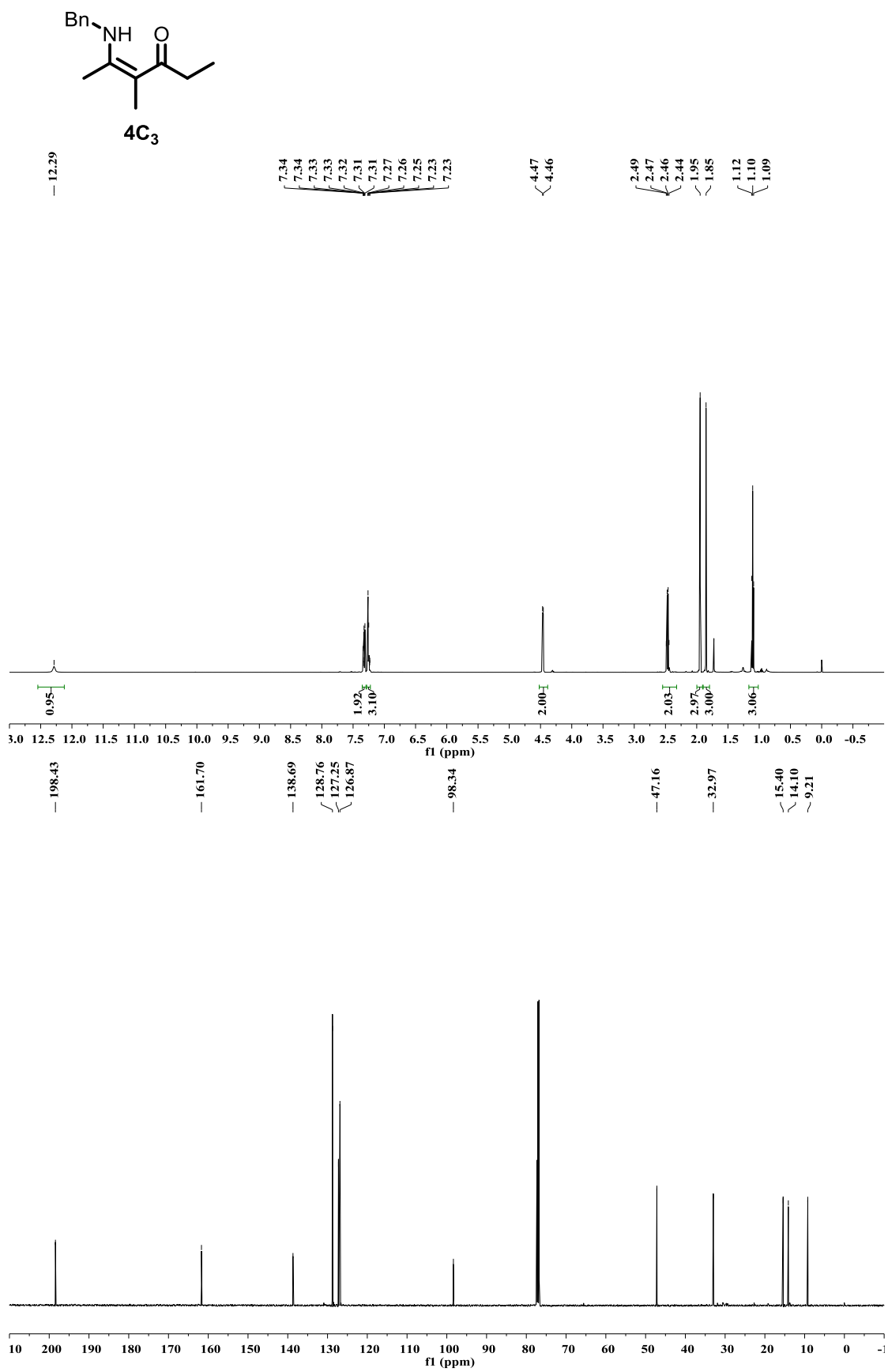


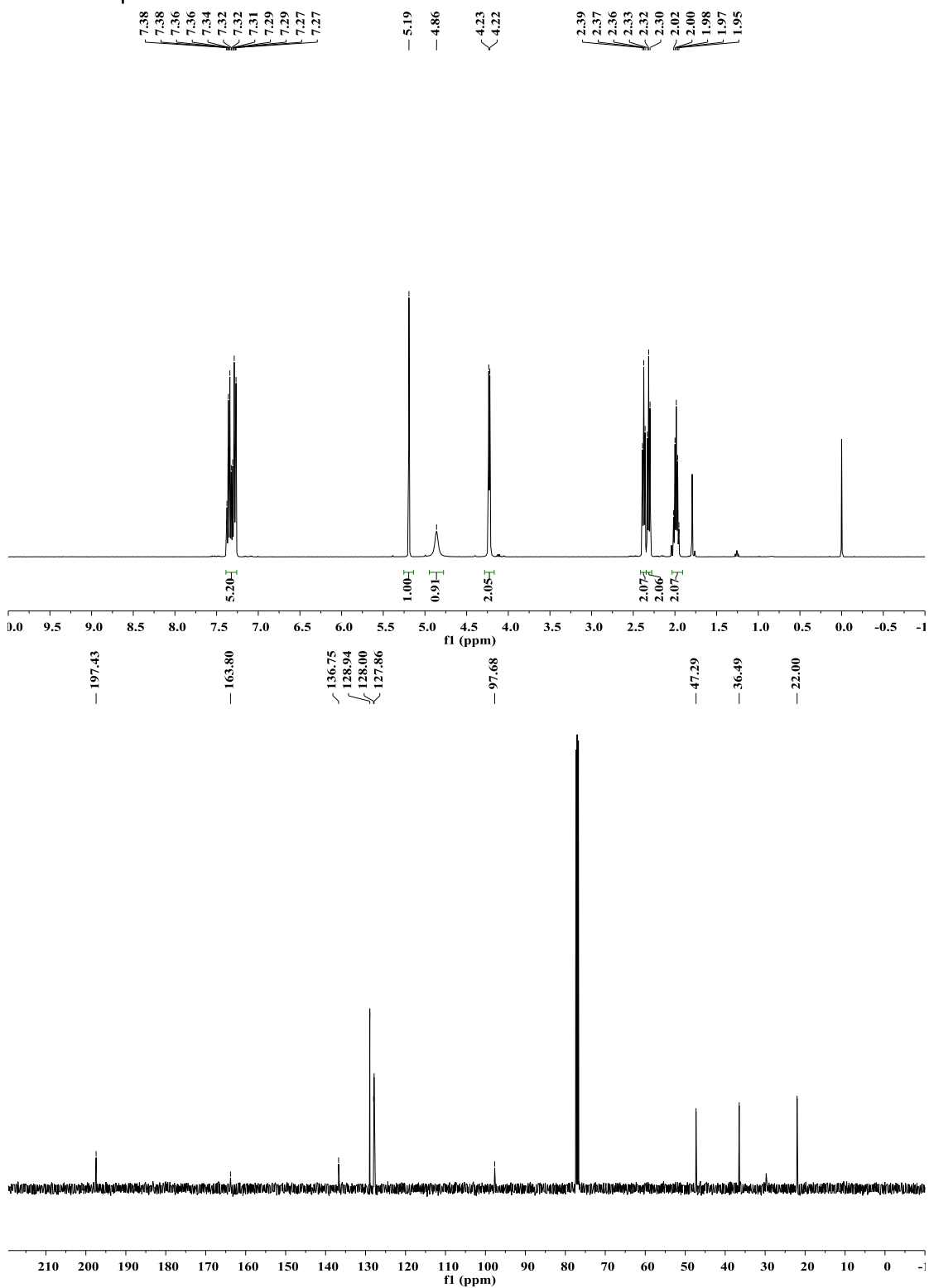
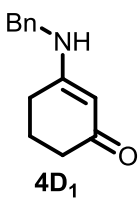


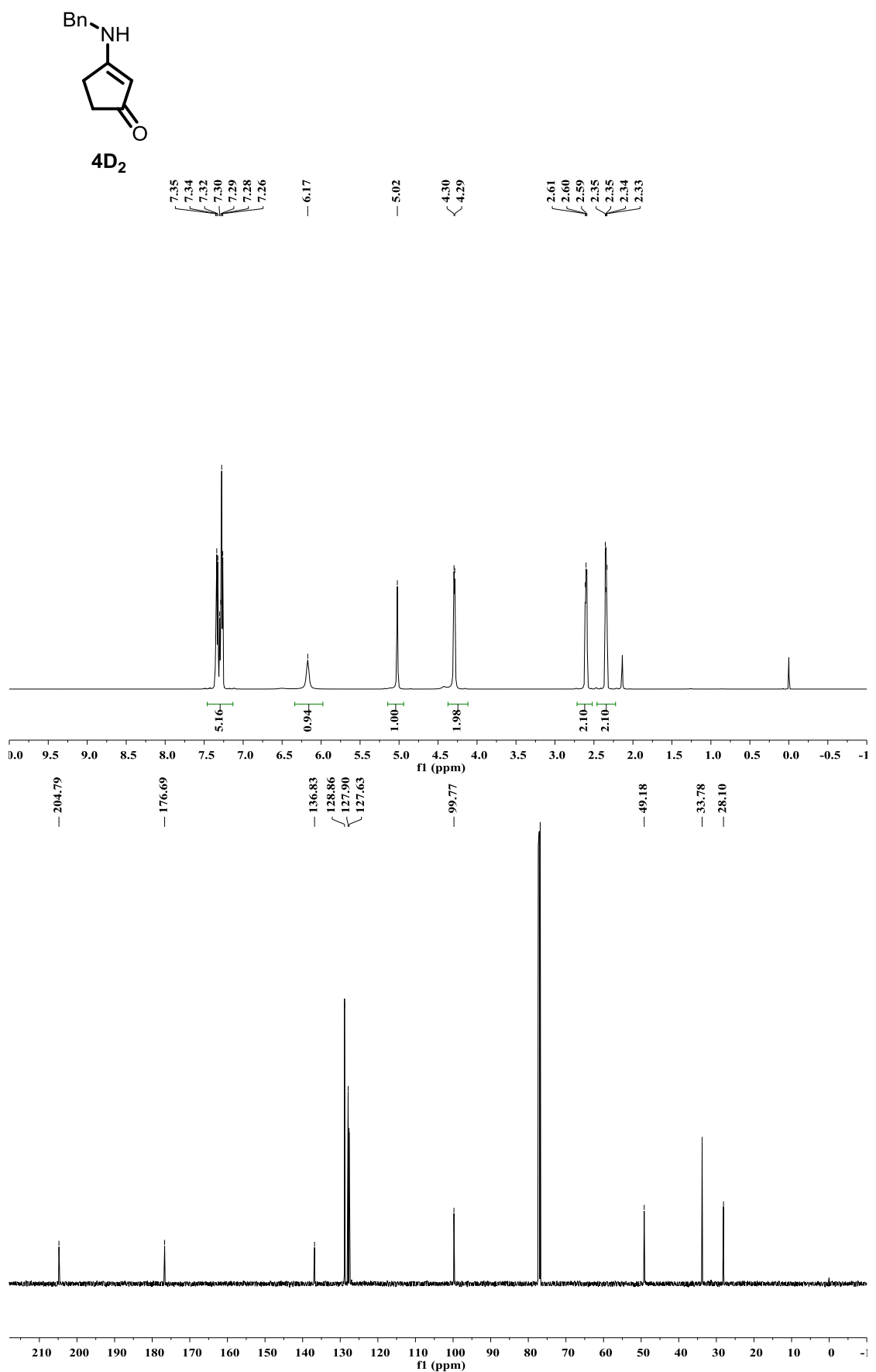


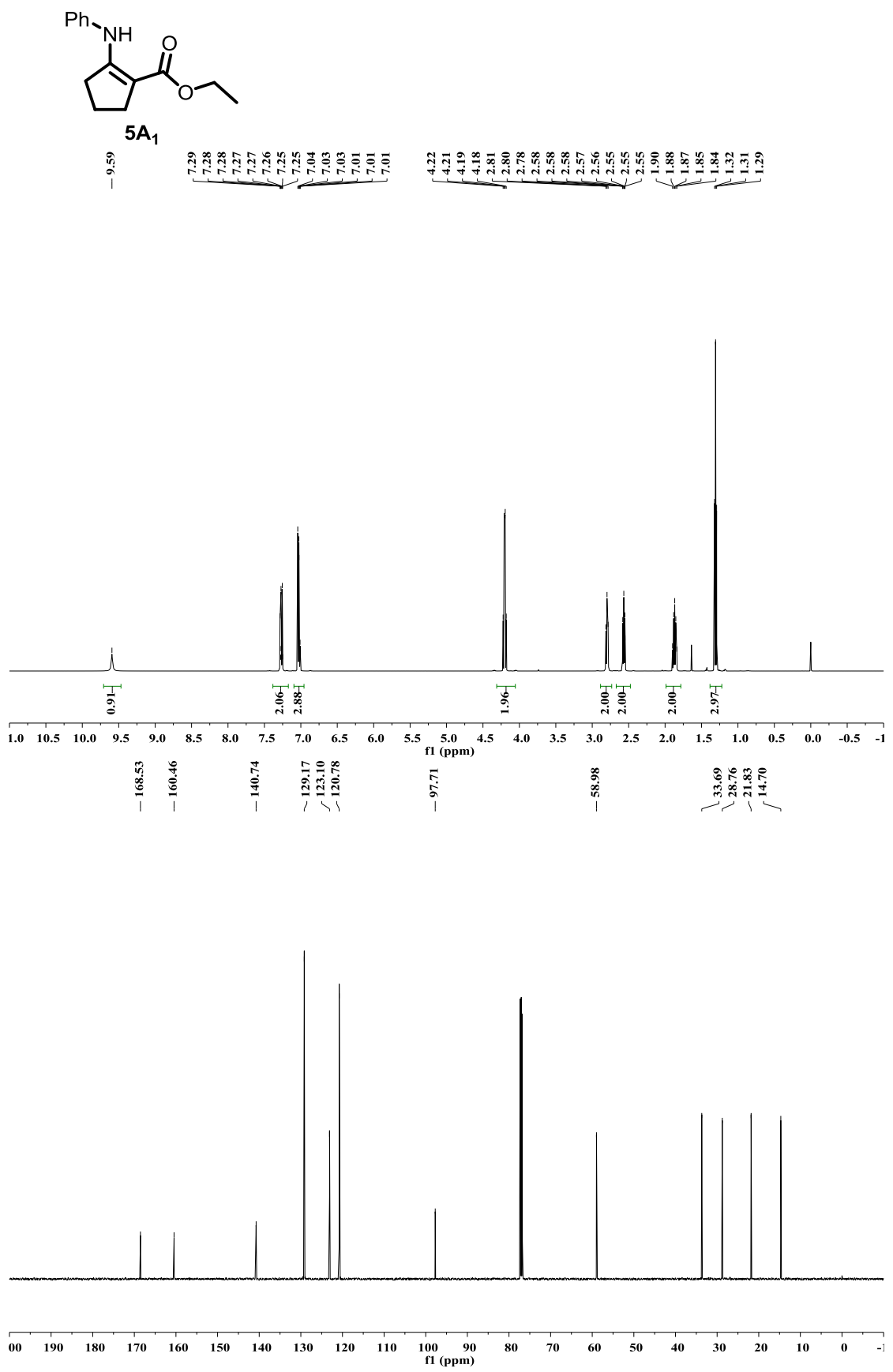


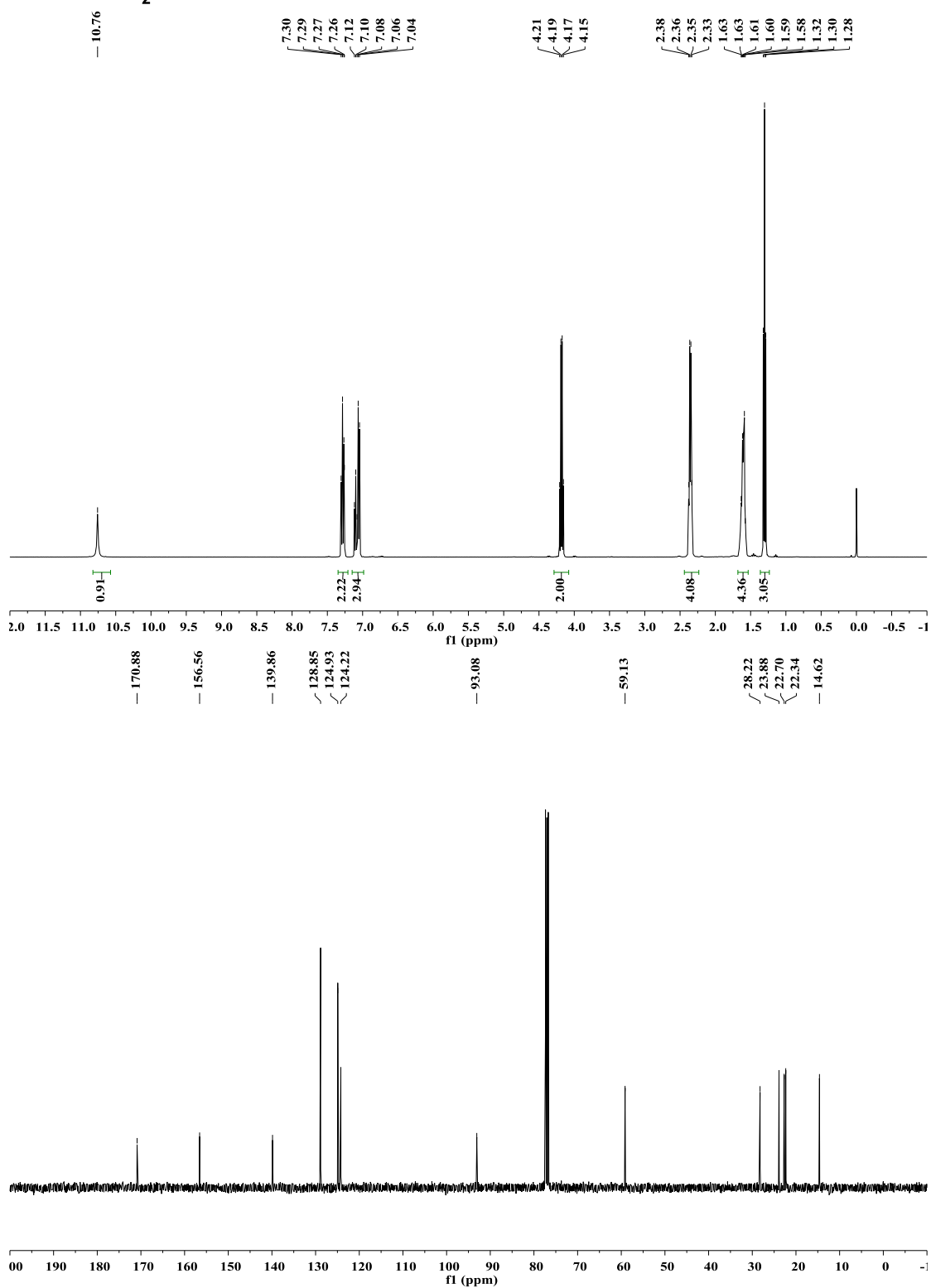
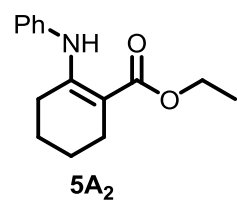


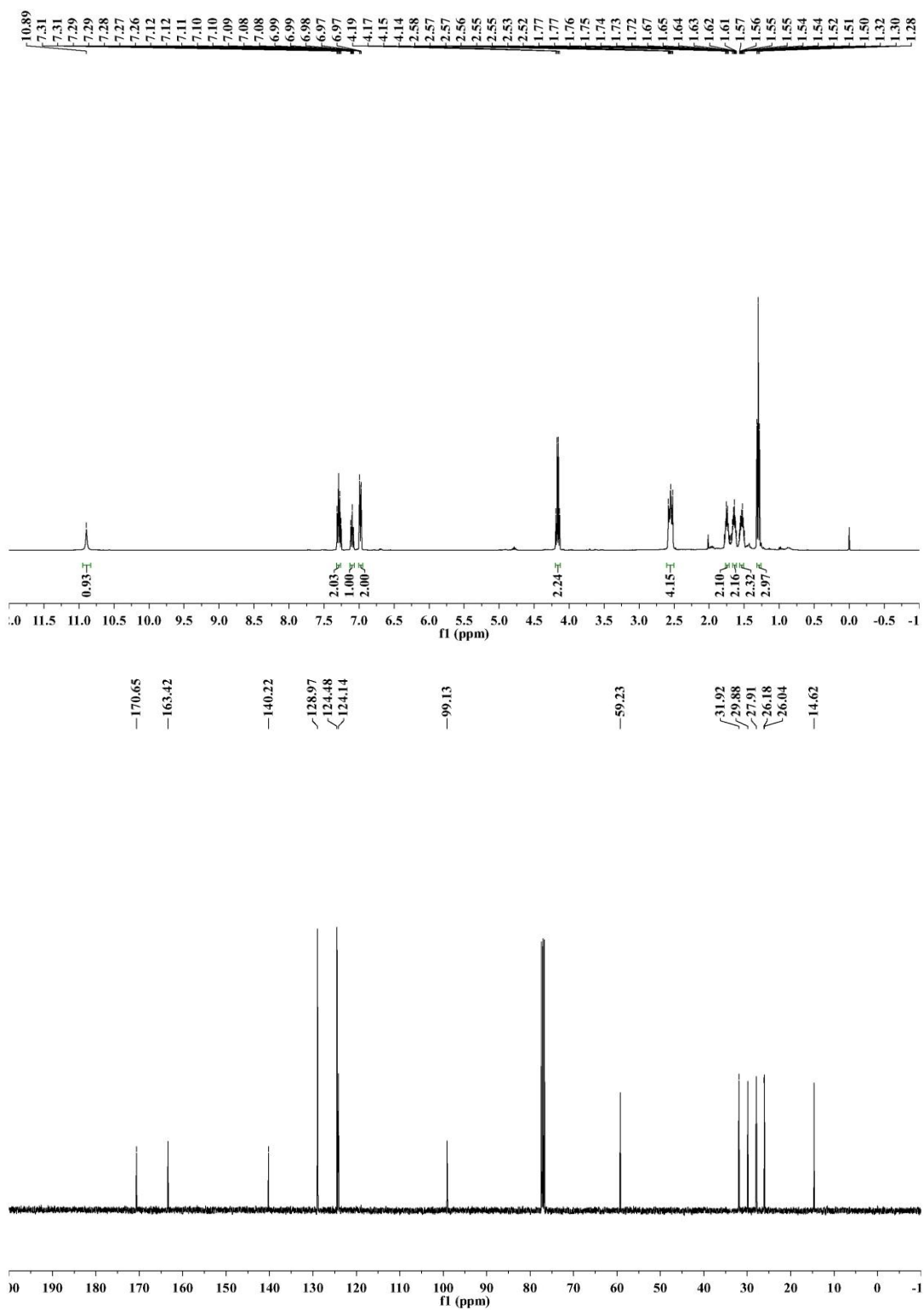
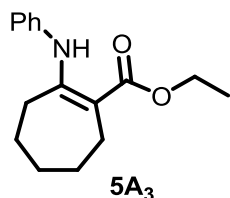


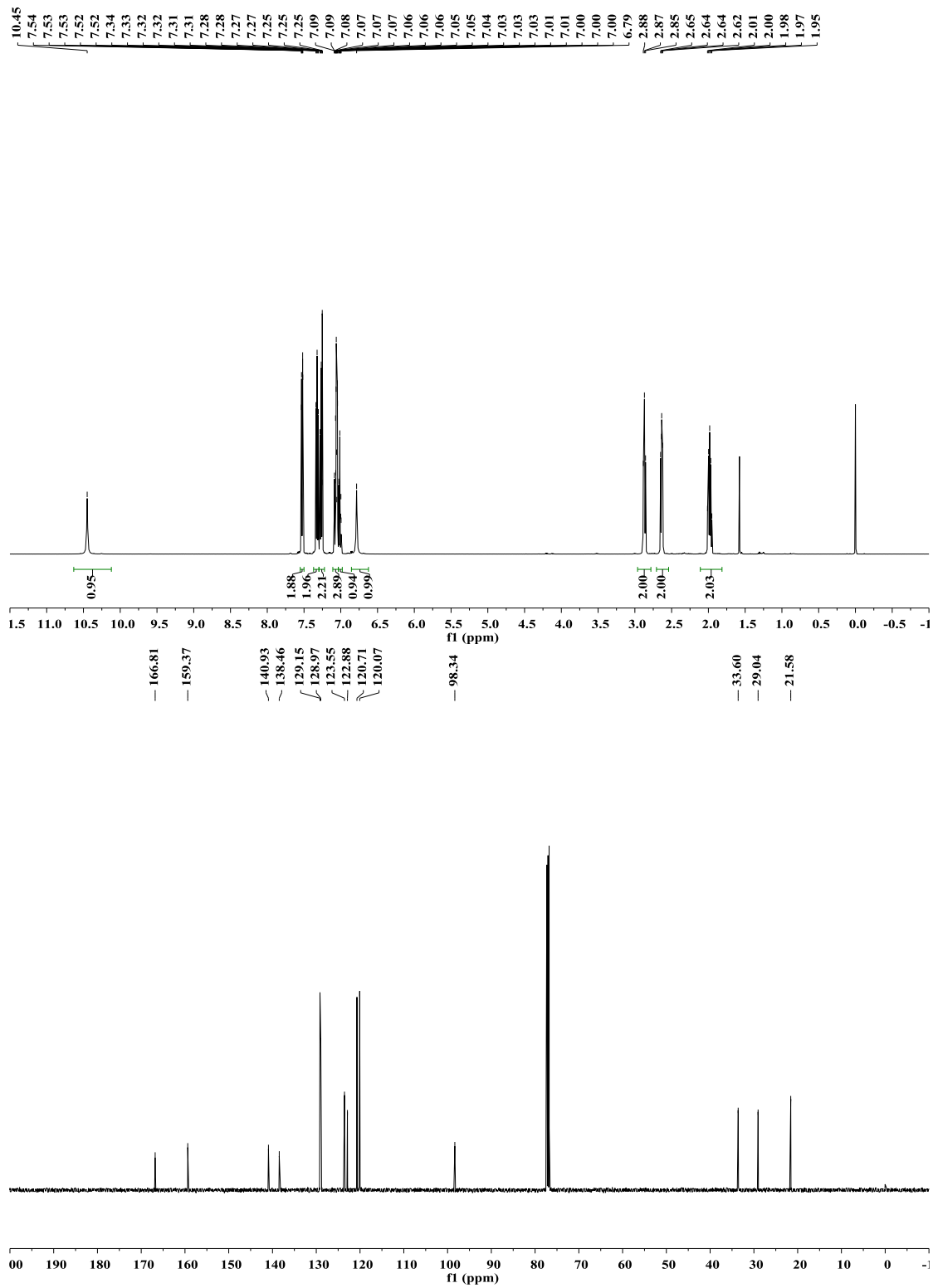
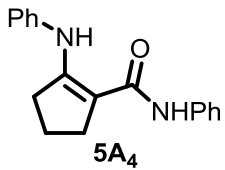


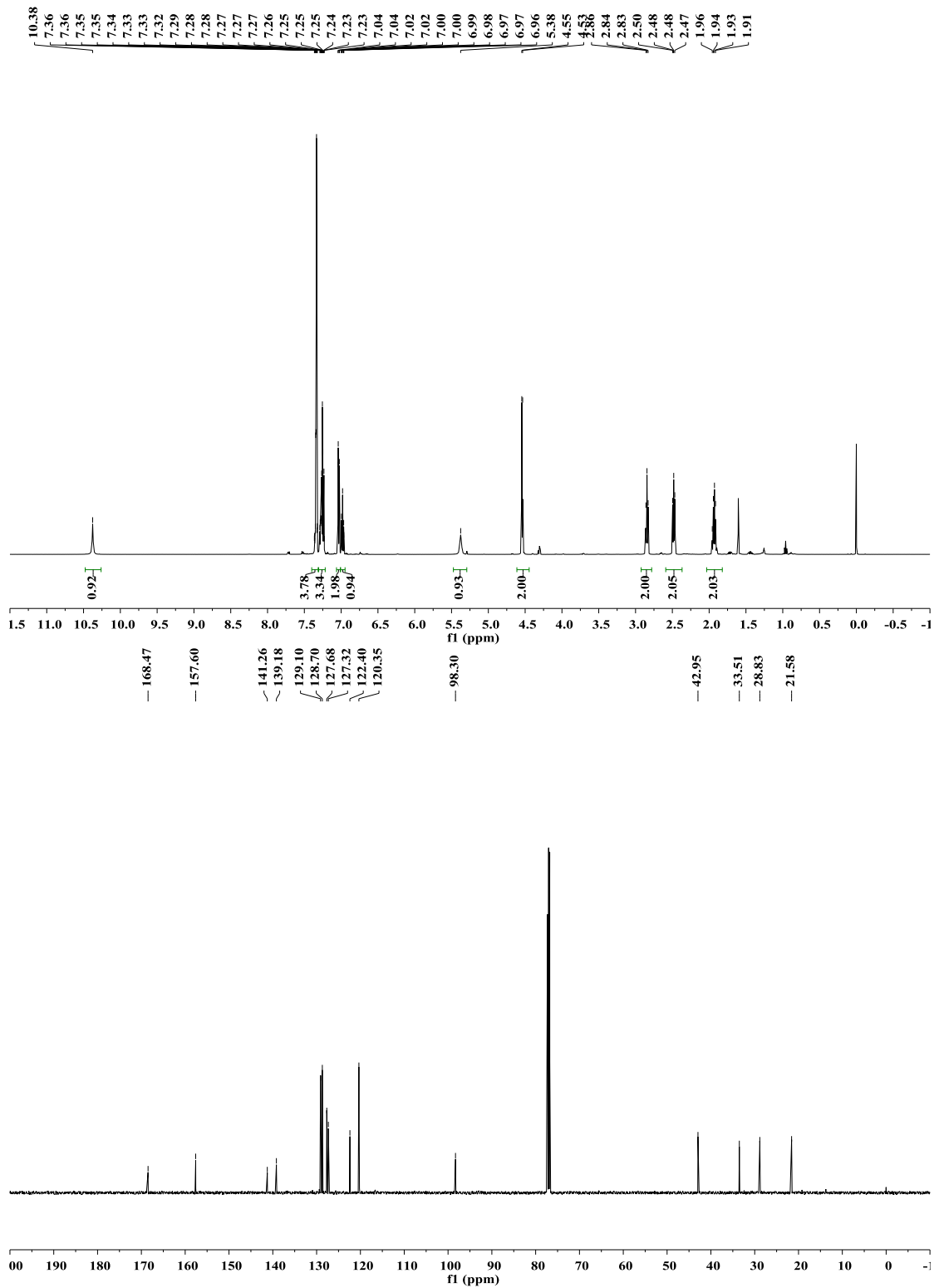
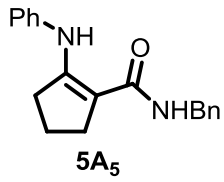


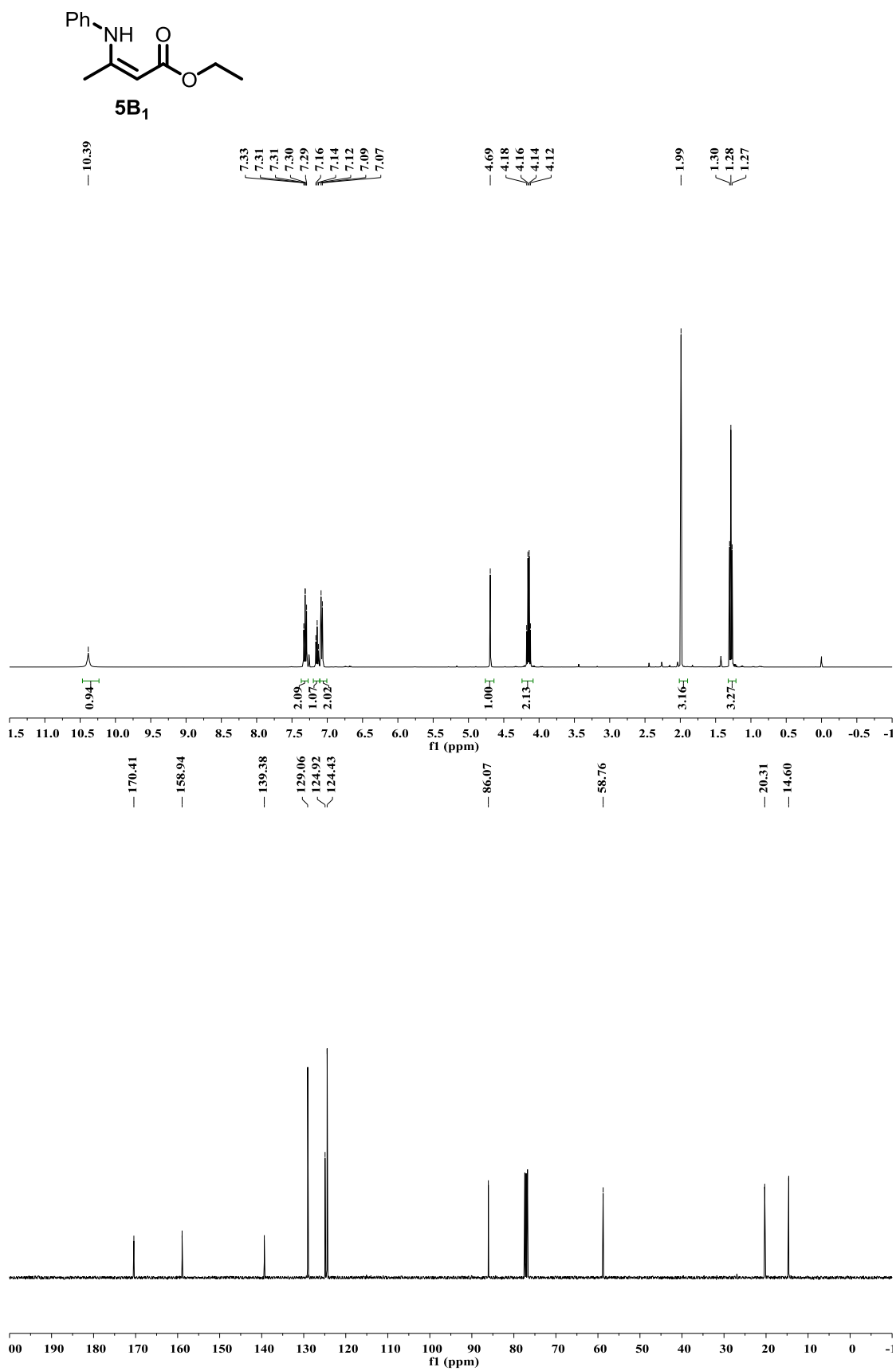


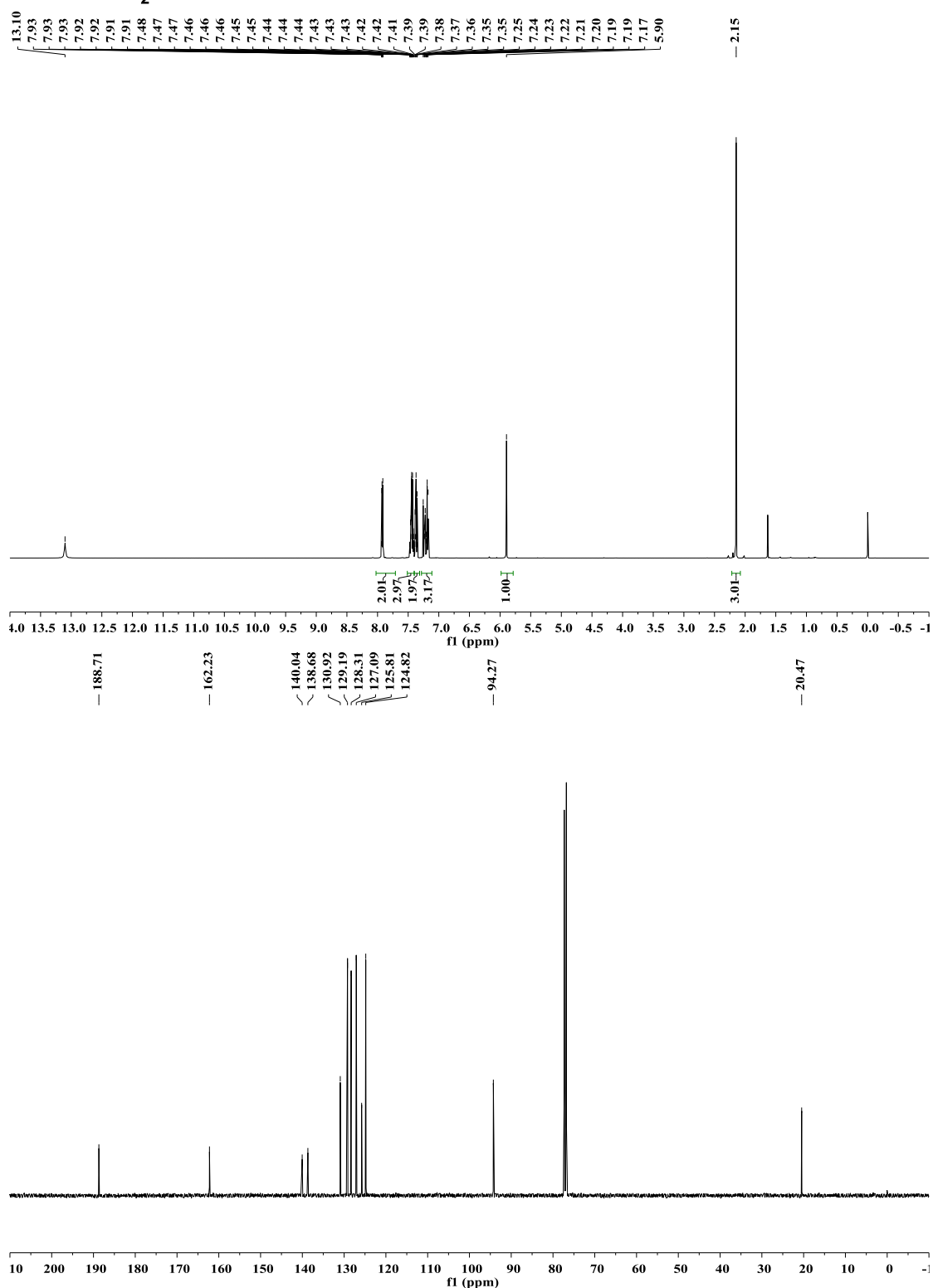
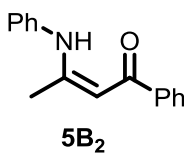


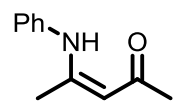




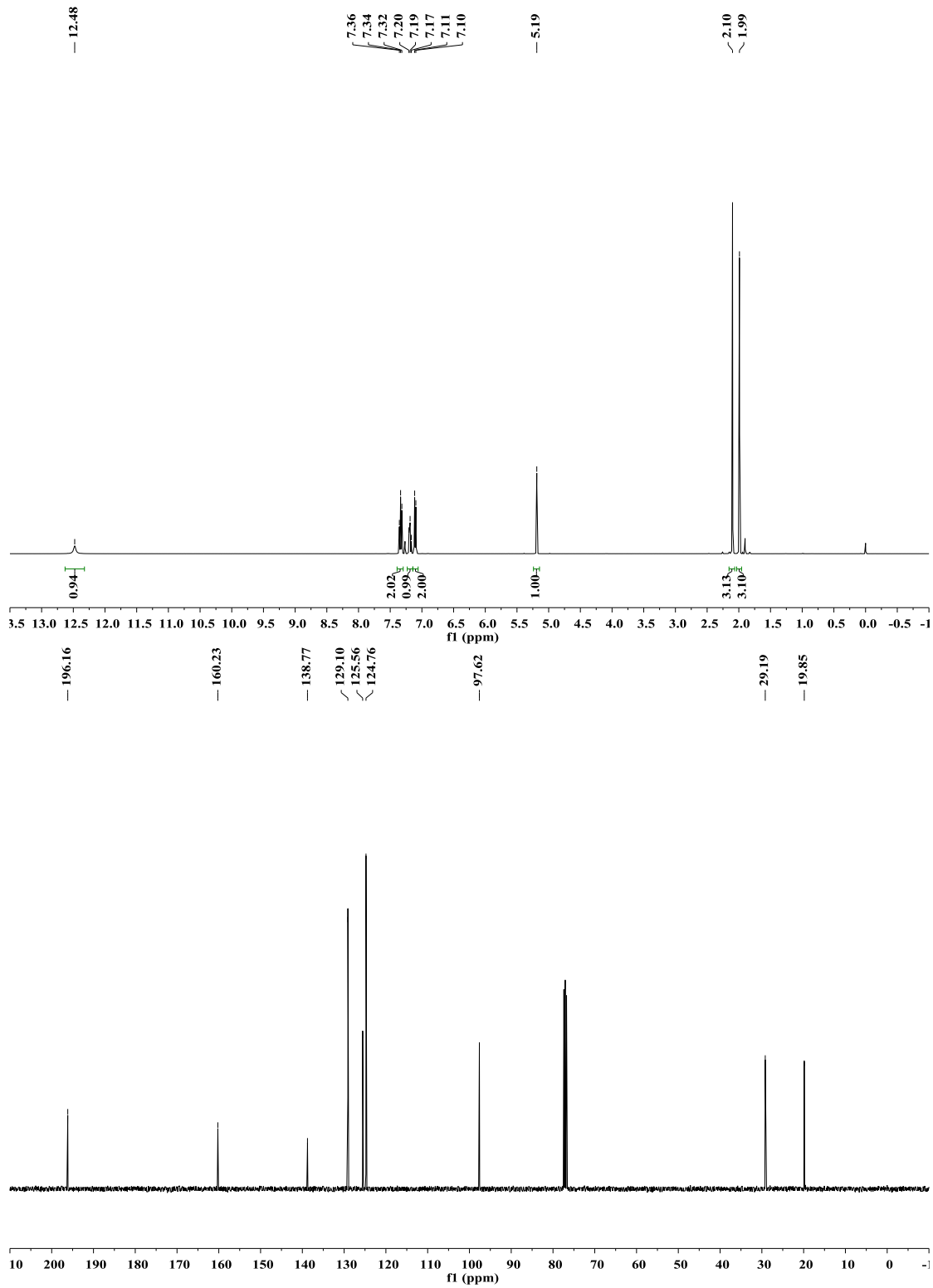


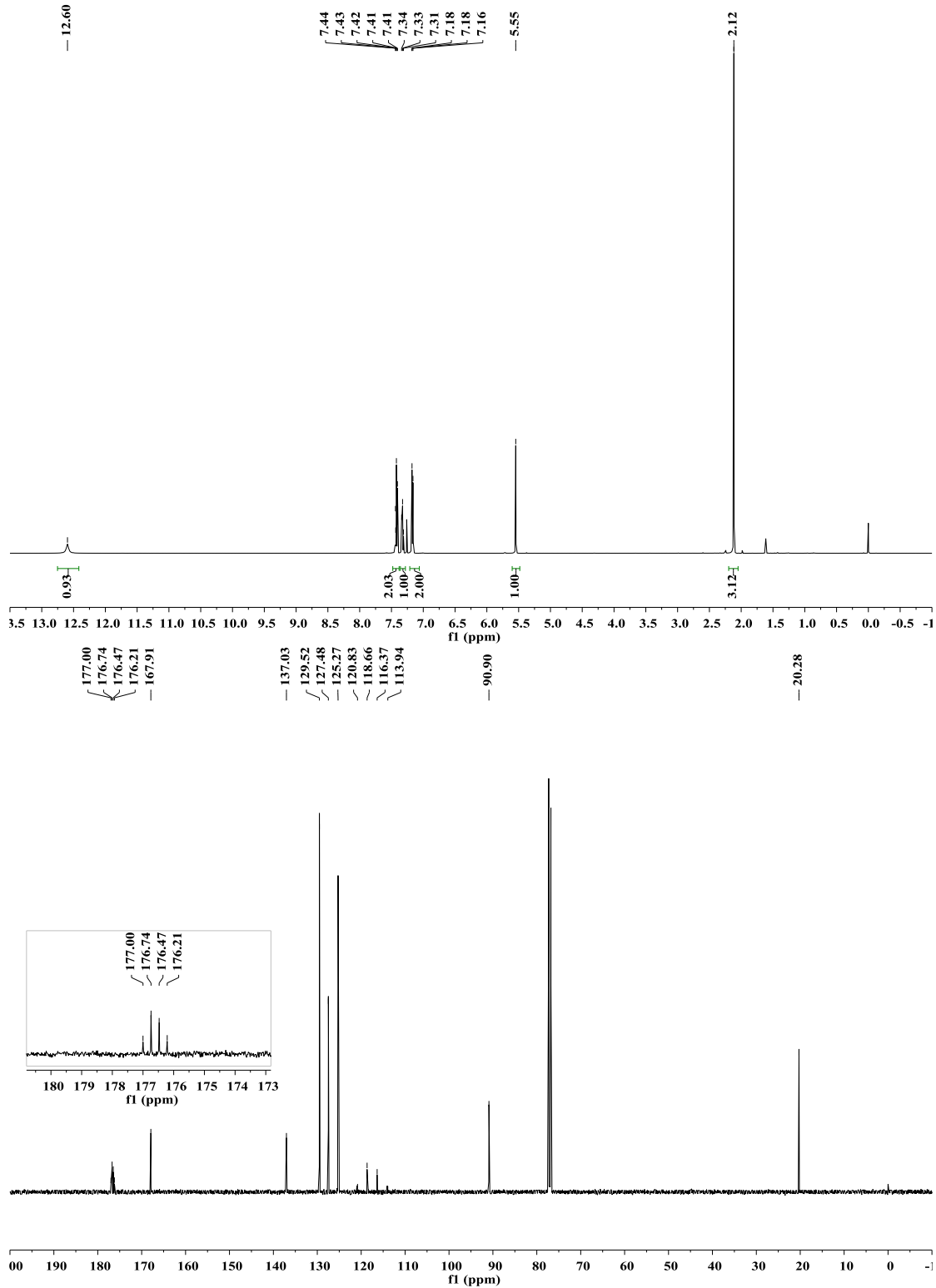
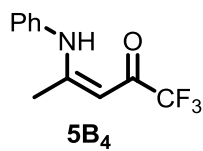


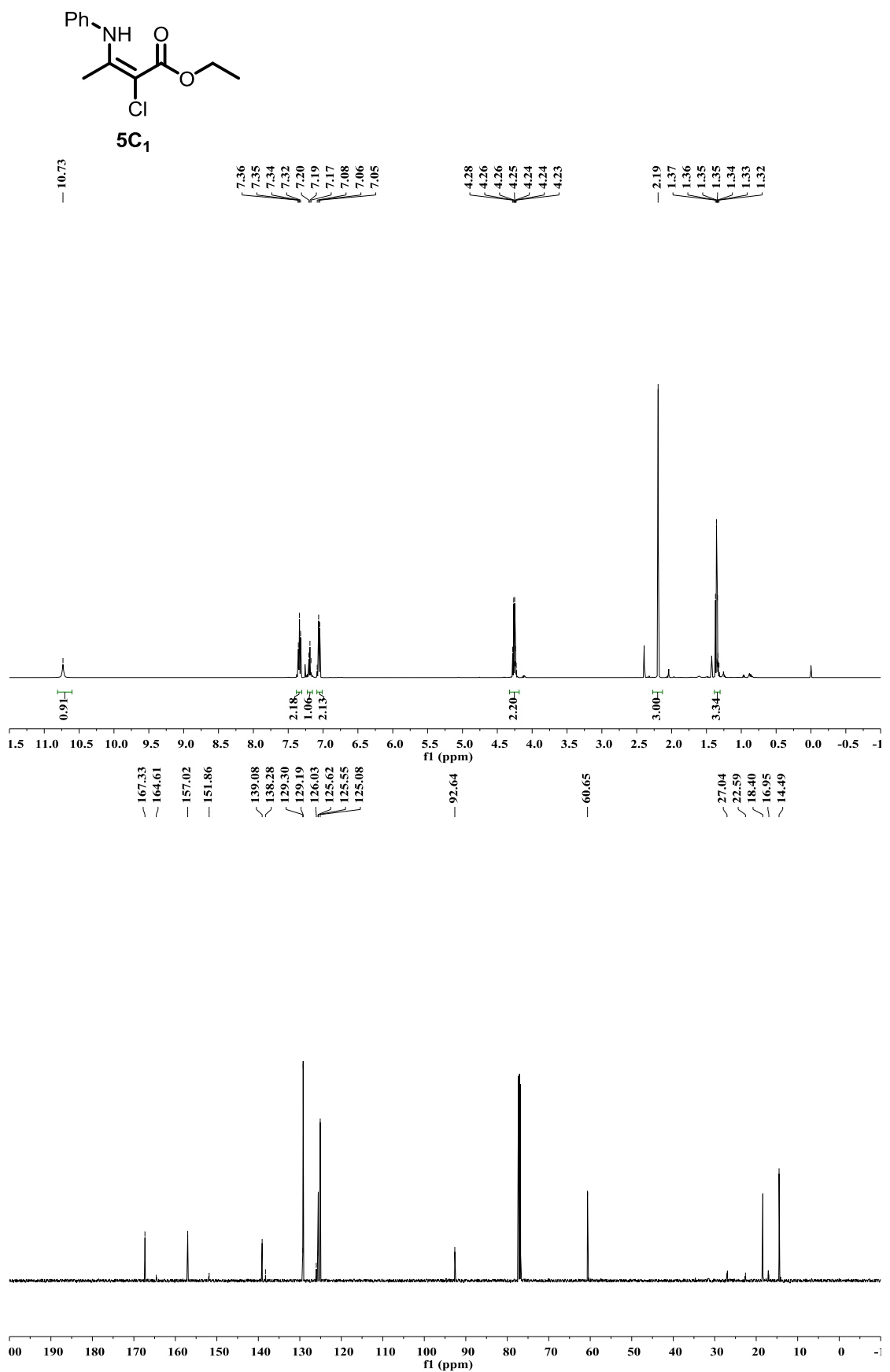


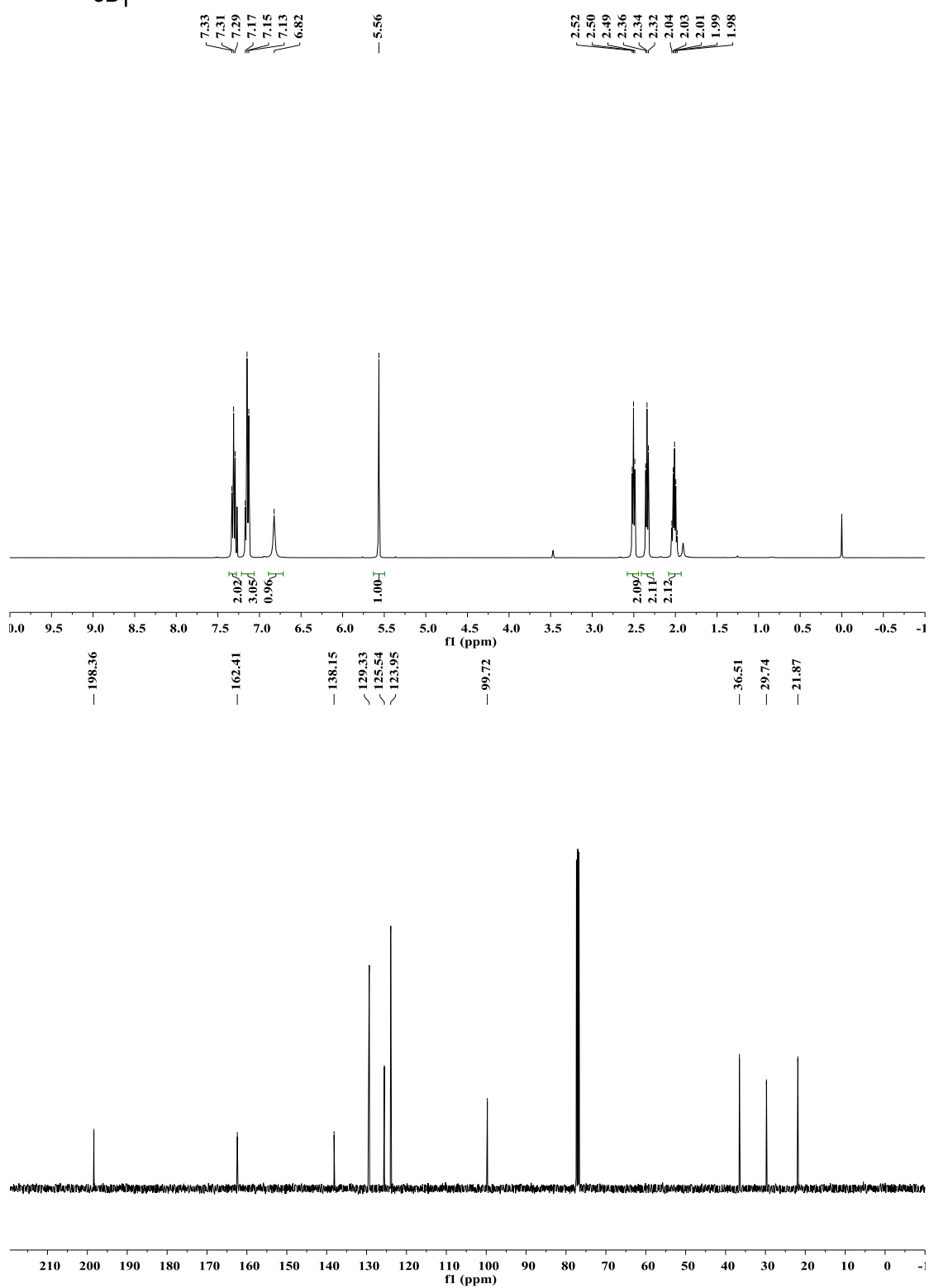
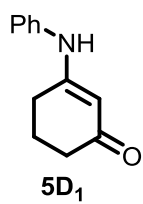


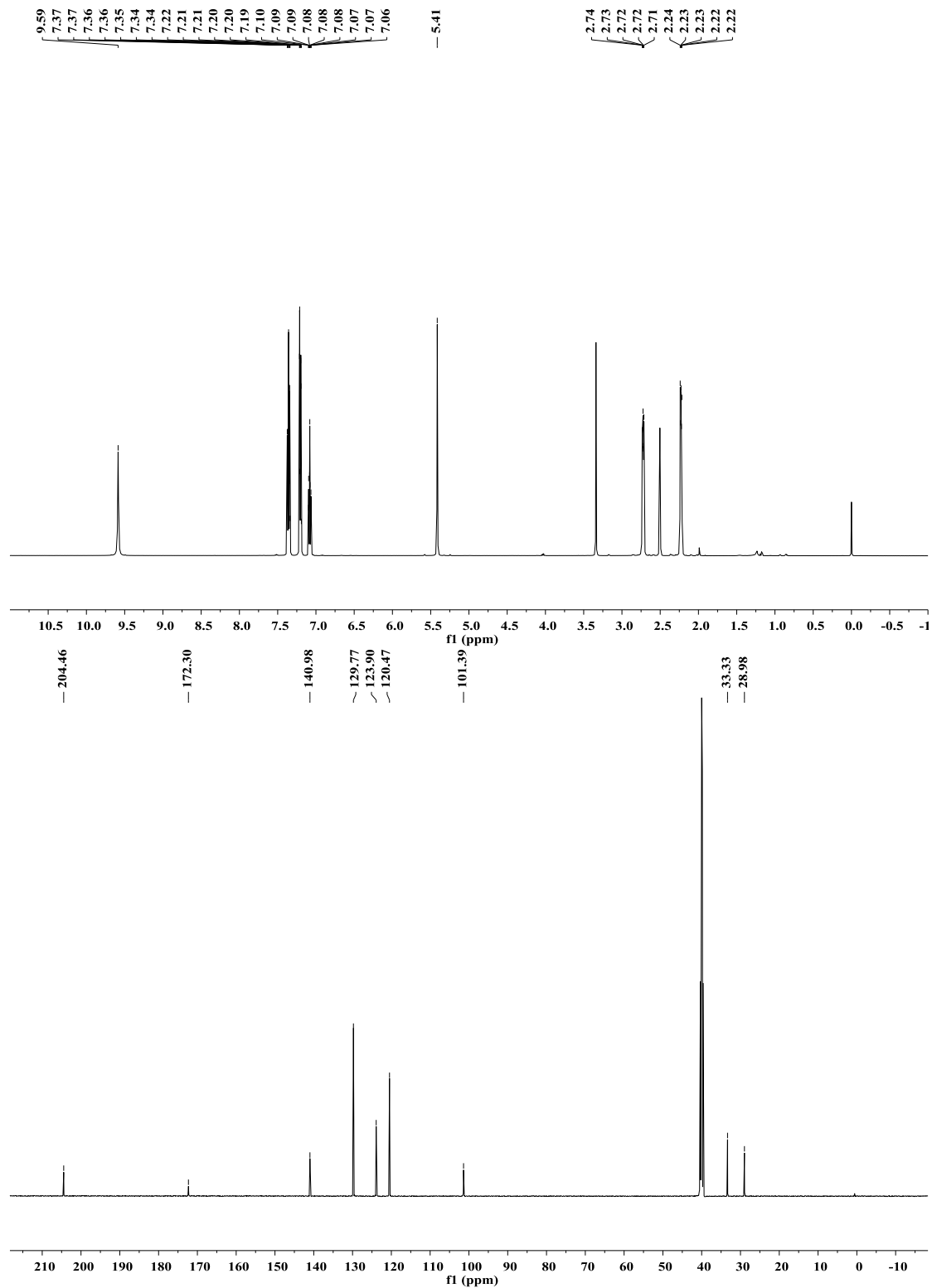
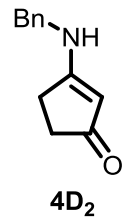
5B₃







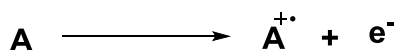




3. Calculation details and additional data

Since Truhlar et al.'s M06-2X hybrid functional was shown to provide accurate predictions of main group thermochemistry,¹ geometry optimizations and frequency computations were performed using Gaussian 09 at the M06-2X/6-311G(d,p) level of theory, in conjunction with the IEF-PCM model to account for the solvation effects of acetonitrile.¹⁻³ Free energies include unscaled zero-point vibrational energies. Where indicated, low frequencies (<100 cm⁻¹) were corrected in the vibrational component of the entropy using a free rotor approximation according to the method of Grimme et al., since entropy associated with these loose vibrational modes was the most prone to computational error.⁴ The quasi-harmonic oscillator corrections were obtained using the GoodVibes.⁵ NBO analysis was conducted at the same level of geometry optimization using NBO package build-in Gaussian 09.⁶

The oxidation potentials of enamines were calculated using the free energies of enamine and enamine radical cation according the equation below.

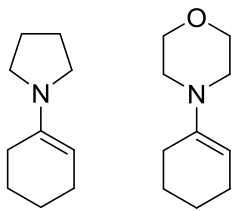


$$E = (G(\text{A}^{\cdot+}) + G(\text{e}^-) - G(\text{A})) / F - E^{\circ/\text{SCE}} \quad (\text{Eq. S1})$$

The value of -0.86 kcal/mol for the gas phase energy of the electron based on the Fermi-Dirac statistical formalism is employed.⁷ $E^{\circ/\text{SCE}}$ is the standard potential of the saturated calomel electrode (SCE) in acetonitrile (value = 4.429 V).⁸

We benchmarked several conventional density functions to calculated the oxidation potential of enamine **9H** (Table S1). The experimental oxidation peak potential of **9H** is 0.361 V (vs. SCE).⁹ This approach also gave an accurate prediction oxidation potential of enamine **22H**.⁹ M06-2X hybrid functional gave the best results and it has been shown to provide accurate predictions of redox potentials in DFT methods.¹⁰

Table S1. Tested several density functions for prediction of oxidation potentials (V vs. SCE).



9H 22H

Experimental E_p 0.361 V 0.574 V

function	Basis set	Solvating model	$E_{ox}(9H)$
B3LYP	6-311g(d,p)	pcm	0.172
PBE	6-311g(d,p)	pcm	0.108
PBE0	6-311g(d,p)	pcm	0.141
M06-2X	6-311g(d,p)	pcm	0.326 0.567^a
M06L	6-311g(d,p)	pcm	0.107
ω B97XD	6-311g(d,p)	pcm	0.178
B97D	6-311g(d,p)	pcm	0.026

^a Calculated oxidation potentials of enamine **22H**.

Table S2. Comparison of experimental and calculated oxidation potentials (V vs. SCE) of enamines deriving from β -ketocarbonyls

Enamines	Experimental oxidation		Calculated oxidation potentials
	peak potentials		
1A₁	0.85		0.91
1A₅	0.68		0.83
1C₂	0.79		0.93
2B₃	1.21		1.23
3A₁	0.99		0.99
3A₃	0.86		0.92
3A₄	0.81		0.91
3B₁	1.17		1.28
3B₂	1.30		1.32
3B₃	1.24		1.27

3C₁	1.13	1.25
3C₂	0.87	0.92
3C₃	0.88	0.91
3D₁	1.22	1.28
4C₂	0.96	1.04
5A₁	1.11	1.14
5A₂	1.06	1.14
5B₄	1.72	1.80
5D₂	1.42	1.51
6C₂	1.10	1.05

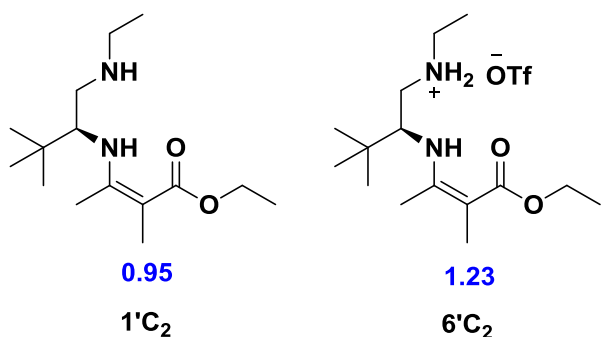
Table S3. Calculated oxidation potentials (V vs. SCE) of enamines in different conformations and relative free energies (in parentheses).

Secondary enamines

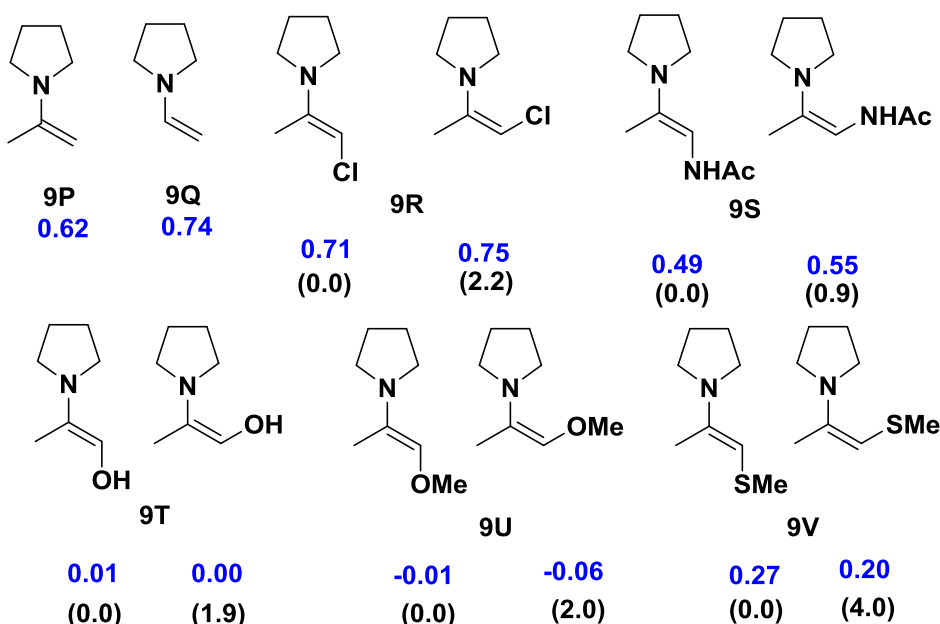
	1E 0.52 (0.0)		1F 0.51 (0.0)		1G 0.48 (0.0)		1I 0.41 (0.0)		1J 0.38 (0.4)
	2E 0.63 (0.2)		2F 0.64 (0.0)		2G 0.52 (0.0)		2I 0.54 (0.0)		2J 0.45 (0.0)
	3E 0.60 (0.0)		3F 0.54 (0.02)		3G 0.44 (0.0)		3I 0.47 (0.0)		3J 0.38 (1.4)
	4E 0.75 (0.0)		4F 0.73 (0.0)		4G 0.65 (0.0)		4I 0.63 (0.0)		4J 0.54 (1.4)
	5E 0.89 (0.5)		5F 0.82 (0.0)		5G 0.80 (0.0)		5I 0.76 (0.0)		5J 0.68 (1.1)
	6E 0.87 (0.0)		6F 0.76 (0.0)		6G 0.79 (0.0)		6I 0.73 (0.1)		6J 0.71 (0.0)
	7E 0.59 (0.0)		7F 0.53 (0.0)		7G 0.46 (0.0)		7I 0.44 (0.0)		7J 0.36 (0.0)
	8E 0.72 (0.0)		8F 0.60 (0.0)		8G 0.54 (0.0)		8I 0.57 (0.0)		8J 0.42 (0.0)
	1E 0.47 (0.5)		1F 0.63 (1.2)		1G 0.38 (2.6)		1I 0.41 (0.9)		1J 0.35 (0.0)
	2E 0.62 (0.0)		2F 0.66 (2.4)		2G 0.49 (1.2)		2I 0.52 (1.3)		2J 0.40 (0.2)
	3E 0.57 (0.2)		3F 0.68 (0.0)		3G 0.36 (1.2)		3I 0.53 (0.5)		3J 0.36 (0.0)
	4E 0.67 (0.6)		4F 0.77 (1.9)		4G 0.62 (0.5)		4I 0.63 (1.1)		4J 0.55 (0.0)
	5E 0.84 (0.0)		5F 0.93 (1.2)		5G 0.74 (0.8)		5I 0.76 (0.7)		5J 0.68 (0.0)
	6E 0.85 (0.5)		6F 0.94 (0.6)		6G 0.71 (1.8)		6I 0.66 (0.0)		6J 0.53 (2.3)
	7E 0.52 (0.4)		7F 0.64 (0.4)		7G 0.41 (1.7)		7I 0.46 (0.7)		7J 0.24 (0.4)
	8E 0.69 (0.02)		8F 0.73 (1.0)		8G 0.48 (2.2)		8I 0.52 (2.5)		8J 0.44 (0.2)

Tertiary enamines

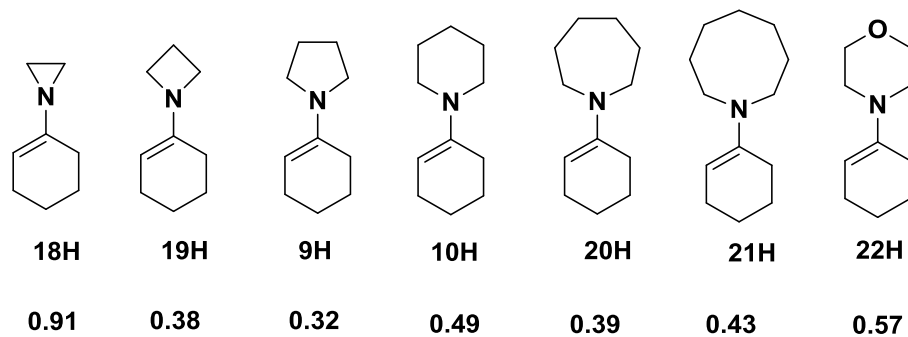
	9E 0.45 (0.0)		9F 0.51 (0.0)		9G 0.31 (0.0)		9I 0.39 (0.5)		9J 0.20 (0.1)
	10E 0.53 (0.0)		10F 0.53 (0.0)		10G 0.49 (0.0)		10I 0.40 (0.8)		10J 0.31 (1.5)
	11E 0.64 (0.0)		11F 0.64 (0.0)		11G 0.55 (0.0)		11I 0.58 (1.3)		11J 0.44 (1.0)
	12E 0.52 (0.0)		12F 0.55 (0.0)		12G 0.42 (0.0)		12I 0.48 (0.0)		12J 0.47 (0.0)
	13E 0.56 (0.0)		13F 0.60 (0.0)		13G 0.36 (0.0)		13I 0.45 (0.4)		13J 0.38 (0.0)
	14E 0.77 (0.0)		14F 0.77 (0.0)		14G 0.61 (0.0)		14I 0.68 (0.0)		14J 0.57 (0.0)
	15E 0.84 (0.0)		15F 0.82 (0.0)		15G 0.80 (1.0)		15I 0.78 (0.0)		15J 0.82 (0.0)
	16E 0.89 (0.0)		16F 0.84 (0.0)		16G 0.89 (0.0)		16I 0.89 (0.8)		16J 0.92 (1.6)
	17E 0.85 (0.0)		17F 0.79 (0.0)		17G 0.75 (0.0)		17I 0.71 (0.8)		17J 0.87 (0.0)
	9E 0.47 (3.4)		9F 0.62 (4.9)		9G 0.37 (2.4)		9I 0.42 (0.0)		9J 0.22 (0.0)
	10E 0.52 (4.5)		10F 0.53 (5.3)		10G 0.52 (3.5)		10I 0.40 (0.0)		10J 0.36 (0.0)
	11E 0.69 (2.4)		11F 0.77 (2.7)		11G 0.62 (1.8)		11I 0.61 (0.0)		11J 0.49 (0.0)
	12E 0.55 (2.9)		12F 0.65 (4.3)		12G 0.60 (0.1)		12I 0.49 (0.1)		12J 0.37 (2.5)
	13E 0.58 (2.6)		13F 0.67 (4.3)		13G 0.51 (0.7)		13I 0.55 (0.0)		13J 0.34 (1.8)
	14E 0.79 (2.7)		14F 0.85 (4.7)		14G 0.69 (0.6)		14I 0.65 (0.5)		14J 0.51 (2.6)
	15E 0.96 (0.6)		15F 0.97 (0.8)		15G 0.98 (0.0)		15I 0.83 (0.2)		15J 0.78 (1.3)
	16E 1.00 (4.1)		16F 1.11 (6.5)		16G 1.08 (2.2)		16I 0.82 (0.0)		16J 0.87 (0.0)
	17E 0.89 (3.5)		17F 0.96 (3.0)		17G 0.91 (0.8)		17I 0.75 (0.0)		17J 0.73 (2.3)



Scheme S1. Calculated oxidation potentials (V vs. SCE) of enamines deriving from 1', 6' and C₂. The numbers in parentheses are the relative free energies.



Scheme S2. Calculated oxidation potentials (V vs. SCE) of enamines deriving from acetaldehyde and α -substituted acetones. The numbers in parentheses are the relative free energies.



Scheme S3. Calculated oxidation potentials (V vs. SCE) of enamines deriving from cyclohexanone and various cyclic amines.

4. Reference

1. (a) Zhao, Y.; Truhlar, D. G. Density Functionals with Broad Applicability in Chemistry. *Acc. Chem. Res.* **2008**, *41*, 157-167. (b) Zhao, Y.; Truhlar, D. The M06 Suite of Density Functionals for Main Group Thermochemistry, Thermochemical Kinetics, Noncovalent Interactions, Excited States, and Transition Elements: Two New Functionals and Systematic Testing of Four M06-Class Functionals and 12 Other Functionals. *Theor. Chem. Acc.* **2008**, *120*, 215-241.
2. Gaussian 09, Revision D.01, Frisch, M. J.; Trucks, G. W.; Schlegel, H. B.; Scuseria, G. E.; Robb, M. A.; Cheeseman, J. R.; Scalmani, G.; Barone, V.; Mennucci, B.; Petersson, G. A.; Nakatsuji, H.; Caricato, M.; Li, X.; Hratchian, H. P.; Izmaylov, A. F.; Bloino, J.; Zheng, G.; Sonnenberg, J. L.; Hada, M.; Ehara, M.; Toyota, K.; Fukuda, R.; Hasegawa, J.; Ishida, M.; Nakajima, T.; Honda, Y.; Kitao, O.; Nakai, H.; Vreven, T.; Montgomery, Jr., J. A.; Peralta, J. E.; Ogliaro, F.; Bearpark, M.; Heyd, J. J.; Brothers, E.; Kudin, K. N.; Staroverov, V. N.; Keith, T.; Kobayashi, R.; Normand, J.; Raghavachari, K.; Rendell, A.; Burant, J. C.; Iyengar, S. S.; Tomasi, J.; Cossi, M.; Rega, N.; Millam, J. M.; Klene, M.; Knox, J. E.; Cross, J. B.; Bakken, V.; Adamo, C.; Jaramillo, J.; Gomperts, R.; Stratmann, R. E.; Yazyev, O.; Austin, A. J.; Cammi, R.; Pomelli, C.; Ochterski, J. W.; Martin, R. L.; Morokuma, K.; Zakrzewski, V. G.; Voth, G. A.; Salvador, P.; Dannenberg, J. J.; Dapprich, S.; Daniels, A. D.; Farkas, O.; Foresman, J. B.; Ortiz, J. V.; Cioslowski, J.; Fox, D. J. Gaussian, Inc., Wallingford CT, 2009.
3. (a) Cancès, E.; Mennucci, B.; Tomasi, J. A New Integral Equation Formalism for the Polarizable Continuum Model: Theoretical Background and Applications to Isotropic and Anisotropic Dielectrics. *J. Chem. Phys.* **1997**, *107*, 3032-3041. (b) Tomasi, J.; Mennucci, B.; Cancès, E. The IEF Version of the PCM Solvation Method: An Overview of a New Method Addressed to Study Molecular Solutes at the QM ab Initio Level. *J. Mol. Struct. (Theochem)* **1999**, *464*, 211-226. (c) Tomasi, J.; Mennucci, B.; Cammi, R. Quantum Mechanical Continuum Solvation Models. *Chem. Rev.* **2005**, *105*, 2999-3093.
4. (a) Grimme, S. Supramolecular Binding Thermodynamics by Dispersion-Corrected Density Functional Theory. *Chem. Eur. J.* **2012**, *18*, 9955-9964. (b) Alecu, I. M.; Zheng, J.; Zhao, Y.; Truhlar, D. G. Computational Thermochemistry: Scale

- Factor Databases and Scale Factors for Vibrational Frequencies Obtained from Electronic Model Chemistries. *J. Chem. Theory Comput.* **2010**, *6*, 2872-2887. (c) Ribeiro, R. F.; Marenich, A. V.; Cramer, C. J.; Truhlar, D. G. Use of Solution-Phase Vibrational Frequencies in Continuum Models for the Free Energy of Solvation. *J. Phys. Chem. B* **2011**, *115*, 14556-14562.
- 5. Funes-Ardoiz, I.; Paton, R. S. GoodVibes, v2.0.1; 2017, DOI: 10.5281/zenodo.884527.
 - 6. NBO Version 3.1, Glendening, E. D.; Reed, A. E.; Carpenter, J.; Weinhold, E. F.
 - 7. (a) Marenich, A. V.; Ho, J. Coote, M. L.; Cramer, C. J.; Truhlar, D. G. Computational Electrochemistry: Prediction of Liquid-Phase Reduction Potentials. *Phys. Chem. Chem. Phys.* **2014**, *16*, 15068-15106. (b) Bartmess, J. E. Thermodynamics of the Electron and the Proton. *J. Phys. Chem.* **1994**, *98*, 6420-6424.
 - 8. Isse, A. A.; Gennaro, A. Absolute Potential of the Standard Hydrogen Electrode and the Problem of Interconversion of Potentials in Different Solvents. *J. Phys. Chem. B* **2010**, *114*, 7894-7899.
 - 9. Schoeller, W. W.; Niemann, J.; Rademacher, P. On the Electrochemical Oxidation of Enamines. *J. Chem. Soc., Perkin Trans. 2* **1988**, 369-373.
 - 10. Isegawa, M.; Neese, F.; Pantazis, D. A. Ionization Energies and Aqueous Redox Potentials of Organic Molecules: Comparison of DFT, Correlated ab Initio Theory and Pair Natural Orbital Approaches. *J. Chem. Theory Comput.* **2016**, *12*, 2272-2284.